Cortical mechanisms of visual motion integration

János Attila Perge

Book design by: **János A. Perge**
Artistic consultant: **Robert van Sluis**
Printed by: **Febodruk B.V. Enschede**

ISBN: 90-393-39686

CORTICAL MECHANISMS OF VISUAL MOTION INTEGRATION

Corticale mechanismen van visuele bewegingsintegratie

(met een samenvatting in het Nederlands)

PROEFSCHRIFT

Ten verkrijging van de graad van doctor aan de Universiteit Utrecht op gezag van de Rector Magnificus, Prof. DR. W. H. Gispen, ingevolge het besluit van het College voor Promoties in het openbaar te verdedigen op dinsdag 7 Juni 2005 des middags te 14.30 uur

door

JÁNOS ATTILA PERGE

Geboren op 17 December 1976, Balassagyarmat, Hongarije

Promotor: PROF. DR. ALBERT V. VAN DEN BERG
Functionele Neurobiologie, Faculteit Biologie
Hemholtz Instituut
Universiteit Utrecht

Co-promotor: DR. RICHARD J. A. VAN WEZEL
Functionele Neurobiologie, Faculteit Biologie
Helmholtz Instituut
Universiteit Utrecht

Co-promotor: DR. IR. MARTIN J. M. LANKHEET
Functionele Neurobiologie, Faculteit Biologie
Helmholtz Instituut
Universiteit Utrecht

Contents

Chapter 1

Introduction

Local motion detection and global motion integration

Our visual system is constantly bombarded by moving patterns and objects projected onto our retina. Detection and analysis of these motion signals is one of the most important functions of the visual system. Visual motion processing is essential for survival of visually oriented organisms in a continuously changing environment when catching prey, escaping from predators or orienting itself during self-motion. The evolutionary pressure for motion processing has led to a sophisticated motion detection system with specialized front-end motion detectors. These primary motion detectors provide local motion measurements of a visual scene. To extract useful information from a changing visual scene these local motion measurements have to be integrated into a global motion percept.

A natural scene can consist of multiple objects that move in different directions or at different speeds. In such a situation, two different processes play an important role. First, different local motion signals belonging to a single object must be integrated. On the other hand, local motion signals belonging to different objects have to be segregated. These processes of motion integration and segregation occur both space and time, and depend on the spatio-temporal layout of speed and direction.

There are many approaches, both experimental and theoretical, that are currently used to understand how the visual system performs these complex operations. Neuroanatomy provides structural information of motion related areas. Neurophysiological methods make it possible to record neural activity of individual neurons or small groups of neurons in visually sensitive brain regions. Functional magnetic resonance imaging (fMRI) allows non-invasive measurements of global brain activation in presence of cognitive tasks. Computational modeling applies simulations to understand complex brain functions. Finally, psychophysics measures the ability of humans or animals to perform a visual task in order to define the system properties of the visual system and to understand how the underlying physiology works.

In this thesis, I will use neurophysiological single unit recordings combined with human psychophysical measurements to derive a quantitative understanding of visual motion integration. This approach has the potential to bridge the gap between the cellular level of neurophysiological measurements on animals and the behavioral level of psychophysical tests on humans. My research is focused on two visual motion sensitive areas in the macaque brain, namely middle temporal (MT) and medial superior temporal (MST) areas. The advantage of these well-studied areas in visual motion research is that both of them are accessible for neurophysiological

measurements, while their role in visual motion processing and higher cognitive functions has been demonstrated. Neurophysiological studies revealed profound attentional effects in these areas, while correlation of cell activities with perceptual abilities revealed a close link to perception (Treue and Maunsell, 1996; Britten et al., 1996). Furthermore, microstimulation in MT and MST alters the animal's judgement of motion direction, manipulates saccades and smooth pursuit eye movements (motor control), and affects performance on a visual working memory task (Celebrini and Newsome, 1995; Nichols and Newsome, 2002; Groh et al, 1997; Salzman et al., 1992; Bisley et al., 2001).

In this thesis, I will discuss multiple aspects of cortical motion integration and segregation, both in the spatial and temporal domain. I will mainly discuss two motion sensitive cortical areas, which comprise the main subject of the thesis, MT and MST. The following section provides a brief overview on basic physiological properties of motion sensitive neurons in these areas. Examples of motion integration and segregation are also provided. This summary of literature will serve as background information for the other chapters of this thesis. The literature on cortical mechanisms of motion processing is abundant, and I do not attempt to provide an encyclopedic review of all the research. Exhaustive reviews on cortical motion pathways can be found elsewhere (Britten, 2004; Albright and Stoner, 1995; Maunsell and Newsome, 1987; Parker and Newsome, 1998).

The Middle Temporal (MT) area

Area MT is one of the most extensively studied visual regions. Its name was derived from its anatomical location in the owl monkey (Allman and Kaas, 1971), although its anatomical location in macaques or humans differs. The other commonly used name is V5, but the original name MT will be used throughout this thesis. The main anatomical features of MT are dense myelination and reciprocal connections with primary visual cortical area V1 (Ungerleider and Mishkin, 1979; Van Essen et al., 1981; Zeki, 1974). It receives input also from Lateral Geniculate Nucleus of thalamus (LGN), V2 and V3 as well projects onto a range of visual areas along the superior temporal sulcus (MST, FST, STP), parietal lobe (VIP, LIP, 7a), the frontal lobe (area 46, FEF, SEF), the brainstem (DTN, NOT), midbrain (superior colliculus), and cerebellum (Fig.1). Area MT is retinotopically organized, i.e. retinal locations correspond well to MT anatomical locations. Additionally, area MT is bilateral, and receives contralateral visual input. MT in one hemisphere represents the visual field on the opposite side.

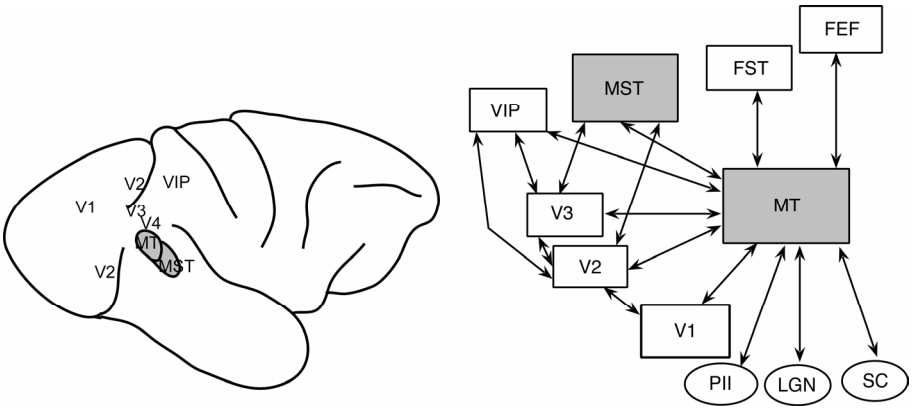

Fig. 1. Location and main connections of areas MT and MST. **A)** Schematic drawing of the macaque brain with the most important motion related areas including MT and MST. **B)** Main anatomical connections of MT and MST. Abbreviations: MT, middle temporal, LGN, Lateral Geniculate Nucleus, MST, Medial Superior Temporal, VIP, Ventral Intraparietal, FST, Fundus of the Superior Temporal sulcus, FEF, Frontal Eye Field, PII, Pulvinar nucleus, SC, Superior Colliculus

Motion sensitivity of area MT neurons

One of the most remarkable features of area MT is its large number of directionally selective neurons. Direction selectivity means that these cells respond best for motion in a particular direction, called the preferred direction. The response decreases as the direction of motion differs more and more from this preferred direction. Generally, the response is the lowest for the direction opposite to the preferred direction, which is called the antipreferred or null direction. For some MT neurons, motion in the antipreferred direction can also have a suppressive effect on the responses (Albright, 1984; Britten et al., 1983, Maunsell and Van Essen, 1983). The dependence of response strength on motion direction is referred to as its direction tuning (Fig. 2). Chapter two will discuss new findings related to the time course of MT direction tuning.

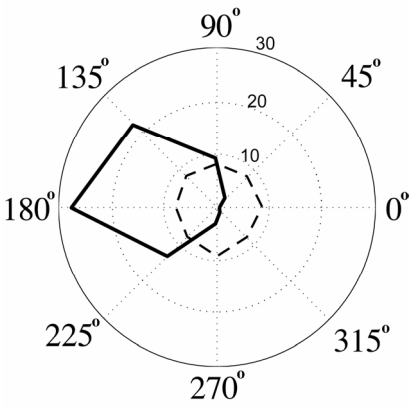

Fig. 2. Direction tuning of an example MT neuron. The polar angles indicate stimulus direction, and the radial dimension indicates the average response magnitude in spikes/sec. The dashed inner circle indicates the spontaneous activity.

Neurons with similar direction tuning properties are organized into a regular, columnar pattern. This means that direction tuning is consistent across cortical layers within a column, but changes gradually or even abruptly across the surface. In owl monkeys, where MT lies exposed on the cortical surface, optical imaging shows a consistent map of cortical columns (Geesaman et al., 1997). In Old World monkeys such as the Rhesus macaque, MT sits deep in the sulcus; therefore, it cannot be visualized by optical imaging. However, the columnar organization can still be recognized by measuring direction-tuning curves along a series of electrode penetrations (Albright, 1984).

Area MT neurons are not only tuned for the direction but also for the speed of motion. MT cells are typically bandpass tuned with the largest responses at medium speeds (Albright, 1984; Lagae et al., 1993; Maunsell and Van Essen, 1983). Preferred speeds increase with eccentricity (Maunsell and Van Essen, 1983). Neurons with similar speed tuning are not as neatly organized into columns for direction, but a patchy organization for speed in MT is present (Ditterich et al., 2003)

Spatial properties of area MT neurons

An important characteristic of MT neurons is the structure of their receptive fields. Neurons in MT respond to moving stimuli only within a limited part of the visual field known as the receptive field. Receptive field sizes vary across the visual field depending on their distance from the fixation point. The diameter of receptive fields is small at the fixation point, and grows larger at increasing eccentricity. On average the diameter of MT receptive fields is 0.8 times the eccentricity in degrees (Maunsell and Van Essen, 1983).

For 50% of MT neurons, the responses can be greatly influenced by stimuli outside the classically defined receptive field (Allman et al., 1985). Stimuli in this surrounding region by definition do not evoke responses, but can modulate the responses to stimuli in the classical receptive field. The modulation is antagonistic, because it is maximally suppressive when the presented stimulus in the surrounding region is in the preferred direction. In some cases, modulation is facilitatory when the presented stimulus in the surround is in the antipreferred direction (Allman et al., 1985). Throughout this thesis, the antagonistic surround as part of the receptive field will be considered, and references to the classical receptive field together with its surround as the center-surround receptive field will be made. Cells that lack the antagonistic surround respond to wide-field motion, and they are anatomically separated from cells with center-surround receptive fields (Born and Tootell, 1992). Center-surround receptive fields might be useful for segregating local motion signals in a noisy visual environment. Chapter three will analyze the spatial and temporal characteristics of center-surround receptive fields.

Motion integration in area MT

Models of motion integration have emphasized a two-stage process. Neurons at the first stage analyze local and ambiguous motion signals and neurons at the second stage integrate these signals into a global motion signal. This process has been illustrated by a "plaid" stimulus, which consists of two superimposed sine-wave gratings with different orientations. Local motion detectors only respond to motion perpendicular to the grating's orientation. A plaid, however, is perceived to move coherently in a direction equal to the vector sum of the separate components. Direction selective neurons in V1 respond mostly to the direction of the individual components of the plaid (component selective cells), whereas a subpopulation of MT neurons responds to the direction of the plaid (pattern selective cells). Component and pattern selective cells reflect the integration of local motion signals into a global motion signal (Movshon et al., 1985).

Temporal properties of area MT neurons

Analysis of visual motion processing cannot be complete without the investigation of the time course of responses. The temporal delay between stimulus onset and the start of the response, called the response latency, varies substantially in MT. The shortest latencies are 30-35 ms, and the median latency is approximately 90 ms (Heuer and Britten, 1999; Maunsell, 1986; Raguel et al, 1999).

When MT neurons are stimulated with continuous motion, the initial response is large, but it settles rapidly (within about 30-80 ms) to a lower

response level. This transient-sustained response pattern is a short-term adaptation, and it is functionally different from adaptation over a longer time such as seconds or tens of seconds (Lisberger and Movshon, 1999, Priebe et al., 2002a,b, van Wezel and Britten, 2002). Prolonged adaptation in the preferred direction sharpens direction-tuning curves (Kohn and Movshon, 2004).

The investigation of the time course of the responses also revealed that complex neural computations such as selectivity to the global motion direction of a moving plaid take time to develop. In the initial part of the responses, pattern selective neurons also signal the components of the moving plaid and the global representation of the plaid develops gradually during the responses (Pack and Born, 2001; Pack et al., 2001; Smith et al., 2005).

Medial superior temporal (MST) area

The medial superior temporal (MST) area is located close to area MT (Fig. 1), and it receives direct input from MT. Similarly to MT, the majority of cells in MST also show directionally selective responses to moving stimuli. The receptive fields are much larger than those in MT are, and many of them include the fovea. Cells in dorsal MST preferentially respond to movements of a wide textured field, whereas those in the ventral MST preferentially respond to movements of a small object (Sugita and Tanaka, 1991; Tanaka et al., 1993).

Dorsal MST cells respond selectively to optic flow patterns (or complex motion) that are projected onto the retina as the observer moves in its environment (Sakata et al., 1985, 1994, Saito et al., 1986, Duffy and Wurtz, 1991, Orban et al., 1992). Examples of optic flow patterns are expansion, contraction, clockwise rotation, counterclockwise rotation, or a combination of them, which are known as ‘spiral space’ (Graziano et al., 1994). Some of the dorsal MST cells show an extensive invariance for changes in the position of the complex motion patterns (Saito et al., 1986; Lagae et al., 1994).

Cells in ventral MST show similarities with center-surround cells in MT. These cells respond to background movement behind a stationary object and movement in the opposite direction of an object on a stationary background (Sugita and Tanaka, 1991; Tanaka et al., 1993). Compared to the responses of MT center-surround cells, these neurons carry precise information about the direction of an object’s relative movement on the background (Tanaka, 1993).

In short, MST receptive fields are larger and more complex than those in MT are, and they integrate motion signals along complex motion trajectories. Their sensitivity to optic flow provides valuable information about the three-dimensional layout of the environment and about self-motion. These characteristics indicate that motion integration has substantially progressed from MT to MST. Comparing MT to MST responses is therefore valuable for understanding mechanisms of visual motion integration. This approach is a promising way to reveal the neuronal mechanisms by which we successfully navigate and operate in our open and complex environment.

Outline of the thesis

The main results of this thesis are based on single-unit recordings in cortical area MT and MST of fixating monkeys. This work addresses the temporal and spatial characteristics of direction tuning of motion sensitive neurons. Some of the findings inspired psychophysical measurements with human observers. Those results are also reported here.

Chapter two investigates how direction selectivity of MT neurons changes in time. This work is a successful application of the Motion Reverse Correlation method developed in our laboratory to measure directional responses in the cat and monkey (Borghuis et al., 2003). The method also allowed us to analyze the temporal integration properties of MT neurons.

Chapter three extends the full-field measurements of motion sensitivity in Chapter two to multiple spatial locations. This provides detailed spatio-temporal maps of MT receptive field properties.

Inspired by the neurophysiological results of Chapter three, we conducted psychophysical experiments with human observers to investigate the perceptual consequences of delayed MT receptive field surrounds in human motion perception. This work is described in Chapter four.

Chapter five describes how MST neurons integrate responses to stimulus pairs with different motion directions. This analysis is related to the reverse correlation analysis of temporal combinations of different motion directions described in Chapter two, and provides new insight in cortical mechanisms of complex motion integration.

References

Albright, T. D. (1984). Direction and orientation selectivity of neurons in visual area MT of the macaque. J Neurophysiol 52, 1106-1130.

Albright, T. D., and Stoner, G. R. (1995). Visual motion perception. Proc Natl Acad Sci U S A 92, 2433-2440.

Allman, J. M., and Kaas, J. H. (1971). Representation of the visual field in striate and adjoining cortex of the owl monkey (Aotus trivirgatus). Brain Res 35, 89-106.

Allman, J., Miezin, F., and McGuinness, E. (1985). Direction- and velocity-specific responses from beyond the classical receptive field in the middle temporal visual area (MT). Perception 14, 105-126.

Bisley, J. W., Zaksas, D., and Pasternak, T. (2001). Microstimulation of cortical area MT affects performance on a visual working memory task. J Neurophysiol 85, 187-196.

Borghuis, B. G., Perge, J. A., Vajda, I., van Wezel, R. J., van de Grind, W. A., and Lankheet, M. J. (2003). The motion reverse correlation (MRC) method: a linear systems approach in the motion domain. J Neurosci Methods 123, 153-166.

Born, R. T., and Tootell, R. B. (1992). Segregation of global and local motion processing in primate middle temporal visual area. Nature 357, 497-499.

Britten, K. H., Shadlen, M. N., Newsome, W. T., and Movshon, J. A. (1993). Responses of neurons in macaque MT to stochastic motion signals. Vis Neurosci 10, 1157-1169.

Britten, K. H., Newsome, W. T., Shadlen, M. N., Celebrini, S., and Movshon, J. A. (1996). A relationship between behavioral choice and the visual responses of neurons in macaque MT. Vis Neurosci 13, 87-100.

Britten, K. H. (2004). The Middle Temporal area: Motion processing and the link to Perception. In The visual neurosciences, L. M. Chalupa, and J. S. Werner, eds. (London), pp. 1203-1215.

Celebrini, S., and Newsome, W. T. (1995). Microstimulation of extrastriate area MST influences performance on a direction discrimination task. J Neurophysiol 73, 437-448.

Ditterich, J., Mazurek, M. E., and Shadlen, M. N. (2003). Microstimulation of visual cortex affects the speed of perceptual decisions. Nat Neurosci 6, 891-898.

Duffy, C. J., and Wurtz, R. H. (1991). Sensitivity of MST neurons to optic flow stimuli. I. A continuum of response selectivity to large-field stimuli. J Neurophysiol 65, 1329-1345.

Geesaman, B., Born, R., Andersen, R., and Tootell, R. (1997). Maps of complex motion selectivity in the superior temporal cortex of the alert macaque monkey: a double-label 2-deoxyglucose study. Cer Cortex 7, 749-757.

Graziano, M. S., Andersen, R. A., and Snowden, R. J. (1994). Tuning of MST neurons to spiral motions. J Neurosci 14, 54-67.

Groh, J. M., Born, R. T., and Newsome, W. T. (1997). How is a sensory map read Out? Effects of microstimulation in visual area MT on saccades and smooth pursuit eye movements. J Neurosci 17, 4312-4330.

Heuer, H. W., and Britten, K. H. (1999). Response normalization by middle temporal neurons. II: effects of contrast. submitted.

Kohn, A., and Movshon, J. A. (2004). Adaptation changes the direction tuning of macaque MT neurons. Nat Neurosci 7, 764-772.

Lagae, L., Raiguel, S., and Orban, G. A. (1993). Speed and direction selectivity of macaque middle temporal neurons. J Neurophys 69, 19-39.

Lagae, L., Maes, H., Raiguel, S., Xiao, D. K., and Orban, G. A. (1994). Responses of macaque STS neurons to optic flow components: a comparison of MT and MST. J Neurophysiol 71, 1597-1626.

Lisberger, S. G., and Movshon, J. A. (1999). Visual motion analysis for pursuit eye movements in area MT of macaque monkeys. J Neurosci 19, 2224-2246.

Maunsell, J. H. R., and Van Essen, D. C. (1983). Functional properties of neurons in the middle temporal visual area (MT) of the macaque monkey: I.

Selectivity for stimulus direction, speed and orientation. J Neurophysiol 49, 1127-1147.

Maunsell, J. H. R. (1986). Physiological evidence for two visual systems. In Matters of Intelligence, L. Vaina, ed. (Dordrecht, Reidel).

Maunsell, J. H., and Newsome, W. T. (1987). Visual processing in monkey extrastriate cortex. Annu Rev Neurosci 10, 363-401.

Movshon, J. A., Adelson, E. H., Gizzi, M. S., and Newsome, W. T. (1985). The analysis of moving visual patterns. In Study group on pattern recognition mechanisms, C. Chagas, R. Gattass, and C.
Gross, eds. (Vatican City, Pontifica Academia Scientiarum), pp. 117-151.

Nichols, M. J., and Newsome, W. T. (2002). Middle temporal visual area microstimulation influences veridical judgments of motion direction. J Neurosci 22, 9530-9540.

Orban, G. A., Lagae, L., Verri, A., Raiguel, S., Xiao, D., Maes, H., and Torre, V. (1992). First-order analysis of optical flow in monkey brain. Proc Natl Acad Sci U S A 89, 2595-2599.

Pack, C. C., and Born, R. T. (2001). Temporal dynamics of a neural solution to the aperture problem in visual area MT of macaque brain. Nature 409, 1040-1042.

Pack, C. C., Berezovskii, V. K., and Born, R. T. (2001). Dynamic properties of neurons in cortical area MT in alert and anaesthetized macaque monkeys. Nature 414, 905-908.

Parker, A. J., and Newsome, W. T. (1998). Sense and the single neuron: probing the physiology of perception. Annu Rev Neurosci 21, 227-277.

Priebe, N. J., Churchland, M. M., and Lisberger, S. G. (2002). Constraints on the source of short-term motion adaptation in macaque area MT. I. the role of input and intrinsic mechanisms. J Neurophysiol 88, 354-369.

Priebe, N. J., and Lisberger, S. G. (2002). Constraints on the source of short-term motion adaptation in macaque area MT. II. tuning of neural circuit mechanisms. J Neurophysiol 88, 370-382.

Raiguel, S. E., Xiao, D. K., Marcar, V. L., and Orban, G. A. (1999). Response latency of macaque area MT/V5 neurons and its relationship to stimulus parameters. J Neurophysiol 82, 1944-1956.

Saito, H., Yukie, M., Tanaka, K., Hikosaka, K., Fukada, Y., and Iwai, E. (1986). Integration of direction signals of image motion in the superior temporal sulcus of the macaque monkey. J Neurosci 6, 145-157.

Sakata, H., Shibutani, H., Kawano, K., and Harrington, T. L. (1985). Neural mechanisms of space vision in the parietal association cortex of the monkey. Vision Res 25, 453-463.

Sakata, H., Shibutani, H., Ito, Y., Tsurugai, K., Mine, S., and Kusunoki, M. (1994). Functional properties of rotation-sensitive neurons in the posterior parietal association cortex of the monkey. Exp Brain Res 101, 183-202.

Salzman, C. D., Murasugi, C. M., Britten, K. H., and Newsome, W. T. (1992). Microstimulation in visual area MT: effects on direction discrimination performance. J Neurosci 12, 2331-2355.

Smith, M. A., Majaj, N. J., and Movshon, J. A. (2005). Dynamics of motion signaling by neurons in macaque area MT. Nat Neurosci 8, 220-228.

Sugita, Y., and Tanaka, K. (1991). Occlusion-related cue used for analysis of motion in the primate visual cortex. Neuroreport 2, 751-754.

Tanaka, K., Sugita, Y., Moriya, M., and Saito, H. (1993). Analysis of object motion in the ventral part of the medial superior temporal area of the macaque visual cortex. J Neurophysiol 69, 128-142.

Treue, S., and Maunsell, J. H. (1996). Attentional modulation of visual motion processing in cortical areas MT and MST. Nature 382, 539-541.

Ungerleider, L. G., and Mishkin, M. (1979). The striate projection zone in the superior temporal sulcus of Macaca mulatta: location and topographic organization. J Comp Neurol 188, 347-366.

Van Essen, D. C., Maunsell, J. H., and Bixby, J. L. (1981). The middle temporal visual area in the macaque: myeloarchitecture, connections, functional properties and topographic organization. J Comp Neurol 199, 293-326.

van Wezel, R. J., and Britten, K. H. (2002). Multiple uses of visual motion. The case for stability in sensory cortex. Neuroscience 111, 739-759.

Zeki, S. M. (1974). Functional organization of a visual area in the posterior bank of the superior temporal sulcus of the rhesus monkey. J Physiol 236, 549-573.

Chapter 2

Temporal dynamics of direction tuning in motion sensitive macaque area MT

János A. Perge, Bart G. Borghuis, Roger J.E. Bours, Martin J.M. Lankheet and Richard J.A. van Wezel

J Neurophysiol 93, 2104-2116, 2005

Abstract

We studied the temporal dynamics of motion direction sensitivity in macaque area MT using a motion reverse correlation paradigm. Stimuli consisted of a random sequence of motion steps in eight different directions. Cross-correlating the stimulus with the resulting neural activity reveals the temporal dynamics of direction selectivity. The temporal dynamics of direction selectivity at the preferred speed showed two phases along the time axis: one phase corresponding to an increase in stimulus probability for the preferred direction at short latencies, and a second phase corresponding to a decrease in stimulus probability for the preferred direction at longer latencies. The strength of this biphasic behavior varied between neurons from weak to very strong and was uniformly distributed. Strong biphasic behavior suggests optimal responses for motion steps in the anti-preferred direction followed by a motion step in the preferred direction. Correlating spikes to combinations of motion directions corroborates this distinction. The optimal combination for weakly biphasic cells consists of successive steps in the preferred direction whereas for strongly biphasic cells it is a reversal of directions. Comparing reverse correlograms to combinations of stimuli to predictions based on correlograms for individual directions revealed several non-linear effects. Correlations for successive presentations of preferred directions were smaller than predicted, which could be explained by a static non-linearity (saturation). Correlations to pairs of (nearly) opposite directions were larger than predicted. These results show that MT neurons are generally more responsive when sudden changes in motion directions occur, irrespective of the preferred direction of the neurons. The latter non-linearities cannot be explained by a simple static non-linearity at the output of the neuron, but most likely reflect network interactions.

Introduction

In visual motion analysis local motion signals have to be integrated into globally meaningful motion signals. This requires effective spatial and temporal summation of comparable motion signals, especially in a visual environment with low signal-to-noise ratio. On the other hand, the brain should also detect and process spatio-temporal differences in motion. Detection of differences in the direction or speed of motion is critically important in figure-background segregation, object localization or breaking camouflage. Because requirements for efficient integration essentially differ from those for detecting motion differences, one could expect that brain areas involved in motion processing contain motion detectors that integrate or differentiate motion signals.

In primates, the middle temporal area (area MT or V5) plays an important role in motion perception (Newsome and Paré, 1988; Salzman et al., 1992; Britten et al., 1996). Neurons in area MT respond selectively to a particular subset of directions and speeds of motion within their receptive field (Dubner and Zeki, 1971; Maunsell and Van Essen, 1983; Albright, 1984; Mikami et al., 1986). Numerous studies have established a close link between processes of integration/segregation in motion perception and the response characteristics of MT neurons (Movshon et al., 1985; Britten et al., 1992; Snowden et al., 1991; Britten and Newsome, 1998; Buracas et al, 1998; Rudolph and Pasternak, 1999; Britten and Heuer, 1999; Treue et al., 2000; Pack and Born, 2001; Heuer and Britten, 2002; Pack et al., 2004). Directional interactions underlying motion segregation and integration have been studied extensively in MT neurons. Most of these studies concerned simultaneous, spatial interactions between different parts of the receptive field and showed that MT neurons differ with respect to the degree of spatial segregation and integration. For instance, for a subset of MT neurons the response to the preferred direction in the receptive field center is suppressed by the same direction in the surrounding area (Allman et al., 1985; Born and Tootell, 1992; Raiguel et al., 1995; Xiao et al., 1995; Born, 2000). This phenomenon, often referred to as center-surround antagonism, makes neurons with strong antagonistic surrounds excellent candidates for playing an important role in spatial segregation of differently moving objects. Other MT neurons either lack surrounds or have reinforcing surrounds and integrate motion over large areas of the visual field to encode information about global motion. Other studies showed different degrees of motion integration, for stimuli presented at different positions within the receptive field center (Movshon et al., 1985; Rodman and Albright, 1989; Pack and Born, 2001). These studies reveal that when MT neurons are stimulated by plaids containing multiple motion components, some neurons respond to the

separate components while others, the so-called “pattern neurons”, respond to the global pattern.

Center-surround antagonism and component/pattern selectivity indicate how the spatial receptive field organization of MT neurons contributes to the integration or segregation of simultaneous motion cues. On the other hand, the temporal aspects of motion integration and segregation in area MT have received less attention. Recent work by Priebe et al. (2002a,b) showed that MT neurons demonstrate different degrees of short-term motion adaptation, which would make them differentially sensitive to temporal motion contrast. They also showed specific temporal interactions between stimuli in the preferred and in the antipreferred direction. When two motion directions are presented consecutively, the response to the second stimulus is suppressed if the preceding stimulus moves in the preferred direction, and either enhanced or suppressed if the preceding stimulus moves in the antipreferred direction.

One problem with addressing the topic of temporal motion integration and segregation is that it has been difficult to isolate the response to single motion steps, which form the basic signals on which segregation and integration processes act. Whenever multiple motion steps in the same direction are used, the basic response to individual stimuli is confounded by effects of temporal integration and/or associated adaptation. Recently we introduced a motion reverse correlation paradigm, which allows us to study the basic response of MT neurons to individual stimuli (Borghuis et al., 2003). In this paradigm stimuli consisted of a sequence of motion steps in random directions. Reverse correlation of spike occurrences and motion steps reveals the time course of relative responses to single motion steps in different directions. The method also offers the possibility to analyze responses to consecutive steps, and study directional interactions in time.

The purpose of the present paper was to study the temporal, rather than the spatial aspects of motion integration and segregation in area MT using the motion reverse correlation method. We are focusing on two questions. First, to what extent do MT neurons differ in their time course of responses to single motion steps at their preferred speed? Second, what is the effect of consecutive motion steps in different motion directions? We find different types of responses to single motion steps, showing different degrees of temporal integration and segregation. Responses to consecutive motion steps show that the increased sensitivity of MT neurons to opposite directions is not limited to the antipreferred/preferred combination, but increased sensitivity can also be found for other near opponent combinations of directions. These special non-linear effects may be due to specific network interactions. Because interactions are quantified at high temporal resolution

(in the order of milliseconds), they provide important clues to the structure of the underlying network of motion detectors.

Materials and Methods

Two adult male rhesus macaques (Macaca Mulatta) participated in this study. Before the experiments, each monkey was implanted surgically with a head holding device, a search coil for measuring eye movements using the double induction technique (Reulen and Bakker 1982, Malpeli, 1998), and a stainless steel recording cylinder placed over a craniotomy above the left occipital lobe. The surgical procedures were performed under N_2O/O_2 anaesthesia supplemented with isoflurane. After recovery the monkeys were trained to fixate a rectangular spot (0.4x0.4 deg) on a black background. During the experiments each monkey sat in a primate chair 57 cm from a cathode-ray tube display. Eye movement recordings were sampled at 500 Hz. For accurate fixation the monkeys had to maintain their viewing direction within a virtual fixation window around the fixation point (2° diameter). While correctly fixating, the monkey was rewarded with water or juice every three seconds. Breaking fixation resulted in pausing the presentation of stimuli and a lack of reward. Stimulus presentations were restarted after 300 ms of correct fixation. Animal procedures used in this study were approved by the Animal Use Committee (DEC) of the Utrecht University and procedures were according to national and international guidelines.

Neuronal recordings

During experimental sessions a parylene insulated Tungsten microelectrode (0.5-2 MΩ at 1 kHz) was inserted manually through a guide tube and then manipulated by a micro-positioning controller. Area MT was identified by the recording position and depth, the transition between grey matter, white matter and sulci along the electrode track, and by its functional properties. These are, among others, the prevalence of direction selective units, the similarity in direction tuning for nearby single unit recordings, the receptive field size according to eccentricity and the change of direction tuning along the electrode penetration. We have no histological confirmation of the recording sites because both monkeys are currently being used in other experiments. Single unit recordings were carried out by using standard extracellular methods. Spike times were registered with 0.5 ms resolution for on-line analysis and data storage, using a Macintosh G4 computer with National Instruments PCI 1200 data acquisition board.

Stimuli and experimental procedure

The monitor (Sony Trinitron Multiscan 500 PS) was driven by an ATI Rage graphics card. The refresh rate was 75 Hz (1152x870 pixels) for early experiments in monkey A (42% of 114 cells recorded in monkey A), and 120 Hz (1024x768 pixels) in the other experiments. The stimulus was a high density binary random dot pattern in a rectangular field (14x14 deg), consisting of 50% black and 50% white dots and surrounded by a black background (Julesz, 1971). Mean luminance of the stimulus was 48 cd/m^2. A dot size of 0.14x0.14 deg was used for 42% of the cells in monkey A, and 0.20x0.20 deg for all of the remaining cells.

The dot pattern was positioned over the receptive field center as determined by hand mapping. The dot pattern was shifted each monitor frame (8.3 ms at 120 Hz and 13.3 ms at 75 Hz) or every second monitor frame (17 ms at 120 Hz and 27 ms at 75 Hz). The size of the shift ranged between 0.07-0.42 degrees (in steps of 0.07 degrees) optimized for each cell to elicit the most activity. The shifts occurred in any of 8 directions (from 0 deg to 315 deg, in steps of 45 deg, where 0 deg corresponds to rightward motion and 90 deg to upward motion) in a pseudo-random order. Each motion step was presented 700-1400 times, in a randomized order. A movie demonstration of the direction tuning stimulus can be also viewed at our website (http://www-vf.bio.uu.nl/lab/NE/publications/JP/methods.html). Stimulus generation, data collection and monitoring of the monkeys' performance was done by custom made software written in programming language C. Offline data analysis was done in MATLAB.

Data analysis

Stimulus generation and data analysis was performed using the motion reverse correlation method previously described elsewhere (Borghuis et al. 2003). Note that our stimulus is different from luminance contrast reverse correlation methods (e.g. DeValois et al., 2000; Livingstone et al., 2001; Cook and Maunsell, 2004), in which motion selectivity is computed from a second-order analysis of the response to dynamically positioned stationary dots (or bars) at different locations in the receptive field. Since we use full field motion steps, in our method the stimulus is much more effective in eliciting spikes, which facilitates a detailed analysis of the response to consecutive motion steps. In our method reverse correlograms were computed for each motion direction by reverse correlating the occurrence of motion steps with the spike train. Reverse correlograms for each direction were converted to relative probabilities by dividing the number of stimulus occurrences at each pre-spike time by the total number of stimuli at that time. Values for each stimulus, normalized in this way, range from 0 to 1, where 0 indicates zero relative probability for a given stimulus to occur at

that time before a spike and a value of 1 indicates perfect correspondence (each spike preceded by a given stimulus at the specified time before a spike).

The value of equal probability (the baseline of the reverse correlograms) corresponds to a level of 1/n, where n is the number of stimuli in the set. In our experiments 8 different directions resulted in an equal probability level of 0.125. Note that the equal probability level is not identical to spontaneous activity. This value indicates that the effect of a particular stimulus is similar to the mean effect across the whole set of stimuli.

Our results would be identical whether correlating the stimuli to the spikes (reverse correlation) or the spikes to the stimuli (forward correlation). However, the main reason to use reverse correlation in this paper is that our stimulus consists of motion impulses with very short intervals (8-24 msec). Therefore, the correlogram is not only the average effect of one specific stimulus, but also the average effect of the preceding and following stimuli that are used. If we presented our data in conventional stimulus-response histograms, one could get the false impression that the responses are only the result of one particular stimulus.

The reverse correlograms obtained for the individual directions are not independent. Since we use a limited set of motion directions we only obtain information on relative probability levels. An increased probability for one direction inevitably leads to a decreased probability level for the other directions. As a result, we cannot differentiate between excitatory effect for one stimulus direction and simultaneous inhibitory effect for another one. Moreover, the choice of stimuli might affect reverse correlograms obtained for a specific response. However, for direction experiments, as we report in this paper, the tuning properties were found not to depend on the number of directions, as long as they were properly balanced. Borghuis et al. (2003) analyzed the effect of the number of directions in a single experiment on direction tuning. They found that, although the absolute probability values changed, there were no significant differences between tuning curves obtained with 4, 8 and 16 directions, except for the obvious increase in sampling resolution.

In most cases one is not primarily interested in the raw correlation values, but rather the statistical significance of those correlations. The noise level of the correlograms may fluctuate with the mean firing rate and with the total length of a measurement. Noise levels therefore differ between cells and between measurements. We estimated the noise level in each recording by analyzing a time period of 100 ms following spikes. Because stimuli

occurring after a spike cannot have any effect on its occurrence, deviations from chance level in this part of the correlogram are by definition uncorrelated and reflect the noise in the correlogram. The noise level was quantified by the standard deviation relative to the equal probability level, for all stimuli together. We used an arbitrary level of 3 standard deviations for defining significant excursions in the reverse correlograms. The chance that reverse correlograms surpassed this level spontaneously was very small.

The reverse correlogram with the highest probability value corresponds to the preferred direction while the stimulus direction 180 degrees away from the preferred direction is defined as antipreferred direction. In nearly all of the cases antipreferred reverse correlograms also had the lowest probability values. As shown in an earlier publication (Borghuis, 2003) the preferred direction determined with this reverse correlation technique is in accordance with preferred direction measured with hand-mapping techniques or conventional stimuli (moving random dot patterns and gratings).

The large number of stimulus repetitions also allows us to study temporal interactions between stimuli. To this end, we computed the correlation between spikes and combinations of successive motion directions. This analysis can reveal interactions between a specific combination of motion directions, as well as the time course of such interactions. This second-order reverse correlation is similar to the first-order correlation described above, except that each direction is subdivided in 8 subclasses, one for each motion direction preceding the stimulus. Second-order reverse correlation thus results in 64 correlograms describing direction combination occurrences as a function of pre-spike time. In our second-order analysis the first and second stimuli occurred successively. However, it is also possible to obtain correlograms for motion steps that are separated by one or several others. As a convention we used the occurrence of the last motion step in the sequence as time zero in the correlogram.

First-order and second-order reverse correlograms were smoothed by sliding window averaging with a Gaussian profile. We used a standard deviation of 8 ms that was found to remove most of the noise without affecting the overall shape of the function and its main parameters.

To link the temporal profile of reverse correlograms to the temporal profile of responses to long duration stimulation we performed an additional measurement. After measuring the direction tuning curves of 31 neurons with the reverse correlation technique we also recorded the responses to continuously moving random dot patterns. The dot patterns were presented in the preferred direction for the duration of 1 second and were repeated ten times. Other parameters of the stimulus such as speed, dot size and pattern size were identical to the motion reverse correlation stimulus. Post Stimulus Time Histograms (PSTHs) with a bin-width of 10 ms were computed and the time course of the histograms was further analysed (see Results).

Results

Motion direction tuning curves were measured with the reverse correlation technique at the preferred step size of MT neurons (see methods) of two male rhesus macaque monkeys for a total of 169 neurons (114 neurons in monkey A, and 55 in monkey S). First we will describe the temporal dynamics of direction tuning in MT neurons, based on individual motion steps. Next, we will analyze the effect of specific combinations of motion directions, and finally we will show how these results differ from the predictions based on tuning to individual steps.

Temporal dynamics of direction tuning

Reverse correlograms for the 8 motion directions are shown for two typical example cells in Fig. 1A and 1B. Direction tuning curves can be obtained at each point in time, based on the correlograms for the 8 different directions. Three examples of these polar direction tuning plots, at different pre-spike times are shown as insets in Fig. 1A and B. The complete temporal profile of direction tuning for these two neurons is shown in a polar plot movie at our website (http : // www-vf. bio.uu.nl /lab /NE /publications /JP / results. html).

Another way to present the time course of direction tuning is to calculate directional vector sums based on the 8 reverse correlograms at each moment in time. For this calculation the length of the vectors is the probability value of the vector sum of the eight correlograms. The direction of the vector sum is upwards for a vector sum in the preferred direction and downwards for the null direction. Figures 1C and 1D show the vector sum representation for each point in time for the example cells in Figs 1A and 1B, respectively. Vector sums calculated in this way provide a good summary of preferred direction and strength of directional selectivity (vector length) as a function of time.

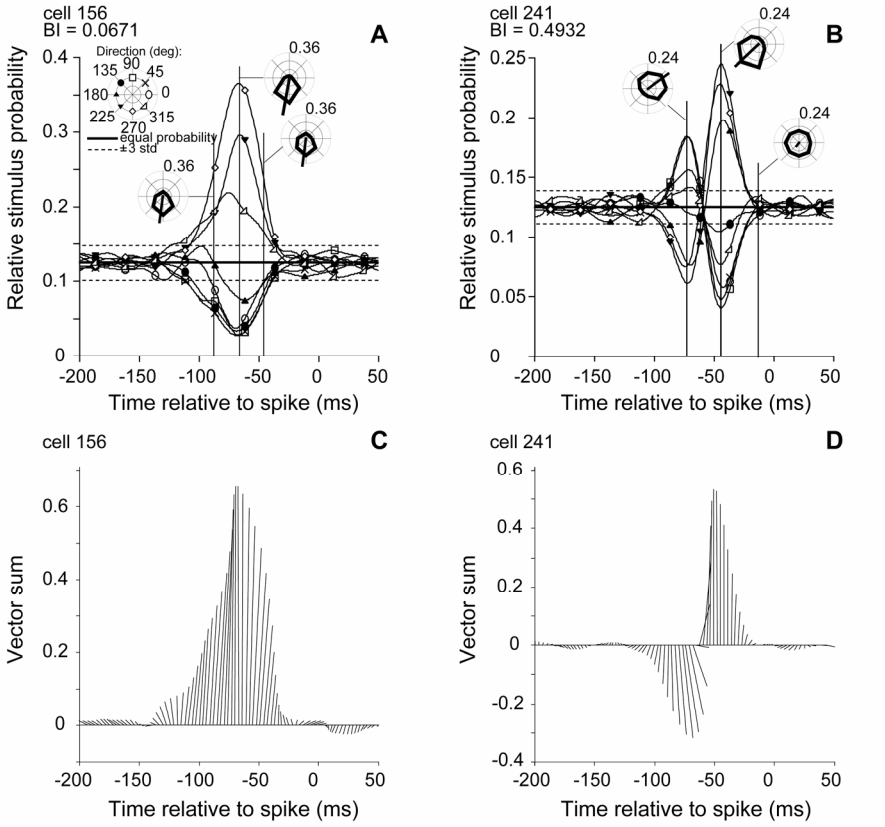

Fig. 1. Time course of direction tuning in MT neurons reveals different response behaviors. (**A**) Neuron without biphasic behavior. (**B**) Neuron with strong biphasic behavior. The 8 reverse correlogram curves represent the relative probability of each stimulus direction before the action potentials. Symbols indicate the motion direction (see insert). Time zero represents the spike occurrences. The solid horizontal line indicates equal probability. Two horizontal dashed lines indicate three standard deviations above or below the equal probability. Three polar plots indicating relative probabilities for certain directions are inserted at three time stamps. The origin of the polar plots is a probability of 0 and the maximum value is indicated on top of the polar plot. The vector sum of these probabilities is indicated by a thick oriented line in the polar plot. A polar plot movie showing the complete temporal progress of the direction tuning can be viewed at our website (http://www- vf. bio. uu. nl /lab /NE /publications /JP/results.html). Directional vector sums of the 8 reverse correlograms show the average stimulus as a function of time before the spikes. (**C**) Directional vector sums of a neuron without biphasic behavior (same neuron as A). (**D**) Directional vector sums of a neuron with strong biphasic behavior (same neuron as B). Longer vectors indicate stronger direction tuning. The direction of the vector sums are up for the preferred direction and down for the antipreferred direction.

The two example cells in Fig. 1 demonstrate the variability in the shape of the reverse correlograms among the recorded MT neurons. The example in Fig. 1A shows for each direction only a single phase, which is either

positive or negative, whereas the example in Fig. 1B reveals two distinct temporal phases, one at short latency and another one with reversed polarity at a longer latency. We will refer to this temporal characteristic as *biphasic behavior*. To characterize the level of biphasic behavior over the whole population we computed for each cell a biphasic index:

$$\text{Biphasic Index} = \frac{\text{maximum excursion of the antipreferred reverse correlogram from the equal probability level}}{\text{maximum excursion of the preferred reverse correlogram from the equal probability level}} \quad (1)$$

The biphasic index thus expresses the ratio between the maximum excitatory effect of preferred and antipreferred stimuli. Those two maxima are at different points in time (see Fig. 1B). A low biphasic index value corresponds to lack of biphasic behavior (Fig. 1A) and a high value to strong biphasic behavior (Fig. 1B). Figure 2 shows the distribution of biphasic index values across the population of recorded MT neurons. The mean biphasic index for all of the cells was 0.19 ± 0.14 (n=169). As Fig. 2 shows, the distribution of biphasic behavior for the population forms a unimodal distribution.

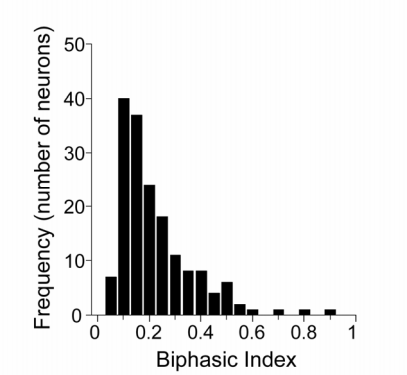

Fig. 2. The degree of biphasic behavior varies in the population. Frequency distribution of the biphasic index over the population (see Formula 1. in the Results section). A biphasic index of 0 means complete lack of biphasic behavior. Two outliers are not shown in this graph. The average biphasic index was 0.19 ± 0.14 (n = 169).

The example cell in Fig. 1B shows a reversal of optimal direction. At a latency of about 45 ms the correlogram shows its maximum, corresponding to the cell's preferred direction. At a latency of about 70 ms, however, the directional preference is changed by about 180 degrees. To characterize the directional change for the strongly biphasic neurons we calculated the difference in vector direction between the two phases. For this analysis we chose 25% of the neurons with the highest biphasic index (n=42). Fig 3A shows the distribution of direction differences between the two peaks in the biphasic profiles (measured in the clockwise direction). On average the change in direction was 170 ± 25 deg. Most cells show a directional difference of about 180 deg, i.e., a direction reversal.

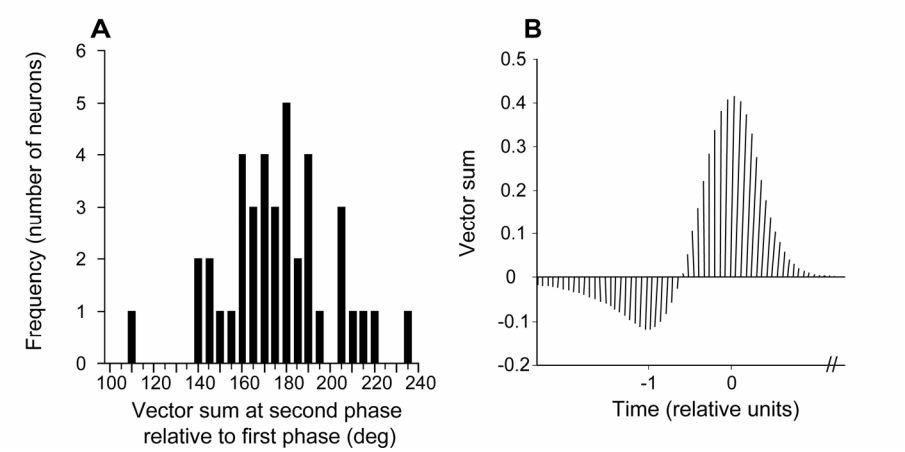

Fig. 3. The temporal change in direction tuning of the strongly biphasic neurons (25% of the neurons with the highest biphasic index). (**A**) Distribution of angular differences between directional vector sums at the first and second phase. The average difference was 170 ± 25 deg. Three outliers are not shown in this plot. (**B**) Directional vector sums as a function of time averaged over the strongly biphasic neurons. Vector direction and length indicate the average stimulus direction and tuning strength in Cartesian coordinates. Longer vectors indicate stronger direction tuning. Directions up and down represent the preferred and antipreferred directions respectively. Time zero and minus one represent the peak latency of the first and the second phase respectively.

To further characterize the time course of directional changes, we summarized the change in time for 25% of the neurons with the highest biphasic index. This analysis allows us to find out whether changes in the direction tuning take place through gradual rotations, or by 180 deg direction reversals. Gradual changes would indicate contributions from multiple directions with different temporal dynamics, whereas direction reversals indicate a change in balance between preferred and antipreferred direction in time. To distinguish between these two possibilities we averaged the directional vector sums of the strongly biphasic neurons. Directional vector sums along the entire time-window were expressed as absolute deviations from the preferred direction (the preferred direction was defined as the vector sum at the peak latency of the phase with the shortest latency). Averaging absolute deviations from the preferred direction avoids possible cancellation of rotations in opposite directions, for different neurons. We also normalized the time scale of each recording to the time difference between the two phases in the correlogram. In this way individual differences in the dynamics of directional changes did not affect the average vector sum. Figure 3B shows the resulting, time-normalized, average vector sum. The average vector sum did not show any sign of gradual rotation, but rather a distinct, abrupt shift from antipreferred to preferred direction. The balance between preferred and antipreferred directions changes in time, but

there is no change in contribution from directional components different from the preferred/antipreferred axis.

The temporal dynamics of the correlograms for different directions were very similar. The differences in peak latencies of the first phase (i.e. the largest excursion of the correlogram from the equal probability level) between the preferred direction and other directions were on average 1 ± 10 ms. There was no statistically significant difference between the peak latencies of the different directions in the population (one-way ANOVA, $F = 0.7$, $p = 0.67$). In 25% of the neurons with the highest biphasic index (n=42) the average difference in peak latency of the second phase was -1 ± 9 ms, with no statistically significant difference (one-way ANOVA, $F= 0.33$, $p= 0.93$).

We analyzed in more detail the relationship between the biphasic index and the shape of the reverse correlogram and other response properties (as summarized in Table 1). The table shows a summary of statistics for several temporal parameters for the whole population, for the 42 (25%) most weakly biphasic cells and for the 42 most clearly biphasic cells. The last column shows the correlation coefficient with the biphasic index. Significant correlations are marked by single ($p<0.05$) or double ($p<0.01$) asterisks.

As is shown in Table 1 the average peak response latency (PL) of the preferred direction for all neurons was 58 ± 10 ms, which is similar to response latencies reported previously based on pseudorandom temporal sequences of preferred and antipreferred stimuli (Bair et al., 2002). Peak latencies did not vary systematically with the biphasic index value in either group. The total width of the profile was on average 54 ms for weakly biphasic cells (W1) and 62 ms for strongly biphasic cells (W3). Even though the example neurons shown in figure 1A and 1B show similar temporal extent, in general the strongly biphasic profile covers a longer time period than the weakly biphasic one. Direction reversals thus require additional time, but are initiated early on. We checked for several parameters, such as FSS, Δt, W1, W2 and W3 (for explanation of these terms see Table 1) whether they varied systematically with the value of the biphasic index. The only parameter that clearly varied with the biphasic index across the total population was the duration of the main peak in the reverse correlogram (W1), defined as the time difference between first and last 'significant' positive excursion for the preferred direction. This duration decreased significantly with increasing levels of the biphasic index, for the total population and for the weakly biphasic group. For strongly biphasic cells however no such dependency was found. The conclusion one can draw from these results is that the temporal dynamics of the short latency response

(W1) changes due to the long latency response of cells with biphasic behavior. In the analysis described above the reverse correlograms were smoothed with a Gaussian sliding window average with a standard deviation of 8 ms. Using a running window average with a smaller standard deviation (4 ms) gives similar results, except that W1 is not significantly correlated to the biphasic index for the weakly biphasic group (r = -0.05).

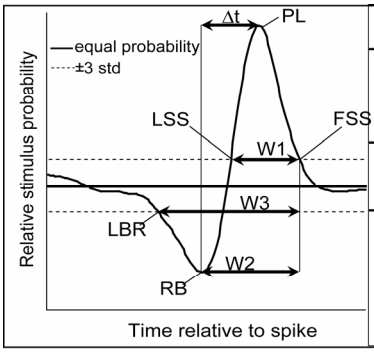

		Mean + SD (ms)	r
Total population (n = 169)	FSS	34 ± 9	0.10
	PL	58 ± 10	-0.13
	W1	47 ± 14	-0.26**
	Spike counts	1715± 1501	-0.01
Monophasic (n = 42)	FSS	35 ± 11	-0.07
	PL	60 ± 12	-0.12
	W1	54 ± 14	-0.33*
Biphasic (n = 42)	FSS	35 ± 8	0.17
	PL	56 ± 8	0.05
	Δt	38 ± 20	-0.06
	W1	40 ± 8	-0.27
	W2	59 ± 22	-0.10
	W3	62 ± 42	-0.06

Table 1. Quantitative analysis of the temporal response profile. Definitions of parameters are explained in the schematic diagram next to the table. A weakly and strongly biphasic group was selected by taking 25% (n=42) of the whole population of neurons with the lowest and 25% with the highest biphasic index respectively. All parameters are calculated for the preferred direction only. The peak latency (PL) and the rebound (RB) were at the latency of the highest and lowest probability values respectively. The first and last significant responses (FSS and LSS respectively) were obtained by starting at PL and stepping back and forth along the time axis until the first and last points were reached where the probability values were still higher than the equal probability level plus three standard deviations. The standard deviation of the noise was calculated for each neuron separately for a 100 ms section of the reverse correlograms after the spike occurrences for all eight directions. The last biphasic response (LBR) was the last significantly low value (where the correlogram was still less than equal probability minus 3 standard deviations). FSS, PL and LSS were computed for all of the cells, and the remaining parameters were computed only for the strongly biphasic neurons. Using these 5 parameters four duration values (W1, W2, W3, and Δt) were calculated as indicated in the schematic diagram. The value 'r' indicates the correlation coefficient between biphasic index and the different parameters. The asterisks indicate significance levels of $p<0.05$ (*) and $p<0.01$(**) respectively. No asterisk indicates a significance level of $p>0.05$.

Biphasic temporal profile and short-term adaptation

Neurons in area MT respond to continuously moving stimuli with a transient-sustained firing pattern. This phenomenon, called short-term adaptation is characterized by a vigorous response to the initial part of the stimulus settling rapidly to a lower firing rate (Priebe and Lisberger, 2002a,b).

To study the relation between biphasic response and short-term adaptation, we recorded the responses of 31 neurons to continuously moving random dot patterns in the preferred direction. To describe the short-term adaptation strength of the resulting histograms we fit the transition from

transient to sustained firing rate with single exponentials similarly as it was described by Priebe and Lisberger (2002a) according to the form

$$R(t) = f_{sus} + (f_{trans} - f_{sus})\, e^{-t/k} \qquad (2)$$

where f_{sus} is the firing rate during the sustained part of the response, f_{trans} is the initial transient level of the response, and k is the time constant of the exponential.

Using the parameters from the fits, short-term adaptation strength was defined as the ratio of transient/sustained response level (TSR) as

$$\mathrm{TSR} = f_{trans} / f_{sus} \qquad (3)$$

Figure 4 shows the transient/sustained ratio of these 31 neurons plotted against their biphasic indices. The figure shows no correlation between the biphasic behavior and adaptation strength (the *r*-value of the linear fit was 0.23, $p>0.05$). This indicates that biphasic responses are probably not due to the same short-term adaptation mechanism that determines the degree of transience in MT cell responses.

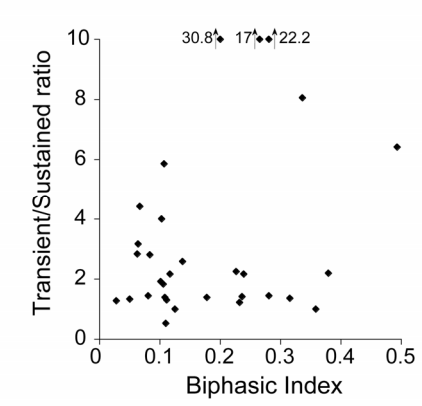

Fig. 4. Biphasic behavior is not correlated with short-term adaptation. Neurons (n = 31) were recorded both with a motion reverse correlation paradigm and a continuously moving random dot display. The continuously moving stimuli were presented in the preferred direction for the duration of 1 second and were repeated ten times. Other parameters of the long duration stimuli were identical with the motion reverse correlation stimulus. Transient/sustained ratio indicates the strength of adaptation to a continuously moving pattern (see text). Each symbol indicates one neuron. The *r*-value of the linear fit was 0.23 ($p>0.05$). 3 extreme outliers are plotted at the top of the figure. Their corresponding transient/sustained ratios are indicated next to the arrows.

Second-order analysis of successive motion directions

In the previous section we showed that a substantial proportion of MT neurons has a biphasic temporal direction tuning profile, which is associated with a reversal of direction preference. In nearly all cells the preferred direction corresponded to the peak in the short latency phase, and the antipreferred direction to the peak in the second phase (at a longer latency).

This finding suggests that the optimal stimulus for a neuron with biphasic characteristics is a change of stimulus direction, from antipreferred to preferred direction. From the results presented so far it is not clear whether biphasic behavior is an inherent property of the cell's response to a single step, or results from specific combinations of stimuli, e.g. a step in the antipreferred direction followed by the preferred direction.

To investigate the contribution of specific combinations of motion directions on the correlograms we performed a second-order analysis on the data. While the first-order analysis as described in the previous paragraphs examines the effect of a single direction on the cell response, second-order reverse correlograms represent the probability of a particular stimulus-combination preceding the spikes. The two stimuli can be consecutive, or separated in time by one or more stimuli. Unless stated otherwise we based the second-order analysis on consecutive stimuli.

The response probabilities over time of 64 (8^2) possible combinations of motion directions are shown in Fig. 5. For the explanation of the figure it is important to note several things. First, a spike is correlated to the occurrence of the *second* presented motion step in the combination. The white spot from about 40-70 ms in the middle vertical panel of Fig. 5A (indicated by the white arrow) is due to the response to the preferred direction, when it was the second stimulus in the combination. The effect of the first stimulus arrives earlier than the second stimulus. Since the first stimulus is coupled to the second one, the effect will appear in the correlograms before the second stimulus. The parallel white stripes in each panel from 20-40 ms correspond to the response to the preferred direction when it was the *first* stimulus in the stimulus pair. Latency differences between the first response (~30 ms) and the second response (~60 ms) are directly related to the motion step delay (in this case 27 ms, two frames at a monitor refresh rate of 75 Hz). The second-order reverse correlogram of the neuron with low biphasic index in Fig. 5A shows that probability levels are highest for the preferred/preferred combination. Probabilities decrease as the first stimulus deviates from the preferred direction. This reflects that combinations of successive steps in the preferred direction have the highest probability of evoking spikes. We find similar probability patterns for the group of cells with a low biphasic index.

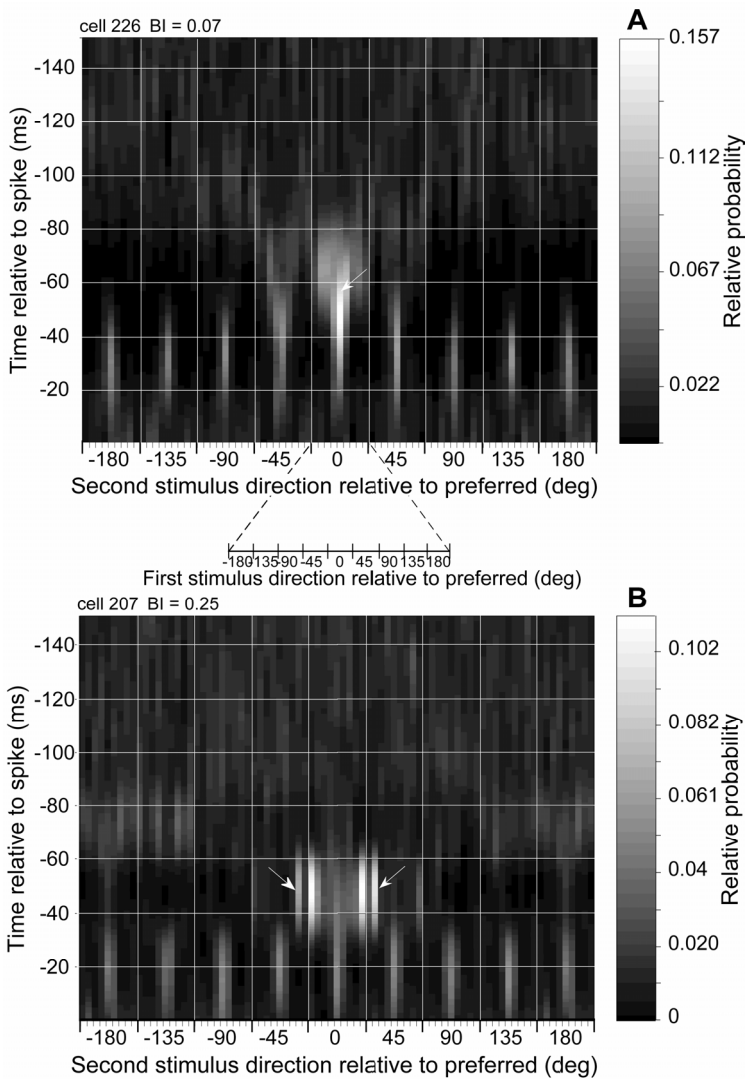

Fig. 5. The effect of stimulus combinations on the response. Second-order reverse correlograms show 64 possible combinations of two stimulus directions. (**A**) An example neuron with a low biphasic index (BI=0.07). (**B**) An example neuron with a high biphasic index (BI=0.25). Each panel in these figures comprises 9 columns representing the relative direction of the second stimulus of a sequence. Nested within each of these columns are 9 smaller columns representing the relative direction of the first stimulus in a pair of motion directions. Directions are relative to the preferred direction; +180 deg and -180 deg stimuli are identical. Dark shading indicates low probability, white spots indicate high probabilities. Spikes are correlated to the second element of the stimulus combination. The correlograms were smoothed with a Gaussian profile (s.d. 8 ms). The white arrow in Fig. 5A indicates a high probability for a preferred/preferred (0/0 deg) stimulus combination. White arrows in Fig. 5B indicate high probability for +135/-45 deg, +180/0 deg and -135/+45 deg stimulus combinations.

Figure 5B shows the second-order reverse correlograms for an example cell with a high biphasic index. In contrast to the previous example in Fig. 5A, this neuron has the highest probability for an antipreferred/preferred stimulus combination. Other high probabilities occur in this cell for the +135/-45 and the -135/+45 combinations, as indicated by the white arrows in Fig. 5B. Generally, neurons with a high biphasic index showed probability patterns with a preference to the antipreferred/preferred directional change. This is exactly what was already suggested by the first-order plot in Fig. 1B, e.g., these neurons respond most optimally to a directional reversal from antipreferred to preferred. Figure 5B also shows that these effects are highly directionally specific. If the second stimulus in the combination deviates plus or minus 45 deg from the preferred direction, the most optimal direction preceding it is not the antipreferred direction, but rather a direction differing by 180 deg.

The second-order analysis for the cell in Fig. 5B was performed for two consecutive motion steps with a temporal interval of 27 ms, which is almost equal to Δt (29 ms) as described in the first-order analysis (Table 1). However, for a substantial number of neurons Δt is in the order of two or more motion step durations. For these neurons second-order reverse correlograms show increased activity for stimulus combinations separated by time intervals longer than one motion step duration. For successive combinations of stimuli these neurons behaved much like the monophasic neurons showing a preference to preferred/preferred combination. Results for combinations of motion steps thus seem to agree qualitatively to what one would predict from combining the profiles for the separate stimuli. In the next section we investigate whether profiles for individual motion steps predict profiles for motion step combinations quantitatively.

Non-linear interactions between successive motion directions

To quantitatively test predictions for second-order correlograms (combinations of motion steps) from first-order profiles (individual motion steps), we multiplied two first-order reverse correlograms and compared the result to the second-order reverse correlograms. Because reverse correlograms reflect probabilities, multiplying two individual correlograms predicts the probability for their combination to occur. (Note, that this is similar to summing the responses when responses would be expressed as firing rates). Since the first stimulus occurs earlier, its reverse correlogram was shifted in time by the duration of one motion step. Differences between measured and predicted second-order profiles indicate direction-specific temporal interactions in the response of MT neurons. Predicted and measured responses for all possible combinations of directions were compared.

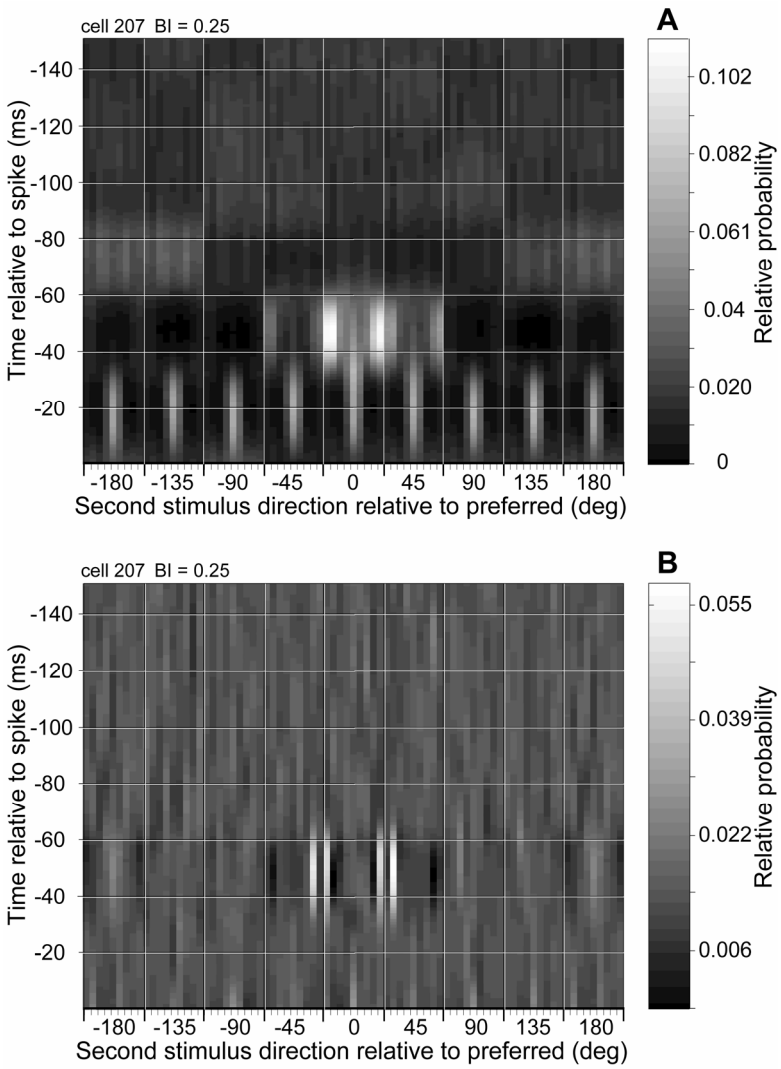

Fig. 6. Linear analysis of the second-order reverse correlation. (A) Predicted second-order reverse correlograms based on individual first-order correlograms. Predictions were obtained by multiplying two first-order correlograms (B) Prediction errors of the second-order reverse correlograms for the example cell shown in Fig. 5B and 6A. The prediction errors show the difference between measured correlograms (Fig. 5B) and linear predictions (Fig. 6A). Conventions are similar to Fig. 5A and B. Positive errors (light) represent stimulus probabilities that are underestimated (prediction is lower than observed), while negative errors (dark) represent probabilities that are overestimated (prediction is higher than the observed response).

Fig 6A shows the predicted second-order reverse correlograms for the same cell whose measured second-order reverse correlogram is shown in Fig 5B. The predicted correlograms are less noisy due to the fact that first-order reverse correlograms are based on a larger number of stimulus occurrences than second-order correlograms (a factor of 8). The fact that correlograms for specific combinations of directions are well described by predictions based on the individual directions shows that the typical biphasic behavior does not result from specific stimulus combinations.

To visualise the differences between the two figures we subtracted the predicted second-order reverse correlograms from the measured second-order reverse correlograms (Fig. 5B - Fig. 6A = Fig. 6B). The remaining prediction errors reveal non-linear interactions between specific motion directions. White spots in Fig. 6B show combinations for which the actual correlation was higher than that predicted from the individual directions. This example cell shows responses that are larger than predicted (white colour) for stimulus combinations of antipreferred/preferred, 135 deg/-45 deg, and -135 deg/45 deg and decreased responses (black colour) for -135/-45, -135/0, 135/0 and 135/45 deg.

To explore the relationship between the biphasic response profile and the level of non-linearity we plotted the biphasic index of each neuron against the prediction errors for antipreferred/preferred and preferred/preferred stimulus combinations. On average, the largest prediction errors were found 6 ms before the peak latency. For this reason we calculated the average prediction error at an 11 ms period around this most informative part centred around 6 ms prior to peak latency. The average prediction error of this 11 ms long period for antipreferred/preferred and preferred/preferred stimulus combinations is shown in Fig. 7.

Neither antipreferred/preferred prediction errors nor preferred/preferred prediction errors showed significant correlation with the biphasic index (*r*-values were 0.08 and 0.01 respectively, $p>0.05$ for both cases). If specific directional interactions contributed significantly to the biphasic temporal response profile, we would expect a relationship between the biphasic index and the level of non-linearity. The most important conclusion from this analysis is that biphasic behavior does not result from specific sequences of stimuli. Therefore it is probably an inherent property of the cell's response to a single motion step. The prediction errors for antipreferred/preferred combinations were on average positive (0.03 ± 0.08) indicating larger responses, while the mean prediction error for preferred/preferred stimulus combination was negative (-0.08 ± 0.1) indicating lower responses as expected from linear summation. Furthermore, prediction errors for

antipreferred/preferred combination were significantly higher than those for preferred/preferred combinations (paired t-test, $p<0.01$).

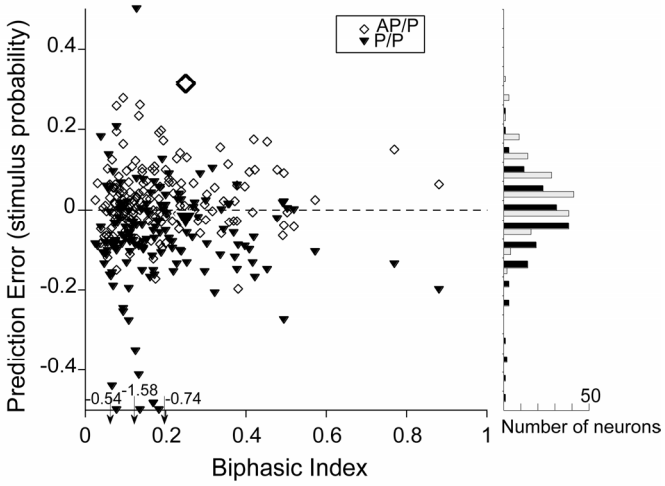

Fig. 7. Biphasic behavior is not due to specific, non-linear interactions between successive stimuli. Relationship between the biphasic index and the level of non-linearity for antipreferred/preferred (AP/P) and preferred/preferred (P/P) combination (see text). Each neuron contributes to two symbols in this figure. The enlarged triangle and diamond indicate example cell 207 (same as Fig. 5B and Fig. 6). 3 extreme outliers are plotted at the bottom of the figure. Their corresponding prediction error values are indicated next to the arrows. The *r*-value of a linear fit for antipreferred/preferred and for preferred/preferred combination was 0.08 and 0.01 respectively ($p>0.05$ for both cases).

Similarly as we calculated the mean prediction error for antipreferred/preferred and preferred/preferred combinations we calculated the mean prediction error for all combinations of directions. These averages summarize non-linear interactions between successive stimuli over the entire population (Fig. 8A). On average, the largest negative prediction error occurred for the preferred/preferred combination (black colour). This indicates that for this combination the prediction is higher than the measured response. Positive prediction errors were observed for 180, 135 and 90 deg directional changes (dark colour) irrespective of the preferred direction. The average prediction error was 14% for the preferred/preferred second-order reverse correlogram and 10% for the antipreferred/preferred second-order reverse correlogram. In general, neurons had similar interaction patterns except that the strongly biphasic neurons showed somewhat larger prediction errors. The prediction error for preferred/preferred combination was 11% in the weakly biphasic group and 20% in the strongly biphasic group. For the

antipreferred/preferred combination it was 6% in the weakly biphasic group and 14% in the strongly biphasic group.

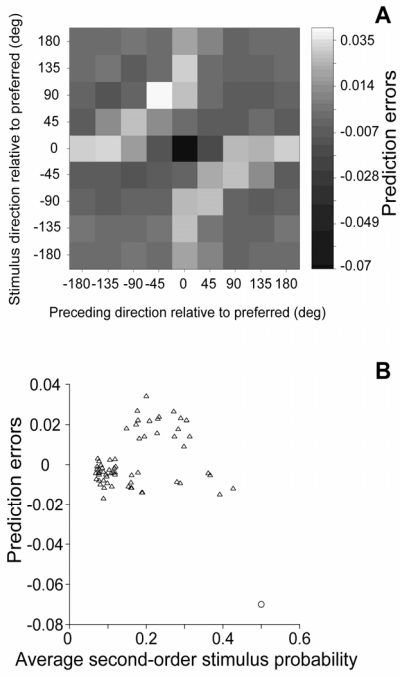

Fig. 8. Prediction errors for different combinations of stimulus directions. For each combination of two consecutive directions the prediction errors were averaged over the whole population. The average prediction error of an 11 ms long section (centered at 6 ms prior to response latency) is shown. (**A**) Negative interactions occur for preferred/preferred stimulus combination and positive interactions between near opposing stimuli (180, 135 and 90 degrees change). Shading indicates negative interactions (response probability is lower than the linear prediction) and light colors indicate positive interactions (response probability is higher than linear prediction). The color scale of the figure is logarithmic to visualize the positive interactions between stimulus combinations with angular differences of near 180 deg. The same data is represented in a linear way in panel B. (**B**) Prediction errors as shown in Fig. 8A plotted as a function of the average second-order stimulus probability level at the same time segment of the correlograms. Each symbol represents a combination of two consecutive motion directions. The open circle represents the preferred/preferred combination.

The prediction error for the preferred/preferred combination can be explained by a simple static non-linearity at the output of the neuron. If a preferred stimulus follows a preferred stimulus, the neuron responds less than the sum of the two responses due to saturation. However, for opposite motion directions the responses are higher than predicted, which cannot be explained by a static non-linearity at the output of the neuron. In Fig. 8B the average prediction error for the cell population is plotted against the average second-order stimulus probabilities. This plot shows that only specific combinations of directions show prediction errors, and that prediction error is not correlated with the absolute probability level. The prediction errors for specific (nearly) opposite combinations of directions are therefore not the result of a static non-linearity at the output of the neuron, but could reflect for instance specific network interactions before or within MT.

In the analysis described above we investigated the effect of successive stimulus combinations on the response. It is also possible to investigate the

effect of stimulus combinations, which are separated in time by other stimuli. To this end, we analysed the level of non-linearity for increasing temporal separation. For this analysis we chose 11 strongly biphasic neurons with a Δt around 24 ms (the duration of 3 motion steps). We computed the prediction errors for each cell for the temporal separation of 1,2,3 or 4 motion steps between stimuli (separation of 1 motion step means successive stimulus combinations). We found decreasing prediction errors in all cases, as the temporal separation between the stimulus combinations increased, suggesting that the strongest non-linearity occurs between successive stimuli. If biphasic profiles were due to non-linear interactions between specific motion steps separated by Δt, we would expect the strongest non-linearity for these neurons at the temporal separation of 3 motion steps. Since this is not the case these results support the conclusion that biphasic behavior does not result from the specific non-linear directional interactions that are shown in Fig. 8A for two opposite consecutive motion directions.

Discussion

Biphasic responses

We examined the dynamics of direction tuning and the effect of directional changes at the preferred step size of MT neurons. The temporal profiles of the reverse correlograms, describing relative responses to individual motion steps at different directions, showed different degrees of biphasic behavior. Preferred directions for neurons with a low biphasic index did not change over time. Direction tuning of neurons with a high biphasic index on the other hand showed a directional change from antipreferred to preferred direction over time.

Reversal effects are a common feature of reverse correlograms and have been described in different visual areas, for instance for luminance contrast reverse correlograms of neurons in the retina (Rowe and Palmer, 1995), Lateral Geniculate Nucleus (Reid et al., 1991, 1997; Cai et al., 1997), and primary visual cortex (Reid et al., 1991; DeAngelis et al., 1995; DeValois et al., 2000; Mazer et al., 2002; Dragoi et al., 2002; Ringach et al., 1997, 2003). A substantial fraction of motion sensitive neurons in area MT can have similar biphasic correlograms in the motion domain, as is shown by our results and other recent work (Bair and Movshon, 2004; Bair et al. 2002). However, a recent report by Cook and Maunsell (2004) reports only a very small fraction of MT neurons with biphasic behaviour. The question arises how these differences in degree of biphasic behaviour can be explained.

Possible explanations for differences in biphasicness could be related to known differences in MT cell spatial response characteristics like center-surround organization and ‘plaid’ versus “component” responses (Movshon

et al., 1985; Rodman and Albright, 1989; Allman et al., 1985; Xiao et al., 1995; Born, 2000). Further investigation would be necessary to establish whether such a correlation exists. Most probably more important factors that determine the degree of biphasicness are stimulus attributes like spatial frequency, temporal frequency, speed, contrast etc. Some reports (Bair et al., 2002; Bair and Movshon, 2004) indeed show that speed, spatial frequency and contrast can change the shape of the reverse correlogram. This could also be the explanation why Cook and Maunsell (2004) hardly found any biphasic neurons in their sample of MT neurons, since their stimulus (dynamic noise) was different from the stimulus we used (field movement impulse stimulus). Our results show that the phase reversal of the correlograms occurs simultaneously for all directions. Furthermore, the peak latencies of the first and second phase of reverse correlograms for different directions are similar. This indicates that probabilities for different directions change with similar dynamics.

Priebe and Lisberger (2002a,b) have intensively investigated short-term adaptation in MT neurons that is related to transient responses. At first sight our results on biphasic responses seem to be correlated with short-term adaptation. A biphasic profile for individual responses would predict effects similar to short-term adaptation, with vigorous responses to the initial part of the stimulus settling rapidly to a lower firing rate. Similar to the distribution of adaptation strength reported by Priebe and Lisberger we find a wide, unimodal distribution for the biphasic effect. However we do not find a correlation with the transient behavior of the neurons. This indicates that biphasic responses are not due to the same short-term adaptation mechanism that determines the degree of transience in MT cell responses.

Weak and strong biphasic characteristics seem to correspond well to different requirements for motion sensitive cells tuned for either optimal temporal integration or segregation. In order to construct a useful representation of moving patterns in the outside world two mechanisms always compete. Sometimes motion directions need to be integrated over time to detect the overall flow of moving objects. On the other hand motion direction differences need to be segmented to distinguish differently moving objects. Our results show that the competition between temporal motion integration and segregation is reflected in responses to single motion steps, at the level of MT.

Second-order characteristics

We examined temporal interactions by measuring the effect of combinations of successive stimuli in 8 different directions. Weakly biphasic cells showed an increased firing probability for a motion step, after a preceding step in the preferred direction. Strongly biphasic cells on the other hand showed a decreased firing probability after a preceding step in the preferred direction. This is in accordance with previous reports that show that the response to the preferred direction strongly depends on the preceding motion direction (Bair et al., 2002; Priebe and Lisberger, 2002a,b). Stimulation with the preferred direction decreases the response to a successive preferred direction (short-term adaptation), and stimulation with the antipreferred direction either decreases or increases the responses to successive preferred directions.

The comparison of correlograms for specific combinations to the correlograms for individual motion steps shows that they to a large extent follow from the profiles for individual steps through simple linear summation. In addition, we also found evidence for 'non-linear', directionally specific interactions. Prediction errors for the second-order reverse correlograms clearly showed two different types of non-linear interactions. First, we found negative prediction errors (a lower response than predicted) for successive presentations of motion steps in the preferred direction. This might either reflect short-term adaptation or a saturation-type of non-linearity. The second, more interesting non-linear interaction that we found were positive prediction errors for antipreferred/preferred combinations (facilitation). This effect was found both for weakly and strongly biphasic neurons, and did not correlate with the biphasic index. The facilitation is in line with interactions along the preferred-antipreferred axis described previously (Bair et al., 2002; Priebe and Lisberger, 2002a,b). Our results for different combinations of directions furthermore show that similar facilitatory effects are also found for combinations other than preferred and antipreferred, as long as they differ by about 180 deg (facilitation to near opposing directions). Facilitation was observed for directional changes of about 180 deg, irrespective of a cell's preferred direction. The directionally specific interactions that we found were not related to the activity level of a cell, and therefore cannot be due to a simple static non-linearity at the output of MT neurons.

The observed facilitatory interactions for near opposite directions are not consistent with a divisive normalization model as proposed by several studies to account for spatial integration in MT (Simoncelli and Heeger, 1998; Britten and Heuer, 1999). In divisive normalization models the gain of the output of a single MT neuron is set by the average activity of all MT neurons tuned to different directions. Such models can account for instance

for the fact that the firing rate to a combination of two stimuli in the receptive field presented simultaneously is predicted by the average of the responses when they are presented separately (Britten and Newsome, 1990; Ferrera and Lisberger, 1997; Recanzone et al. 1997; Britten and Heuer, 1999). This model cannot account for the temporal integration effects found in our study, because the effect is directionally specific and not global, and because normalization would lead to decreased activity rather than facilitation. Furthermore we find the largest non-linear interactions on average 6 msec before the peak of the response. It is unlikely that normalization would peak even before the maximum response level is achieved. The simplest model to account for our data would be specific facilitatory input from oppositely tuned combinations of motion sensitive neurons for all motion directions at the input of MT, for instance from V1.

Our results show that area MT neurons are generally more responsive when sudden changes in motion directions occur, irrespective of the preferred direction of the neurons. This specific non-linear mechanism might play an important role in signalling relevant changes in the pattern of motion and provide additional information for directing eye movements and attracting attention to interesting parts of the visual field.

Acknowledgements
This study was supported by the Innovational Research Incentives Scheme (VIDI) of the Netherlands Organization for Scientific Research (NWO) and the Interuniversity Attraction Poles Programme (IUAP) of the Belgian Science Policy. We thank Ildiko Vajda for helpful discussions and providing parts of the analysis software. We thank Peter Sterling for useful comments on earlier drafts of the manuscript. Furthermore, we thank Theo Stuivenberg and the other technicians of our lab for technical support.

References
Albright, T. D. (1984). Direction and orientation selectivity of neurons in visual area MT of the macaque. J Neurophysiol 52, 1106-1130.

Allman, J., Miezin, F., and McGuinness, E. (1985). Direction- and velocity-specific responses from beyond the classical receptive field in the middle temporal visual area (MT). Perception 14, 105-126.

Bair, W., Cavanaugh, J. R., Smith, M. A., and Movshon, J. A. (2002). The timing of response onset and offset in macaque visual neurons. J Neurosci 22, 3189-3205.

Bair, W., and Movshon, J. A. (2004). Adaptive temporal integration of motion in direction-selective neurons in macaque visual cortex. J Neurosci 24, 9305-9323.

Borghuis, B. G., Perge, J. A., Vajda, I., van Wezel, R. J.A., van de Grind, W. A., and Lankheet, M. J. M. (2003). The motion reverse correlation (MRC) method: a linear systems approach in the motion domain. J Neurosci Methods 123, 153-166.

Born, R. T. (2000). Center-surround interactions in the middle temporal visual area of the owl monkey. J Neurophysiol 84, 2658-2669.

Born, R. T., and Tootell, R. B. (1992). Segregation of global and local motion processing in primate middle temporal visual area. Nature 357, 497-499.

Britten, K. H., and Heuer, H. W. (1999). Spatial summation in the receptive fields of MT neurons. J Neurosci 19, 5074-5084.

Britten, K. H., and Newsome, W. T. (1990). Responses of MT neurons to discontinuous motion stimuli. Invest Opth and Vis Sci Suppl 31, 238.

Britten, K. H., and Newsome, W. T. (1998). Tuning bandwidths for near-threshold stimuli in area MT. J Neurophysiol 80, 762-770.

Britten, K. H., Newsome, W. T., Shadlen, M. N., Celebrini, S., and Movshon, J. A. (1996). A relationship between behavioral choice and the visual responses of neurons in macaque MT. Vis Neurosci 13, 87-100.

Britten, K. H., Shadlen, M. N., Newsome, W. T., and Movshon, J. A. (1992). The analysis of visual motion: a comparison of neuronal and psychophysical performance. J Neurosci 12, 4745-4765.

Buracas, G. T., Zador, A. M., DeWeese, M. R., and Albright, T. D. (1998). Efficient discrimination of temporal patterns by motion-sensitive neurons in primate visual cortex. Neuron 20, 959-969.

Cai, D., DeAngelis, G. C., and Freeman, R. D. (1997). Spatiotemporal receptive field organization in the lateral geniculate nucleus of cats and kittens. J Neurophysiol 78, 1045-1061.

Cook, E. P., and Maunsell, J. H. (2004). Attentional modulation of motion integration of individual neurons in the middle temporal visual area. J Neurosci 24, 7964-7977.

De Valois, R. L., Cottaris, N. P., Mahon, L. E., Elfar, S. D., and Wilson, J. A. (2000). Spatial and temporal receptive fields of geniculate and cortical cells and directional selectivity. Vision Res 40, 3685-3702.

DeAngelis, G. C., Ohzawa, I., and Freeman, R. D. (1995). Receptive-field dynamics in the central visual pathways. Trends Neurosci 18, 451-458.

Dragoi, V., Sharma, J., Miller, E. K., and Sur, M. (2002). Dynamics of neuronal sensitivity in visual cortex and local feature discrimination. Nat Neurosci 5, 883-891.

Dubner, R., and Zeki, S. M. (1971). Response properties and receptive fields of cells in an anatomically defined region of the superior temporal sulcus in the monkey. Brain Res 35, 528-532.

Ferrera, V. P., and Lisberger, S. G. (1997). Neuronal responses in visual areas MT and MST during smooth pursuit target selection. J Neurophysiol 78, 1433-1446.

Heuer, H. W., and Britten, K. H. (2002). Contrast dependence of response normalization in area MT of the rhesus macaque. J Neurophysiol 88, 3398-3408.

Julesz, B. (1971). Foundations of Cyclopean Perception (Chicago, University of Chicago Press).

Lisberger, S. G., and Movshon, J. A. (1999). Visual motion analysis for pursuit eye movements in area MT of macaque monkeys. J Neurosci 19, 2224-2246.

Livingstone, M. S., Pack, C. C., and Born, R. T. (2001). Two-dimensional substructure of MT receptive fields. Neuron 30, 781-793.

Malpeli, J. G. (1998). Measuring eye position with the double magnetic induction method. J Neurosci Methods 86, 55-61.

Maunsell, J. H., and Van Essen, D. C. (1983). Functional properties of neurons in middle temporal visual area of the macaque monkey. I. Selectivity for stimulus direction, speed, and orientation. J Neurophysiol 49, 1127-1147.

Mazer, J. A., Vinje, W. E., McDermott, J., Schiller, P. H., and Gallant, J. L. (2002). Spatial frequency and orientation tuning dynamics in area V1. Proc Natl Acad Sci U S A 99, 1645-1650.

Mikami, A., Newsome, W. T., and Wurtz, R. H. (1986). Motion selectivity in macaque visual cortex. I. Mechanisms of direction and speed selectivity in extrastriate area MT. J Neurophysiol 55, 1308-1327.

Movshon, J. A., Adelson, E. H., Gizzi, M. S., and Newsome, W. T. (1985). The analysis of moving visual patterns. In Study group on pattern recognition mechanisms, C. Chagas, R. Gattass, and C. Gross, eds. (Vatican City, Pontifica Academia Scientiarum), pp. 117-151.

Newsome, W. T., and Paré, E. B. (1988). A selective impairment of motion perception following lesions of the middle temporal visual area (MT). J Neurosci 8, 2201-2211.

Pack, C. C., Berezovskii, V. K., and Born, R. T. (2001). Dynamic properties of neurons in cortical area MT in alert and anaesthetized macaque monkeys. Nature 414, 905-908.

Pack, C. C., and Born, R. T. (2001). Temporal dynamics of a neural solution to the aperture problem in visual area MT of macaque brain. Nature 409, 1040-1042.

Pack, C. C., Gartland, A. J., and Born, R. T. (2004). Integration of Contour and Terminator Signals in Visual Area MT of Alert Macaque. J Neurosci 24, 3268-3280.

Priebe, N. J., Churchland, M. M., and Lisberger, S. G. (2002). Constraints on the source of short-term motion adaptation in macaque area MT. I. the role of input and intrinsic mechanisms. J Neurophysiol 88, 354-369.

Priebe, N. J., and Lisberger, S. G. (2002). Constraints on the source of short-term motion adaptation in macaque area MT. II. tuning of neural circuit mechanisms. J Neurophysiol 88, 370-382.

Raiguel, S., Van Hulle, M. M., Xiao, D. K., Marcar, V. L., and Orban, G. A. (1995). Shape and spatial distribution of receptive fields and antagonistic motion surrounds in the middle temporal area (V5) of the macaque. Eur J Neurosci 7, 2064.

Recanzone, G. H., Wurtz, R. H., and Schwarz, U. (1997). Responses of MT and MST neurons to one and two moving objects in the receptive field. J Neurophysiol 78, 2904-2915.

Reid, R. C., Soodak, R. E., and Shapley, R. M. (1991). Directional selectivity and spatiotemporal structure of receptive fields of simple cells in cat striate cortex. J Neurophysiol 66, 505-529.

Reid, R. C., Victor, J. D., and Shapley, R. M. (1997). The use of m-sequences in the analysis of visual neurons: linear receptive field properties. Vis Neurosci 14, 1015-1027.

Reulen, J. P., and Bakker, L. (1982). The measurement of eye movement using double magnetic induction. IEEE Trans Biomed Eng 29, 740-744.

Ringach, D. L., Hawken, M. J., and Shapley, R. (2003). Dynamics of orientation tuning in macaque V1: the role of global and tuned suppression. J Neurophysiol 90, 342-352.

Ringach, D. L., Sapiro, G., and Shapley, R. (1997). A subspace reverse-correlation technique for the study of visual neurons. Vision Res 37, 2455-2464.

Rodman, H. R., and Albright, T. D. (1989). Single-unit analysis of pattern-motion selective properties in the middle temporal visual area (MT). Exp Brain Res 75, 53-64.

Rowe, M. H., and Palmer, L. A. (1995). Spatio-temporal receptive-field structure of phasic W cells in the cat retina. Vis Neurosci 12, 117-139.

Rudolph, K., and Pasternak, T. (1999). Transient and permanent deficits in motion perception after lesions of cortical areas MT and MST in the macaque monkey. Cereb Cortex 9, 90-100.

Salzman, C. D., Murasugi, C. M., Britten, K. H., and Newsome, W. T. (1992). Microstimulation in visual area MT: Effects on direction discrimination performance. J Neurosci 12, 2331-2355.

Simoncelli, E. P., and Heeger, D. J. (1998). A model of neuronal responses in visual area MT. Vision Res 38, 743-761.

Snowden, R. J., Treue, S., Erickson, R. G., and Andersen, R. A. (1991). The response of area MT and V1 neurons to transparent motion. J Neurosci 11, 2768-2785.

Treue, S., Hol, K., and Rauber, H. J. (2000). Seeing multiple directions of motion-physiology and psychophysics. Nat Neurosci 3, 270-276.

Xiao, D. K., Raiguel, S., Marcar, V., Koenderink, J., and Orban, G. A. (1995). Spatial heterogeneity of inhibitory surrounds in the middle temporal visual area. Proceedings of the National Academy of Sciences of the United States of America 92, 11303-11306.

Chapter 3

Dynamics of directional selectivity in MT receptive field center and surround

János A. Perge, Bart G. Borghuis, Roger J.E. Bours, Martin J.M. Lankheet and Richard J.A. van Wezel

Submitted to the Journal of European Neuroscience

Abstract

We studied receptive field organization of motion sensitive neurons in macaque middle temporal cortical area (MT) by mapping direction selectivity in space and in time. Stimuli consisted of pseudorandom sequences of single motion steps presented simultaneously at many different receptive field locations. Spatio-temporal receptive field profiles were constructed by cross-correlating stimuli and spikes. The resulting spike-triggered averages revealed center-surround organization. The temporal dynamics of the receptive fields were generally biphasic with increased probability for the preferred direction at short latency (50-70ms) and decreased probability at longer latency (80-100 ms). The response latency of the surround was on average 16 ms longer than that of the receptive field center. Our results show that surround input and biphasic behavior reflect two different mechanisms, both of which make MT cells specifically sensitive to motion contrast in space and time.

Introduction

Motion detection of a moving pattern is easier when the pattern is surrounded by other patterns moving in the opposite direction. This increased sensitivity to motion contrast or relative motion is generally related to center-surround receptive fields of visual motion sensitive neurons. Motion sensitive neurons with a center-surround receptive field organization such as those in cortical area MT are most responsive when motion is presented to the preferred direction in their receptive field center, and the opposite direction in the surrounding area (Allman et al., 1985). Due to the strong link between relative motion perception and the physiological properties of MT neurons, the investigation of spatial and temporal characteristics of center-surround receptive fields can be important for a better understanding of the spatiotemporal properties of relative motion perception.

Spatiotemporal receptive fields can be reconstructed by presenting flashing bright and/or dark stimuli pseudorandomly at different spatial locations and cross-correlating the neuronal spike train to the stimulus sequence. This luminance reverse correlation method has been used extensively to describe receptive fields of retinal neurons (Rowe and Palmer, 1995), the Lateral Geniculate Nucleus (LGN) (Reid et al., 1991, 1997; Cai et al., 1997), and primary visual cortex (V1) (Reid et al., 1991; DeAngelis et al., 1995; DeValois et al., 2000; Mazer et al., 2002; Dragoi et al., 2002; Ringach et al., 1997, 2003). For neurons that behave approximately linearly, such as those in LGN or simple cells in V1, first-order correlation between stimulus and response provides a nearly complete description of spatio-temporal receptive field properties. However, for motion sensitive neurons first-order correlation fails to capture the essential tuning properties like motion direction and speed selectivity. Therefore second-order analysis of stimulus interactions (i.e., the combination of two stimuli presented at different locations and different times) is required to reconstruct the relevant receptive field characteristics.

Second-order analysis of dark and/or bright stimuli has been used to characterize direction selectivity in cat simple and complex cells (Emerson et al., 1992) as well as in motion sensitive macaque area MT (Livingstone et al., 2001, Cook and Maunsell, 2004). One disadvantage in studying motion sensitivity using these luminance reverse correlation techniques is that the motion energy for specific motion directions is very small compared to the motion energy of coherently moving patterns. Luminance-based reverse correlation is therefore limited in revealing complex spatio-temporal receptive field properties of motion sensitive cells. To overcome this problem, Borghuis et al. (2003) proposed a motion reverse correlation

method, which employs a pseudorandom sequence of motion impulses. This motion reverse correlation method is much more effective in eliciting spikes, which allows for a detailed analysis of spatio-temporal receptive field properties of motion sensitive cells.

In this study, we used a spatio-temporal version of the motion reverse correlation paradigm (Borghuis et al., 2003) to investigate the dynamics of directional selectivity in MT receptive field centers and surrounds. We focus on two properties that are important for shaping directional responses in area MT: biphasic behavior and center-surround organization. We have previously shown that many MT cells display biphasic reverse correlation functions, indicating reduced sensitivity after a single step to the preferred direction (Perge et al., 2005). Thus, biphasic behavior makes MT neurons specifically sensitive to temporal motion contrast. Center-surround organization on the other side makes MT cells sensitive to spatial motion contrast. Although MT neurons are sensitive both to spatial and temporal motion contrast, it is unclear whether these characteristics reflect a single mechanism. We describe the dynamics of center and surround responses and show that biphasic response characteristics in the center operates at a time scale distinctly different from delayed surround inhibition.

Materials and methods

Two adult male rhesus macaques (*Macaca Mulatta*) participated in this study. Before the experiments, each monkey was implanted surgically with a head holding device, a search coil for measuring eye movements using the double induction technique (Reulen and Bakker 1982; Malpeli, 1998), and a stainless steel recording cylinder placed over a craniotomy above the left occipital lobe. The surgical procedures were performed under N_2O/O_2 anesthesia supplemented with isoflurane. After recovery, the monkeys were trained to fixate a rectangular spot (0.4x0.4 deg) on a black background. During the experiments, each monkey sat in a primate chair 57 cm from a cathode-ray tube display. Eye movement recordings were sampled at 500 Hz. For accurate fixation, the monkeys had to maintain their viewing direction within a virtual fixation window around the fixation point (2 degrees in diameter). While correctly fixating, the monkey was rewarded with water or juice every three seconds. Breaking fixation resulted in pausing the presentation of stimuli and no reward. Stimulus presentations were restarted after 300 ms of correct fixation. Animal procedures used in this study were approved by the Animal Use Committee (DEC) of Utrecht University, and procedures followed national and international guidelines.

Neuronal recordings

Single unit recordings were carried out by using standard extracellular methods. During experimental sessions, a parylene insulated Tungsten microelectrode (0.5-2 MΩ at 1 kHz) was inserted manually through a guide tube and then manipulated by a micro-positioning controller. Area MT was identified by the recording position and depth, the transition between grey matter, white matter and sulci along the electrode track, and by its functional properties. Among others, these are the prevalence of direction selective units, the similarity in direction tuning for nearby single unit recordings, the receptive field size according to eccentricity and the change of direction tuning along the electrode penetration. We have no histological confirmation of the recording sites because both monkeys are currently being used in other experiments. Spike times were registered at 0.5 ms resolution for on-line analysis and data storage, using a Macintosh G4 computer with a National Instruments PCI 1200 data acquisition board.

Stimuli and experimental procedure

The monitor (Sony Trinitron Multiscan 500 PS) was driven by an ATI Rage graphics card. The refresh rate was 75 Hz (1152x870 pixels) for early experiments in monkey A (10 cells recorded in monkey A), and 120 Hz (1024x768 pixels) in all other experiments. The stimulus was a rectangular field presented on a black background and it was divided into smaller subfields along an invisible grid (Fig. 1). Each subfield contained a high-density binary random dot pattern, consisting of 50% black and 50% white dots (Julesz, 1971). Mean luminance of the stimulus was 48 cd/m^2. A dot size of 0.14x0.14 deg was used for 10 cells in monkey A, and 0.20x0.20 deg for all of the remaining cells.

The stimulus was positioned over the receptive field center as determined by hand mapping. In each subfield pattern the dot pattern was shifted each monitor frame (8.3 ms at 120 Hz and 13.3 ms at 75 Hz) or every second monitor frame (17 ms at 120 Hz and 27 ms at 75 Hz). The size of the shift was 0.14 deg in horizontal and vertical directions and 0.15 deg in diagonal directions. As determined by the motion reverse correlation method, the shifts occurred in either the preferred or the antipreferred direction (Borghuis et al., 2003; Perge et al., 2005) and in a pseudo-random order (Figs. 1A and 1B). The antipreferred direction was defined as the direction opposite to the preferred direction. The dot displays in the subfields were presented simultaneously and the direction in a subfield chosen at each motion step was independent from the directions in other subfields. Between different experiments, the number of subfields varied. The resulting sequence of motion steps effectively stimulated most of our neurons. In case the stimulus did not drive the neuron effectively, the size of the shift was

either increased or decreased in a range of 0.07-0.42 degrees (in steps of 0.07 degrees) until a sufficiently strong response was obtained. The motion steps in the preferred and antipreferred direction in each subfield were each presented 7000-8000 times in a randomized order. This number was increased if the signal-to-noise ratio of the online analysis was judged insufficient. A movie demonstration of the stimulus is available at our website (http://www-vf.bio.uu.nl/lab/NE/publications/JP2/methods.html). Stimulus generation, data collection, and monitoring the monkeys' performance was done by custom made software written in programming language C. Offline data analysis was done in MATLAB.

Stimulus size and the number of subfields were optimized for each cell. We tried to maximize spatial resolution of the measurement by increasing the number of subfields while decreasing their size. However, by decreasing the size of the subfields the effective stimulus energy also decreases substantially. As a result, responses as well as the signal-to-noise ratio in the measurement decrease. Therefore, we needed a balance between sufficient spatial resolution and excitability. We found that subfields of minimally 1.5x1.5 deg stimulated most recorded neurons properly. For cells with insufficient responses, we increased the size of the patches until an adequate response was obtained.

Data analysis

We used the method of spike-triggered averaging (De Boer and Kuyper, 1968) to estimate the properties of spatio-temporal receptive fields in area MT (Figs. 1B and 1C). We calculated the average stimulus preceding the spikes as a function of time, *t*. The stimulus was represented by a temporal sequence of motion impulses for each stimulus patch, where +1 and -1 indicate the occurrence of preferred and antipreferred directions respectively. Spike-triggered averages (STAs) for each location were calculated by calculating the average stimulus value preceding each spike at that location. Thus, the resulting STA fluctuates in time between 1 and –1, where positive values indicate a relatively higher probability for the preferred motion direction and negative values indicate a relatively higher probability for the antipreferred motion direction to occur at time *t* before the spikes. A value of zero indicates that preferred and antipreferred stimulus direction occurred with equal probability at that time. STAs were smoothed by sliding window averaging with a Gaussian profile. Using a standard deviation of 8 ms, most of the noise was removed without affecting the overall shape of the function and its main parameters (Perge et al., 2005).

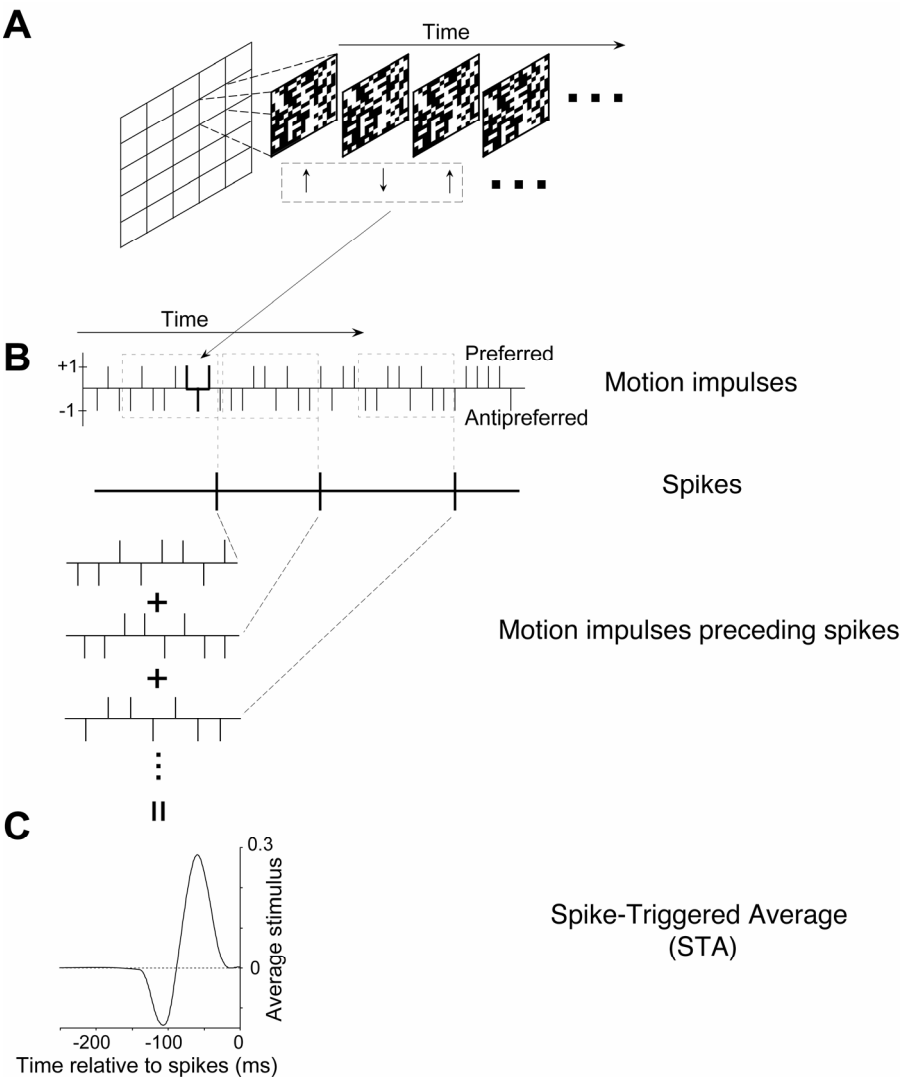

Fig. 1. Illustration of the stimulus and the motion reverse correlation paradigm. **A.** Stimuli were random dot patterns (50% dark and 50% white dots) presented simultaneously at different locations along a grid of squares. Each dot pattern within a subfield of the grid was shifted either to the preferred or antipreferred direction of the neuron in a pseudo-random order. **B.** Representation of the stimulus sequence and the reverse correlation procedure. The values of +1 and –1 indicate motion impulses to the preferred or antipreferred direction, respectively, for one subfield. **C.** Equal length stimulus sequences preceding the spikes were collected and averaged. This results in a spike triggered average (STA) for each individual subfield.

A significance criterion for the STAs was determined by calculating the mean and standard deviation of the STA based on a period of 100 ms following spikes in all subfields. This section of the STA reflects the noise in

the STAs since it indicates random correlations between spikes and stimuli presented after the occurrence of the spikes. We used an arbitrary noise level of four standard deviations for defining significant excursions in the STA.

Results

Spatiotemporal receptive fields were mapped with the spatial reverse correlation technique (see methods) in area MT of two male rhesus macaque monkeys for a total of 56 neurons (40 neurons in monkey A, and 16 in monkey S). Figure 2 shows the results for one example cell. This neuron was tested at 64 locations along an 8x8 grid of subfields with random dot patterns moving simultaneously either in the cell's preferred or antipreferred direction. Responses were reverse-correlated to the stimulus sequence for each subfield of the stimulus (see methods and Fig. 1) resulting in individual STAs for each individual stimulus subfield (Fig. 2A). The two subfields with high values (high probability for the preferred direction) correspond to the center of the receptive field. The subfields with low values correspond to the surround. Since the STAs show the average stimulus in time, Fig. 2A reveals both the temporal dynamics and the spatial characteristics of the receptive field.

The difference in the time course of the STAs is more salient when the STAs are presented on top of each other (Fig. 2B). Two representative STAs were plotted with thicker lines. One STA with large amplitude corresponds to a subfield covering the center of the receptive field and another one with a small negative amplitude corresponds to a subfield covering the surround. The STA corresponding to the center shows strong correlation with the preferred direction peaking at about 60 ms prior to the spikes. At longer delays, however, the STA changes in sign showing a dip at about 110 ms prior to the spikes indicating a stronger correlation with the antipreferred direction. This biphasic characteristic indicates that spike generation is suppressed after the initial response to the preferred motion impulse. For this example MT neuron the time course of STAs in the surround is delayed by 10 ms relative to that for the center. This difference in latency does not correspond to the delayed suppression in the center, which is at about 110 ms. Thus, Fig. 2B shows that for this cell, temporal dynamics for center and surround are clearly different.

A spatial representation of the receptive field can be constructed at each delay of the STAs. These spatial receptive field maps were derived by linear interpolation between probability values of the STAs at adjacent spatial locations. Such receptive field maps are shown for four different delays preceding the spikes (Fig. 2C). The total series of spatial receptive field maps at each delay is shown in a movie (http://www-

vf.bio.uu.nl/lab/NE/publications/JP2/results.html). These maps reveal the spatial organization of a center-surround receptive field structure in time, revealing the different temporal dynamics of center and surround responses.

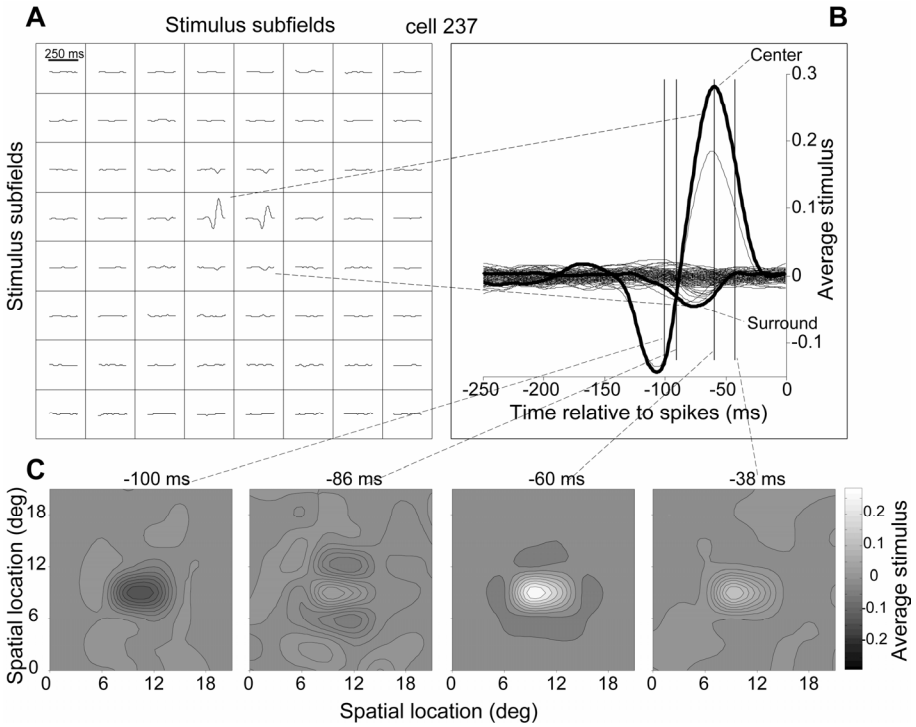

Fig. 2. Spatiotemporal receptive field of one example MT neuron. **A.** The stimulus consisted of an 8x8 grid of stimulus subfields moving independently in either the preferred or antipreferred direction. At each stimulus subfield, the STA for that location is plotted. The rightward point of each individual curve indicates the average stimulus value at 0 msec before the occurrence of a spike (by definition this will always have an average stimulus value of 0). The leftward point of the curve is the average stimulus value 250 msec before a spike occurred. **B.** The same STAs as in A plotted on top of each other. The two thick lines with the large and small amplitude indicate STAs for a center and a surround subfield, respectively. **C.** Spatial receptive field representations shown at four different times before the spikes occurred as indicated by the vertical lines in B. The contour plots were derived by linear interpolation between average stimulus values at adjacent positions in the 8X8 grid. White shading indicates high average stimulus values (higher probability for a preferred direction). Dark shading indicates a low negative average stimulus value (higher probability for an antipreferred direction). The X and Y coordinates indicate the distance from the bottom left of the stimulus field in visual degrees. The distance from the fixation point to the center of the stimulus field was 11.1 deg.

In general, surround responses were relatively weak. Sometimes the surround was radially symmetric (as the example cell in Fig. 2), but very often, it was irregular and patchy. The irregularities partly could arise due to

the limited spatial sampling resolution of our stimulus, since we only used a limited number of subfields (grids of 5x5 to maximum 10x10 subfields). However, for some recordings the irregularities are clearly due to intrinsic inhomogeneities of the receptive field, as has been reported by others (Raiguel et al., 1995).

In Fig. 3, we show how the spatial receptive field changes in time for five example cells that are representative for our whole population. The left hand column of Fig. 3 shows the spatial receptive field maps at the time where STAs reach their maximum value, similar to the –60 ms plot of Fig. 2C. Note that a surround is not necessarily visible in this figure, because the surround generally has a longer latency. To show the spatio-temporal characteristics in a single figure, we plotted space-time diagrams for a cross-section of the receptive field containing both the maximum value for the center and the minimum value for the surround. The center was defined as the subfield with the highest STA value, and the surround was the subfield with the lowest STA value (high correlation with the antipreferred direction) during the short latency phase. The orientation of this cross-section is indicated in the spatial receptive field maps in the left column by the oriented bars. The right column in Fig. 3 shows the resulting space-time plots for the five example cells, and illustrates the diversity in receptive field characteristics that we observed.

For some cells, the latency for the surround was close to that of the negative phase for the center. For these cells, the surround and the long latency negative phase of the center were intermingled (Fig. 3A, the same neuron as presented in Fig. 2). Fig. 3B is an extreme example of such a cell with a biphasic response and surround that are indistinguishable. Figure 3C shows a neuron without a long latency negative phase, which we will label a monophasic response. Some of the other cells such as the example cell in Fig. 3D showed no clear surround. For the last example cell (Fig. 3E), both center and surround show biphasic temporal characteristics. The short latency phase of the surround and the long latency phase of the center are clearly separated in time for this cell. The example cells in Fig. 3 suggest that spatially separable surrounds and biphasic temporal profiles result from different mechanisms. The following section addresses the temporal dynamics of these two features quantitatively.

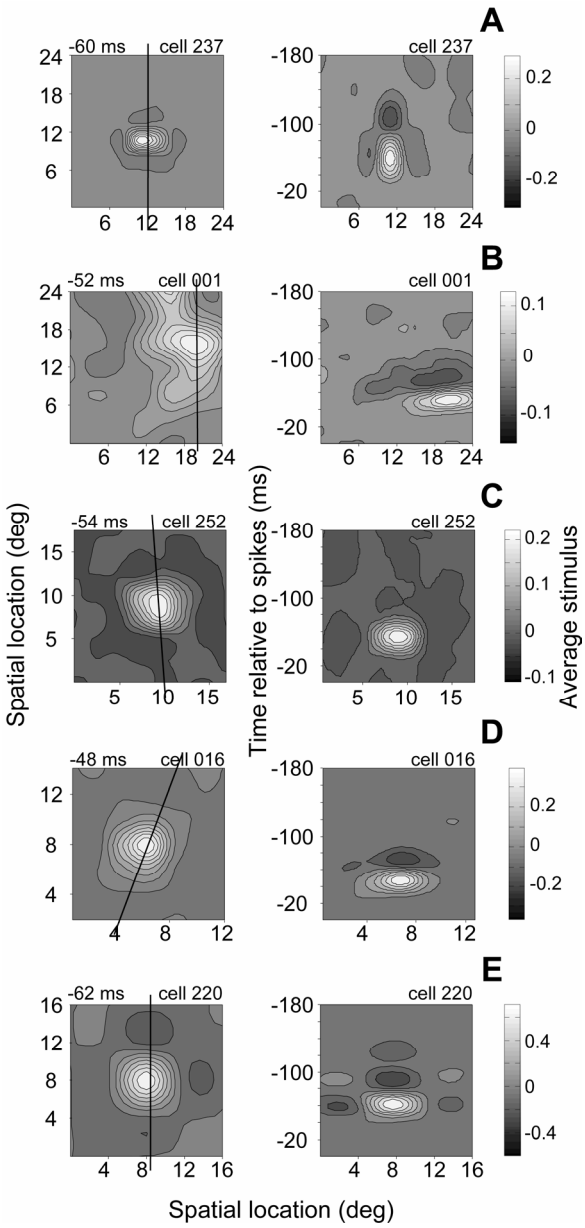

Fig. 3. Spatiotemporal receptive field structure of five example MT neurons. **Left column:** A spatial receptive field representation obtained as indicated in Fig. 2C. The spatial receptive field is shown at the time where the STA reaches its maximum value (similar to the –60 ms plot in Fig. 2C). Figure 3A is the same cell as plotted in Fig. 2. The X and Y coordinates indicate the distance from the bottom left of the stimulus field in visual degrees. The distance from the fixation point to the center of the stimulus field for cells A-E was 11.1, 11.8, 3.9, 6.7 and 5.9 deg, respectively. **Right column:** A representative cross-section of the 2D receptive fields (indicated by oriented bars in the left column) plotted at different times before the spike occurrences.

Differences in center and surround dynamics

To quantify the temporal differences between center and surround for our population of cells, we analyzed the time course of the STAs at different locations in the receptive field. The center of the receptive field was defined by subfields that showed a significant increase in average value. A stimulus subfield was defined as a surround subfield if the STA at that location did not show a significant increase but only a decrease in average stimulus value. Our significance criterium was four standard deviations (see Methods) above or below zero. Using this surround definition, 28/56 neurons (50%) showed the presence of a surround. In the event more subfields fulfilled the criteria for surround (39% of our cell population), we analyzed those subfields as well.

Figure 4A illustrates the model that we used to quantify the temporal changes of center and surround. The model consisted of two Gaussian functions, one for the early (thin black line) and one for the late component (grey line). The time course of the center STA was then described as the difference of these two Gaussians according to the form:

$$DOG_{cen}(t) = A_e * \frac{1}{\sqrt{2\pi * sd_e}} * e^{-\frac{1}{2}\left(\frac{t-\mu_e}{sd_e}\right)^2} - A_l * \frac{1}{\sqrt{2\pi * sd_l}} * e^{-\frac{1}{2}\left(\frac{t-\mu_l}{sd_l}\right)^2} \quad (1)$$

Where A_e and A_l are the surface area of the early and late components, μ_e and μ_l are the time of the peaks of the early and late components, and sd_e and sd_l represent the half-widths of the two Gaussians. The amplitude of the early and late components were obtained from equation 1 for t=μ.

$$Amp_e = \frac{A_e}{\sqrt{2\pi * sd_e}} \quad \text{and} \quad Amp_l = \frac{A_l}{\sqrt{2\pi * sd_l}} \quad (2)$$

The DOG model accurately describes the different types of biphasic profile (the thick dashed line in Fig. 4A). The function describing the surround STA was similar to the function for the center STA except that two additional free parameters (*d* and *g*) were introduced:

$$DOG_{sur}(t) = -g * A_e * \frac{1}{\sqrt{2\pi * sd_e}} * e^{-\frac{1}{2}\left(\frac{t-\mu_e+d}{sd_e}\right)^2} + g * A_l * \frac{1}{\sqrt{2\pi * sd_l}} * e^{-\frac{1}{2}\left(\frac{t-\mu_l+d}{sd_l}\right)^2} \quad (3)$$

where *d* is the delay between center and surround, and *g* is a gain factor to scale the surround amplitude relative to the center. The minus sign before *g* indicates that in our model the surround STA is reversed with respect to the

center STA. In case more subfields fulfilled the criteria for surround, each surround STA was fit separately with different *g* and *d* parameters. The fits were carried out using a least square minimization algorithm (Gauss-Newton method). The choice for our model was arbitrary, and it was chosen because it describes the data well. For example, a difference of gamma functions (Cai et al., 1997) instead of Gaussian functions would provide similar results.

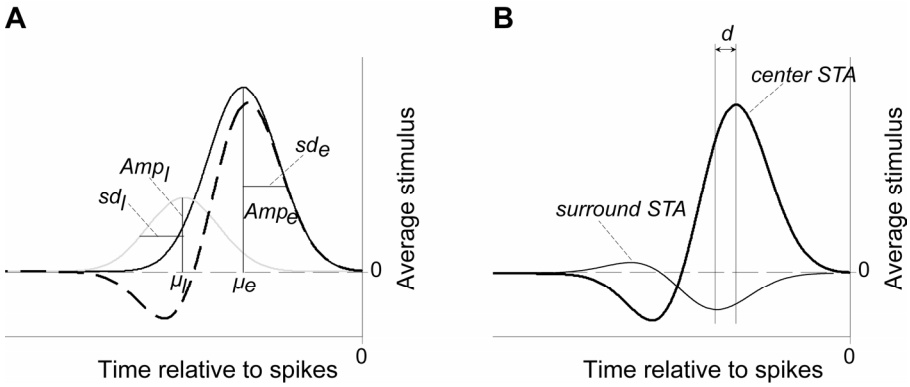

Fig. 4. Illustration of our model describing the temporal dynamics of the spatial receptive field. **A.** The temporal profile of our model consists of an early (thin black line) and late (gray line) Gaussian profile. The difference between the early and late components results in a biphasic profile (dashed black line). *Amp*: Amplitude; *sd*: height at half width; μ: time of the peak. Subscripts *e* and *l* refer to the early and late components, respectively. **B.** The center and surround temporal profiles are both separately constructed according to Fig. 4A. For more details, see the description in the text. *d*: difference in time between the temporal profiles of the center and surround.

It is important to note that we assume similar shapes of the temporal profiles for center and surround. Comparable models with the same assumption have been applied earlier to describe the temporal characteristics of visual receptive fields with delayed surround (Adelson and Bergen 1985, Dawis et al., 1984, Cai et al., 1997). To evaluate the validity of this assumption, we calculated fit errors of surround STAs by subtracting our fit results from the original STAs. We found no systematic fit error over time, which supports our assumption of similarity in shape for center and surround.

First, we analyzed the differences in surround latencies at different spatial locations for the same neuron, for cells with multiple surround subfields under our definition. In general, we found that fit parameters indicating the surround delay relative to the center delay (*d*) were similar within one measurement. For five neurons the number of surround fields was larger than three. For these cells, the average standard deviation of *d* was 5 ms, which was smaller than the variation in *d* within cells (see later). Since

the surround fields showed similar temporal characteristics, we averaged all surround STAs within a measurement. Thus, the following results are based on fit results of the average surround STAs for each cell.

Figure 5 shows the delay of the center early component (μ_e) plotted against the delay of surround early component ($\mu_e + d$). Most of the data points are above the diagonal, indicating longer surround latencies than center latencies. The average delay difference between center and surround was 16 ± 10 ms, which clearly differs from the delay difference of the early and late components both in the center and surround ($\mu_l - \mu_e$, 39 ± 36 ms). We found no significant correlation between the difference of center and surround delay and receptive field eccentricity (r = -0.07 p>0.05), nor did we find significant correlation between the difference of center and surround delay and the average distance of center and surround field (r = 0.01, p>0.05).

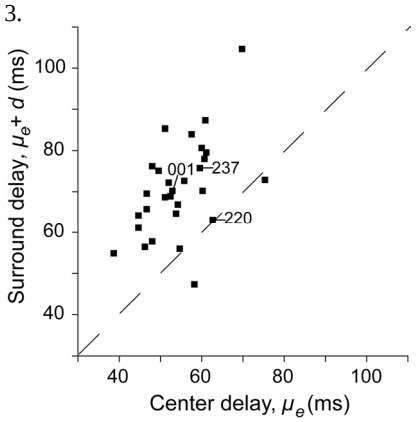

Fig. 5. Surround delay is longer than center delay. Based on the model we describe in Fig. 4, we fitted the STAs for each cell separately, and plotted the center delay (mu_{exc}) versus surround delay ($mu_{exc}+d$). Each symbol indicates one neuron. Only those neurons are shown where the minimum stimulus value of the surround was significant, i.e. more than four standard deviations below zero (50% of the neurons, n=56). The average delay difference between center and surround was 16 ± 10 ms. The dashed line indicates the line of equality. Numbers indicate the cell numbers of the cells shown in Fig. 3.

To characterize the magnitude of biphasic behavior in the population, we computed a biphasic index (BI) for each neuron as the ratio of the amplitudes of the early and late components.

$$BI = Amp_l / Amp_e \quad (4)$$

Thus, a low biphasic index value corresponds to lack of biphasic behavior and a high value to strong biphasic behavior. Figure 6 shows the distribution of biphasic index values across our population of recorded MT neurons. The mean biphasic index for all of the cells was 0.40 ± 0.25 (n=56). As Fig. 6 shows, a broad range of biphasicness was present in the population.

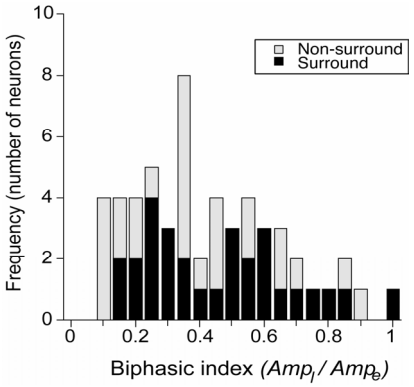

Fig. 6. The distribution of biphasic indices indicating the biphasic temporal characteristics in the population (n=56). A biphasic index of 0 means complete lack of biphasic behavior. Two outliers with a biphasic index > 1 are not shown in this graph. The average biphasic index was 0.40±0.25 (n=56). The black part of the bars indicates the number of neurons with surround using our significance criteria (see text).

The black part of the bars in Fig. 6 indicates the number of neurons with a surround according to our significance criteria described earlier. The figure shows no clear relationship between the presence of surround and the strength of biphasic behavior. To further investigate the relationship between biphasic behavior and surround strength, we plotted the biphasic index against *g*, a fit parameter indicating the strength of the surround relative to the center (Fig. 7). We found no significant correlation between surround strength and biphasicness ($r = -0.04$ $p>0.05$). This finding again indicates that biphasic behavior and surround are not related to each other.

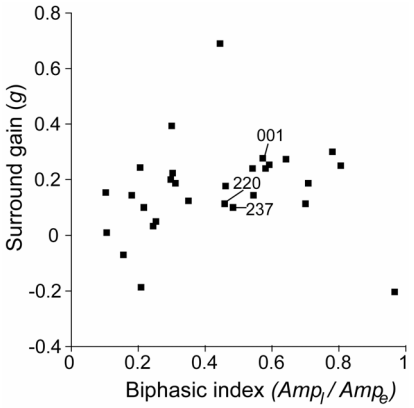

Fig. 7. Strength of biphasic behavior and strength of surround are not correlated. Strength of surround was defined by fit parameter *g* (see text), which indicates the surround amplitude relative to the center amplitude. Each symbol indicates one neuron. The *r*-value of the linear fit was 0.04 ($p>0.05$). Numbers indicate the cell numbers of the cells shown in Fig. 3

Discussion

We have shown two important aspects of the temporal dynamics of area MT receptive fields. First, peak latency for the surround was on average 16 ms longer than that for the center. Second, biphasic behavior for full-field stimuli is also found for local responses in center and surround. Even though the delayed surround response and the biphasic characteristics of the center cannot always be separated in space and time, our results indicate that biphasic behavior does not primarily result from center-surround antagonism.

The delay difference between center and surround that we find is much shorter than the reported 40 ms in owl monkey MT (Allman et al., 1985). This difference might be due to differences in experimental paradigm. Allman et al. (1985) used continuous stimulation in the preferred direction, while we used a time-varying stimulus with two opposite motion directions. Temporal integration of motion responses for preferred and non-preferred directions thus may have affected the latency estimates in different ways.

It is interesting to note that area MT cells show receptive field properties in the motion domain similar to properties of low-level receptive fields in the luminance domain. However, delay differences between center and surround responses are quantitatively different from findings at lower levels. Retinal P cells have a delay difference of 8 ms (Rowe and Palmer, 1995), and this value only increases slightly for LGN (10 ms, Cai et al., 1997) and V1 (9 ms, Bair et al., 2004). In contrast to the findings by Bair et al. for orientation tuning in V1, we found no evidence for a relationship between the strength of the surround and the difference in delay between center and surround. Furthermore, we rarely observed the surround to be faster than the center, which is described in V1 (Bair and Movshon, 2004).

Delayed surround effect might play a role in integrating local motion information into a global motion percept. For instance, it has been shown that area MT neurons first respond to local motion directions and gradually converge to a response to global motion directions (Pack et al., 2001). Related to these reports are studies on pattern selectivity of MT neurons. Pattern direction selectivity is the ability to signal the single direction of a moving plaid instead of the two components of the plaid (Movshon et al, 1985). Again, this ability develops in time during stimulation, though the time course of this effect is tens of milliseconds longer than our reported surround delay (Pack et al., 2001; Smith et al. 2005).

Several different models might explain delayed MT surround responses. A simple candidate would be localized spatial integration of V1 direction

selective responses to establish the center, and more global integration of opposite directions with a reversed sign for the surround. This type of model was very successful in explaining monodirectional aftereffects for bidirectional motion adaptation (Grunewald and Lankheet 1996). It is not clear however where a delay difference of 16 ms would arise in such a model. Other options would be inhibitory input from MT neurons with a receptive field center at the retinal location of the surround, tuned to the same direction (lateral inhibition) (Hartline et al., 1956), or excitatory input from such neurons tuned to the opposite direction (disinhibition) (Allman et al., 1985). Such lateral interactions require time, but again one would not necessarily expect such long delays. Our results do not exclude the possibility that delay differences arise from feedback of higher visual areas (Bair and Movshon, 2004).

Our results show that MT neurons can have strong biphasic characteristics (Perge et al., 2005). This characteristic could arise from short-term adaptation to a preferred stimulus. However, we showed in a previous paper that biphasic characteristics are not correlated with the ratio between the transient and sustained response (Perge et al., 2005), which characterizes short-term adaptation (Priebe et al., 2002). Thus, biphasic responses reflect a different form of adaptation operating at a different time course. In this paper we also show that biphasic responses are not directly related to surround input. We found no correlation between biphasic behavior and surround strength.

One might expect that the delay difference between center and surround could also be observed at the level of motion perception. For V1 neurons, it has been shown that neural responses to temporally interleaved excitatory and inhibitory stimuli match perceptual masking (Macknik and Livingstone, 1998). Human psychophysical studies have shown that direction discrimination of random dots moving in a center patch is strongly influenced by dots moving in the surround (Murakami and Shimojo, 1993, 1995, 1996). Depending on stimulus characteristics like center size, eccentricity, etc., the center dots can seem to move in the opposite direction (induced motion), or move in the same direction (motion capture). Our results suggest that the strength of motion capture and induced motion should be influenced by the timing of center and surround onsets. Further psychophysical studies are required to confirm such a relationship between MT receptive field properties that we describe and motion perception.

Acknowledgements
This study was supported by the Innovational Research Incentives Scheme (VIDI) of the Netherlands Organization for Scientific Research (NWO) and the Interuniversity Attraction Poles Programme (IUAP) of the Belgian Science Policy. We thank Andre Noest for helpful discussions.

References

Adelson, E. H., and Bergen, J. R. (1985). Spatiotemporal energy models forthe perception of motion. J Opt Soc Am A 2, 284-299.

Allman, J., Miezin, F., and McGuinness, E. (1985). Direction- and velocity-specific responses from beyond the classical receptive field in the middle temporal visual area (MT). Perception 14, 105-126.

Bair, W., and Movshon, J. A. (2004). Adaptive temporal integration of motion in direction-selective neurons in macaque visual cortex. J Neurosci 24, 9305-9323.

Borghuis, B. G., Perge, J. A., Vajda, I., van Wezel, R. J., van de Grind, W. A., and Lankheet, M. J. (2003). The motion reverse correlation (MRC) method: a linear systems approach in the motion domain. J Neurosci Methods 123, 153-166.

Cai, D., DeAngelis, G. C., and Freeman, R. D. (1997). Spatiotemporal receptive field organization in the lateral geniculate nucleus of cats and kittens. J Neurophysiol 78, 1045-1061.

Cook, E. P., and Maunsell, J. H. (2004). Attentional modulation of motion integration of individual neurons in the middle temporal visual area. J Neurosci 24, 7964-7977.

Dawis, S., Shapley, R., Kaplan, E., and Tranchina, D. (1984). The receptive field organization of X-cells in the cat: spatiotemporal coupling and asymmetry. Vision Res 24, 549-564. de Boer, R., and Kuyper, P. (1968). Triggered correlation. IEEE Trans Biomed Eng 15, 169-179.

De Valois, R. L., Cottaris, N. P., Mahon, L. E., Elfar, S. D., and Wilson, J. A. (2000). Spatial and temporal receptive fields of geniculate and cortical cells and directional selectivity. Vision Res 40, 3685-3702.

DeAngelis, G. C., Ohzawa, I., and Freeman, R. D. (1995). Receptive-field dynamics in the central visual pathways. Trends Neurosci 18, 451-458.

Dragoi, V., Sharma, J., Miller, E. K., and Sur, M. (2002). Dynamics of neuronal sensitivity in visual cortex and local feature discrimination. Nat Neurosci 5, 883-891.

Emerson, R. C., Bergen, J. R., and Adelson, E. H. (1992). Directionally selective complex cells and the computation of motion energy in cat visual cortex. Vision Res 32, 203-218.

Grunewald, A., and Lankheet, M. J. (1996). Orthogonal motion after-effect illusion predicted by a model of cortical motion processing. Nature 384, 358-360.

Hartline, H. K., Wagner, H. G., and Ratliff, F. (1956). Inhibition in the eye of Limulus. J Gen Physiol 39, 651-673.

Julesz, B. (1971). Foundations of Cyclopean Perception (Chicago, University of Chicago Press).

Livingstone, M. S., Pack, C. C., and Born, R. T. (2001). Two-dimensional substructure of MT receptive fields. Neuron 30, 781-793.

Macknik, S. L., and Livingstone, M. S. (1998). Neuronal correlates of visibility and invisibility in the primate visual system. Nat Neurosci 1, 144-149.

Malpeli, J. G. (1998). Measuring eye position with the double magnetic induction method. J Neurosci Methods 86, 55-61.

Mazer, J. A., Vinje, W. E., McDermott, J., Schiller, P. H., and Gallant, J. L. (2002). Spatial frequency and orientation tuning dynamics in area V1. Proc Natl Acad Sci U S A 99, 1645-1650.

Movshon, J. A., Adelson, E. H., Gizzi, M. S., and Newsome, W. T. (1985). The analysis of moving visual patterns. In Study group on pattern recognition mechanisms, C. Chagas, R. Gattass, and C. Gross, eds. (Vatican City, Pontifica Academia Scientiarum), pp. 117-151.

Murakami, I., and Shimojo, S. (1993). Motion capture changes to induced motion at higher luminance contrasts, smaller eccentricities, and larger inducer sizes. Vision Res 33, 2091-2107.

Murakami, I., and Shimojo, S. (1995). Modulation of motion aftereffect by surround motion and its dependence on stimulus size and eccentricity. Vision Res 35, 1835-1844.

Murakami, I., and Shimojo, S. (1996). Assimilation-type and contrast-type bias of motion induced by the surround in a random-dot display: evidence for center-surround antagonism. Vision Res 36, 3629-3639.

Pack, C. C., Berezovskii, V. K., and Born, R. T. (2001). Dynamic properties of neurons in cortical area MT in alert and anaesthetized macaque monkeys. Nature 414, 905-908.

Perge, J. A., Borghuis, B. G., Bours, R. J., Lankheet, M. J., and van Wezel, R. J. (2005). Temporal dynamics of direction tuning in motion-sensitive macaque area MT. J Neurophysiol 93, 2104-2116.

Priebe, N. J., Churchland, M. M., and Lisberger, S. G. (2002). Constraints on the source of short-term motion adaptation in macaque area MT. I. The role of input and intrinsic mechanisms. J Neurophysiol 88, 354-369.

Raiguel, S., Van Hulle, M. M., Xiao, D. K., Marcar, V. L., and Orban, G. A.

(1995). Shape and spatial distribution of receptive fields and antagonistic motion surrounds in the middle temporal area (V5) of the macaque. Eur J Neurosci 7, 2064.

Reid, R. C., Soodak, R. E., and Shapley, R. M. (1991). Directional selectivity and spatiotemporal structure of receptive fields of simple cells in cat striate cortex. J Neurophysiol 66, 505-529.

Reid, R. C., Victor, J. D., and Shapley, R. M. (1997). The use of m-sequences in the analysis of visual neurons: linear receptive field properties. Vis Neurosci 14, 1015-1027.

Reulen, J. P., and Bakker, L. (1982). The measurement of eye movement using double magnetic induction. IEEE Trans Biomed Eng 29, 740-744.

Ringach, D. L., Hawken, M. J., and Shapley, R. (2003). Dynamics of orientation tuning in macaque V1: the role of global and tuned suppression. J Neurophysiol 90, 342-352.

Ringach, D. L., Sapiro, G., and Shapley, R. (1997). A subspace reverse-correlation technique for the study of visual neurons. Vision Res 37, 2455-2464.

Rowe, M. H., and Palmer, L. A. (1995). Spatio-temporal receptive-field structure of phasic W cells in the cat retina. Vis Neurosci 12, 117-139.

Smith, M. A., Majaj, N. J., and Movshon, J. A. (2005). Dynamics of motion signaling by neurons in macaque area MT. Nat Neurosci 8, 220-228.

Chapter 4

Temporal properties of center-surround interaction in human motion perception

János A. Perge, Remco Suer, Martin J.M. Lankheet, W.A. van de Grind and Richard J.A. van Wezel

Abstract
Motion perception in a small region of the visual field is influenced by motion in the immediately surrounding regions. We studied this influence by a center-surround paradigm, where the perception of motion in a central circular region is influenced (biased) by motion in a surrounding annulus. We investigated the contribution of surround timing to the surround bias. The magnitude of surround bias for different onset delays between center and surround was quantified. Surround fields were presented before, simultaneously, or after center onset in a range of –24 to 24 ms relative to the center onset, and in steps of 8 ms. We found that the temporal shift of the surround in this range of time shifts had no significant effect on the magnitude of surround bias. These results are in contrast to neurophysiological results, which show that the antagonistic surround of motion receptive fields in motion sensitive cortical area MT is on average 16 ms delayed relative to the receptive field center. This finding indicates that the response timing of center-surround neurons is not represented at the level of motion perception.

Introduction

When the moon is seen amidst moving clouds, we might have the impression that the moon is moving rather than the clouds. This phenomenon illustrates the relative nature of visual motion perception: perceived motion in one part of the visual field is influenced by motion at other locations. When a stationary object appears to move in a direction opposite to nearby moving elements, the illusory motion is often referred to as induced movement (see for a review Reinhardt-Rutland, 1988). However, nearby motion can also induce illusory motion of a static target in the same direction (Ramachandran and Cavanagh, 1987). Due to these differences in the direction of induced motion, a distinction has been made between motion contrast (opposite induced motion) and motion assimilation (induced motion in the same direction). Motion contrast can occur between distant visual regions and motion assimilation seems to be limited to nearby regions (Chang and Julesz, 1984; Nawrot and Sekuler, 1990).

Induced motion studies investigated a rather specific aspect of relative motion perception, namely when the test pattern in which induced motion is seen is static. A more general approach has been introduced by a center-surround stimulus paradigm (Murakami and Shimojo, 1993, 1995, 1996), in which the perception of motion in a moving dot display is influenced (biased) by a surrounding annulus of moving dots. Murakami and Shimojo distinguished two types of bias: contrast bias for motion opposite to the inducer and assimilation bias for motion in the direction of the inducer. The authors suggested that their results might reflect the properties of detectors especially sensitive to motion contrast. Where in the visual system might such motion opposition take place, and how would this relate to perceptual phenomena of induction?

Neurons in the middle temporal cortical area (area MT or V5) in primates respond selectively to a particular subset of directions and speeds of motion within their receptive field (Dubner and Zeki, 1971; Maunsell and Van Essen, 1983; Albright, 1984; Mikami et al., 1986). Numerous studies have established a close link between neural activity of MT neurons and motion perception (Britten et al., 1992; Britten and Newsome, 1998). For about 50% of MT neurons, the response to the preferred direction in the receptive field center is suppressed by the same direction in the surrounding area (Allman et al., 1985; Born and Tootell, 1992; Raiguel et al., 1995; Xiao et al., 1995; Born, 1992). This phenomenon, often referred to as center-surround antagonism, makes neurons with strong center-surround receptive fields excellent candidates for playing an important role in relative motion perception.

If center-surround receptive fields in MT take a substantial part in relative motion perception, we might expect that other properties of MT neurons also affect induced motion percepts. It has been shown that the response latency of the surround of MT receptive fields is on average 16 ms longer than the response latency of the center (Perge et al., 2005). However, the perceptual consequence of this delayed surround is unknown. When we relate the activity of MT center-surround neurons to the strength of relative motion perception (or the strength of surround bias), we implicitly assume that the relative increase in firing rates of stimulus driven center-surround neurons also increases the strength of perceived surround bias. The larger the increase relative to other differently tuned neurons the stronger the perceived surround bias. If neurons respond more when presented with optimally timed moving center and surround stimuli, we would expect that the response increase is also reflected in the psychophysical performance in the form of increase in the strength of surround bias.

In this study, we investigated whether timing differences between MT centers and surrounds also affect motion induction. We measured the strength of induced motion for different onset delays between center and surround. If MT center-surround organisation plays a role in perceptual motion induction, we would expect an optimal effect for an onset delay equal to the physiologically identified timing difference. Such a relationship between stimulus timing and perceptional surround bias would strengthen the link between motion perception and the underlying physiological processes in area MT. Negative results would indicate that MT center-surround delays play no role in the strength of motion induction.

Methods

Subjects

One naive subject and two of the present authors participated as observers. All observers had normal bilateral vision.

Equipment

The experiments were done in a dark room. Stimuli were presented on a CRT (Sony FD Trinitron GDM-F520 40.5x30.5 cm) set to a resolution of 1024x768 pixels, and a frame rate of 120 Hz. An Apple Macintosh G4 computer was used for stimulus generation. The subject's head was stabilized with a chin rest at a viewing distance of 171 cm. Stimulus generation and data collection were done by custom made software developed in our laboratory.

Stimulus and task

The stimulus was presented on a black background with a luminance of ~0.01 cd/m^2. A moving random dot pattern was presented on this background behind a circular aperture (center) and was surrounded by an annulus of moving random dots (surround) (Fig. 1). The dot density was 30 dots/deg^2, the diameter of each dot was 0.04deg (1 pixel served as one dot), and the dot velocity was 8 deg/sec in both the center and the surround. The direction of motion in the center or the surround was always horizontal either to the right or left. The motion strength was quantified by the percentage of dots moving coherently in one direction, where 100% coherence corresponds to all dots moving coherently in one direction and a value of 0% to purely random noise. In that case, all dots were redrawn in random locations at each frame-refresh. The center coherence was varied (0-100%), while the surround coherence was kept constant at 50% during the experiments.

Stimuli were presented in the right visual field at 3 deg eccentricity from the fixation point. This eccentricity was based on a previous observation that at this position both assimilation and contrast type biases occur, and that the magnitude of surround bias shows a definite size tuning with a clear optimum (Murakami and Shimojo, 1996). Center dots were white (102 cd/m^2) and the surround dots were red (19 cd/m^2). This color difference was introduced merely to help the perceptual segregation between center and surround. A central fixation bar (0.2 deg in height and 0.04 deg in width) was presented to aid correct fixation. The subjects were asked to maintain fixation and to indicate the direction of center motion in a two-alternative forced-choice task.

We used an intermittent stimulus presentation, consisting of a repetition of short center and surround motion impulses (Fig. 1). One trial consisted of six center and surround impulses. The duration of each motion impulse was 48 ms and it was repeated every 160 ms. The gap between two impulses (112 ms) was left empty and had the same black color as the background. When choosing these parameters, we tried to minimize the duration of the impulses and increase the gap between them. At this short impulse duration, we still found a reasonable surround bias. At even shorter impulse durations both the performance and the perceptual bias were remarkably impaired. The longer gaps between impulses intended to prevent effects of surround impulses on the following center impulses.

In experiment one, we tested which center size evoked the strongest surround bias (Experiment 1.). In this experiment, the center and surround impulses were presented simultaneously. In experiment 2, we investigated the effect of different onset asynchronies between center and surround. The onset of the surround impulses varied from 24 ms before to 24 ms after onset of the center impulses, in steps of 8 ms (1 monitor frame)

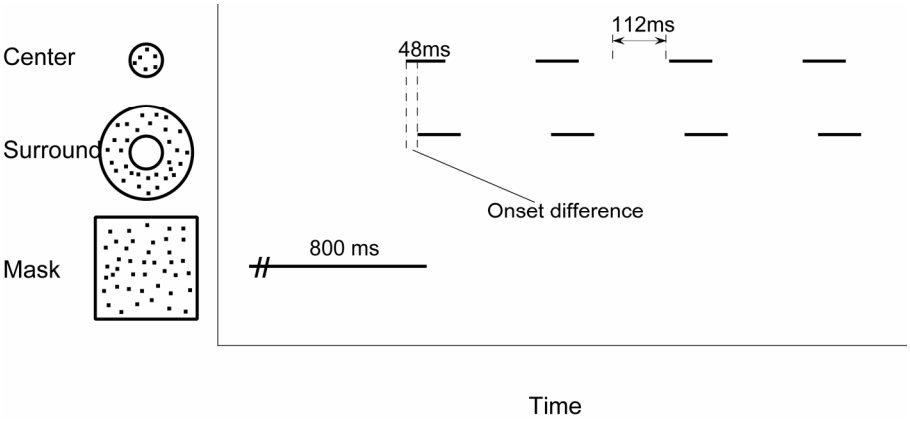

Fig. 1. Schematic illustration of stimulus timing. Each trial started with a mask consisting of a 0% coherent dot display and lasting 800 ms. At the end of the mask presentation, a center and surround random dot pattern was presented as brief (48 ms) motion impulses and repeated 6 times with intervening gaps without any stimulus of 112 ms. The onset time of surround motion impulses could be shifted in steps of 8 ms relative to the onset time of center motion impulses. The range of these delays was –24 to 24 ms. This figure illustrates the case in which surround motion impulses are presented 24 ms later than center motion impulses.

Before each trial, we presented a noise mask with duration of 800 ms to prevent possible adaptation effects from the previous trial. The mask was a random dot pattern of 0% coherence displayed in a rectangular field

covering both the center and the surround area. Its diameter was equal to the surround diameter. The dot density of the mask was equal to that of the center and the surround. At the end of the trial and before the next trial, only the fixation bar was visible on a black background at least for a 300 ms long period. All conditions were presented in a pseudorandom order and each condition was repeated 20 times during the experiment. Due to the long duration of the experiments, the trials were presented in four sessions of equal-length with breaks between the sessions.

Data analysis.
Dots in the center and the surround could move independently either to the left or right. This resulted in four possible configurations: center motion to the right or left combined with surround motion to the same or opposite direction. Since we found no systematic difference between left or right center motion direction, these conditions were pooled in two data sets: one for center and surround in the same and one for center and surround in opposite motion directions. The percentage correct choices for same direction motion were plotted as a function of motion coherence in the center (Fig. 2). The left side of this function corresponds to motion of the center and surround in opposite directions, and the right side corresponds to motion of the center and surround in same directions.

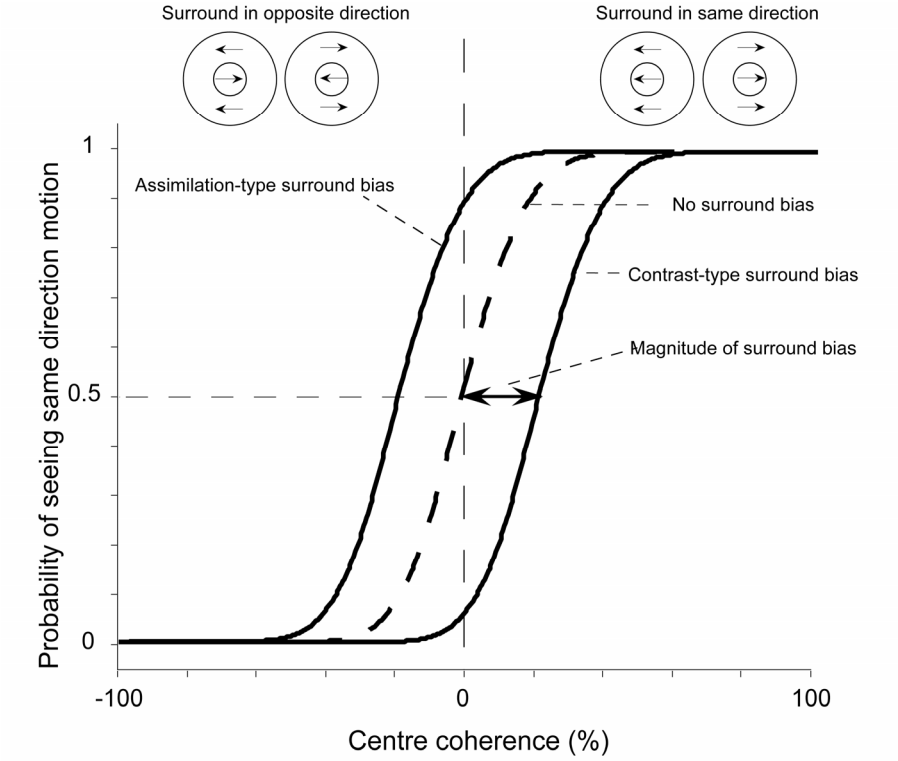

Fig. 2. Representation of surround magnitude. At 0% coherent motion, all dots are refreshed in random locations, which results in no net motion energy in any direction. At increasing coherence the number of signal dots in the center increases. Subjects were instructed to report the motion direction in the center. Since they did not give significantly different results for left and right conditions, those conditions were pooled. As a result, we present the cases where center and surround move either oppositely or in the same direction. The right part of the abscissa indicates the coherence levels of the center region for the same (right or left) motion direction in the surround at 50% coherence. The left part of the abscissa corresponds to right or left motion in the center but opposite direction in the surround. When motion discrimination in the center is not biased by the surround, it is expected that the psychometric function will pass through 0.5 probability at 0% signal (dashed curve). If there is a biasing surround, it is expected that the function will be shifted laterally either to the right (contrast type bias) or to the left (assimilation type bias). The amount of shift (measured as the shift of 0.5 probability point of the function) indicates the magnitude of the surround bias.

In the absence of a surround bias, the psychometric function is expected to reach the 0.5 probability level at 0% coherence. This would indicate equal probability for seeing leftward and rightward motion irrespective of the motion direction in the surround. A bias due to induction by the surround would show up as a shift of the curve along the coherence axis. Positive or negative shifts indicate contrast-type or assimilation-type of bias, respectively. We defined the magnitude of the surround bias as the horizontal shift of the 0.5 probability point of the curve from 0% coherence.

Results

We investigated the effect of a delayed surround onset on the bias induced by surround motion on perceived motion directions in the center. First, we determined the center stimulus size, which generates the strongest contrast-type bias. Second, we measured the magnitude of surround bias at this stimulus size with different surround onset delays.

Experiment 1: Optimal stimulus size

The diameter of the center was varied between 0.5 and 4 deg, in six steps. The surround diameter was always twice as large as the center diameter. Figure 3 shows the surround bias plotted as a function of center size for one subject. The negative values at small center sizes indicate assimilation-type bias. In those cases, the subject has a strong tendency to report a direction for the center similar to that of the surround. For larger center sizes (1.5-3 deg), the positive values indicate contrast-type bias. In those cases, the subject reports the direction opposite to the direction of the surround. The size tuning curve peaks at 1.5 deg, which is in accordance with previous reports at 3 deg eccentricity (Murakami and Shimojo, 1996). Assimilation-type bias at small stimulus sizes and contrast-type bias for larger stimulus sizes is also in line with previous results (Nawrot and Sekuler, 1990). In the next experiments, we used 1.5 deg center size to maximize the strength of surround bias.

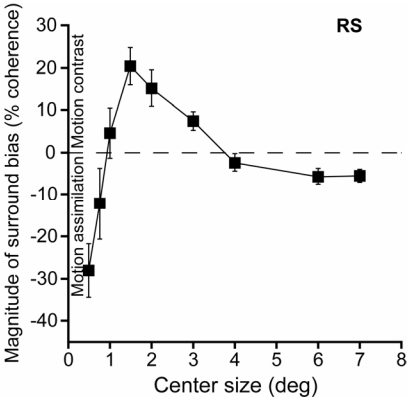

Fig. 3. The magnitude of surround bias obtained for various stimulus sizes. Stimulus was presented at 3 deg eccentricity. Surround diameter was always twice as large as center diameter. Dashed line indicates no surround bias. Positive and negative values indicate contrast and assimilation type bias respectively. Error bars indicate 95% confidence intervals as determined by a bootstrap method after fitting the data with a psychometric function.

Experiment 2: Motion onset differences for center and surround

In this experiment, we tested the effect of small differences in center and surround motion onsets on the strength of induced motion. The surround bias

was determined for seven different ones ranging from –24 to 24 ms in steps of 8 ms. Figure 4 summarizes the results of the three subjects. In general, delay-tuning curves were flat. Subjects had different absolute magnitudes of surround bias, but their bias in our measured range of delays did not depend on the surround delay. One subject (RS) also performed the experiment for foveal stimulus presentation, when the center diameter was 0.75 deg and the other stimulus parameters were identical to the parameters in Experiment 2. Foveal presentation showed no systematic difference in delay tuning (Fig. 4, RS foveal), except that surround bias was stronger, which increased the offset of the tuning curve.

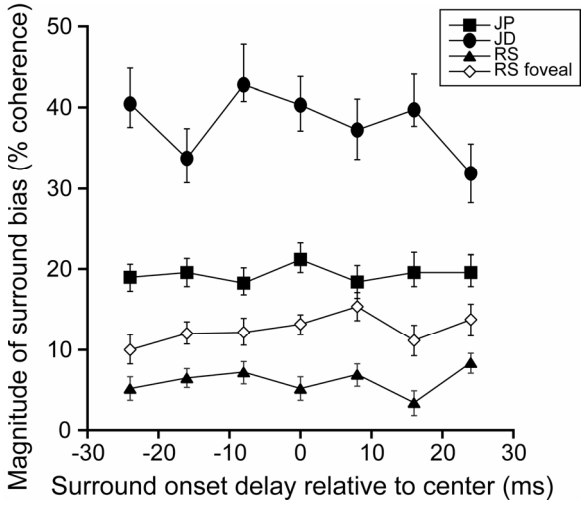

Fig. 4. The magnitude of surround bias obtained for various surround delays. Center was presented at 3 deg eccentricity at 1.5 deg center size (filled symbols). Open symbols indicate one experimental condition with stimulus presentation at the fovea and a 0.75 deg center size.

Discussion

The goal of the current study was to find out whether the strength of induced motion depends on precise timing of center and surround motion onset. Physiological studies have shown that the latency of surround responses in area MT is on average 16 ms longer than that for the center (Perge et al., 2005). If timing differences between receptive field centers and surrounds in area MT influence motion induction, we would expect an optimal surround bias for a delay difference of about -16 ms (surround preceding center). However, we found no clear optimum, indicating that the surround delay in area MT is of no consequence in our task.

The temporal resolution of our paradigm was 8 ms (the monitor frame duration). If the optimal surround delay were smaller than 8 ms, then we would expect a peak in the tuning curves at zero surround delay. Conversely, if the optimal surround delay were somewhat below or above our measured range of surround delays (<-24 ms or >24), we would expect an increase in bias at the lowest or highest measured surround delay, where the delay

approaches its optimal value. The fact that the tuning curves were flat could indicate that the absolute value of the optimal delay is much larger than 24 ms (<<-24 ms or >>24). However, we think that it is more likely that surround delay differences do not reveal themselves in relative motion perception. Any of these possibilities reject the linking hypothesis (Teller, 1980) between the delayed surround (16 ms) in motion sensitive area MT and relative motion perception.

Our center-surround stimulus is likely to activate MT center-surround neurons efficiently; therefore, we presumed that the properties of these neurons such as a delayed surround would be reflected more or less directly in the psychophysically measured surround bias. However, given our results, we cannot exclude the possibility that other motion areas without center-surround delay equally contribute to the psychophysical performance, and as a result cancel out the effect of delayed surrounds in MT. Another possibility for the negative results is that neurophysiological data on MT receptive fields were recorded in monkeys while our psychophysical experiments were done with humans. Despite the striking similarities between the human and monkey visual systems and motion detection capabilities, interspecies differences cannot be excluded.

Other possible explanations are differences in the visual stimulus, for instance, the eccentricity, which was three degrees in the human psychophysical experiments and on average 9±6 deg for the cells recorded in MT. Furthermore, it can not be excluded that MT neural responses are different when performing the psychophysical task due to attention and task specific effects. The only way to exclude all these interspecies, task dependent and stimulus dependent effects would be to record MT neurons in a monkey that is performing the psychophysical task. We do not believe that the negative results are due to the changing coherence level of the center. Response latency of MT neurons does not change considerably at decreasing motion coherence (van Wezel, unpublished observation). Finally, it is also possible that the timing of neural responses is not strictly related to perceptual timing (van de Grind, 2002).

Visual motion perception implies the existence of multiple operations, and these operations could be located at different levels of the visual system. Several properties of our motion perception such as relative motion detection are reflected in motion sensitive area MT (in the form of center-surround receptive fields). Other properties, such as relative insensitivity to short temporal delays of center and surround motion may be reflected at other levels of the visual system or as a result of multiple processes. This indicates

that well-defined physiological events such as center-surround delay do not have to strictly correspond to well-defined psychophysical effects.

References

Albright, T. D. (1984). Direction and orientation selectivity of neurons in visual area MT of the macaque. J Neurophysiol 52, 1106-1130.

Allman, J., Miezin, F., and McGuinness, E. (1985). Direction- and velocity-specific responses from beyond the classical receptive field in the middle temporal visual area (MT). Perception 14, 105-126.

Born, R. T., and Tootell, R. B. (1992). Segregation of global and local motion processing in primate middle temporal visual area. Nature 357, 497-499.

Britten, K. H., Shadlen, M. N., Newsome, W. T., and Movshon, J. A. (1992). The analysis of visual motion: a comparison of neuronal and psychophysical performance. J Neurosci 12, 4745-4765.

Britten, K. H., and Newsome, W. T. (1998). Tuning bandwidths for near-threshold stimuli in area MT. J Neurophysiol 80, 762-770.

Chang, J. J., and Julesz, B. (1984). Cooperative phenomena in apparent movement perception of random-dot cinematograms. Vision Res 24, 1781-1788.

Dubner, R., and Zeki, S. M. (1971). Response properties and receptive fields of cells in an anatomically defined region of the superior temporal sulcus in the monkey. Brain Res 35, 528-532.

Maunsell, J. H. R., and Van Essen, D. C. (1983). Functional properties of neurons in the middle temporal visual area (MT) of the macaque monkey: I. Selectivity for stimulus direction, speed and orientation. J Neurophysiol 49, 1127-1147.

Mikami, A., Newsome, W. T., and Wurtz, R. H. (1986). Motion selectivity in macaque visual cortex: II. Spatio-temporal range of directional interactions in MT and V1. J Neurophysiol 55, 1328-1339.

Murakami, I., and Shimojo, S. (1993). Motion capture changes to induced motion at higher luminance contrasts, smaller eccentricities, and larger inducer sizes. Vision Res 33, 2091-2107.

Murakami, I., and Shimojo, S. (1995). Modulation of motion aftereffect by surround motion and its dependence on stimulus size and eccentricity. Vision Res 35, 1835-1844.

Murakami, I., and Shimojo, S. (1996). Assimilation-type and contrast-type bias of motion induced by the surround in a random-dot display: evidence for center-surround antagonism. Vision Res 36, 3629-3639.

Nawrot, M., and Sekuler, R. (1990). Assimilation and contrast in motion perception: explorations in cooperativity. Vision Res 30, 1439-1451.

Perge, J. A., Borghuis, B. G., Bours, R. J., Lankheet, M. J., and van Wezel, R. J. (2005). Temporal dynamics of direction tuning in motion-sensitive macaque area MT. J Neurophysiol 93, 2104-2116.

Raiguel, S., Van Hulle, M. M., Xiao, D. K., Marcar, V. L., and Orban, G. A. (1995). Shape and spatial distribution of receptive fields and antagonistic motion surrounds in the middle temporal area (V5) of the macaque. Eur J Neurosci 7, 2064.

Ramachandran, V. S., and Cavanagh, P. (1987). Motion capture anisotropy. Vision Res 27, 97-106.

Reinhardt-Rutland, A. H. (1988). Induced movement in the visual modality: an overview. Psychol Bull 103, 57-71.

Teller, D. Y. (1980). Locus questions in visual science. In Visual coding and adaptability, C. S. Harris, ed. (Hilladale, New Jersey).

van de Grind, W. (2002). Physical, neural, and mental timing. Conscious Cogn 11, 241-264; discussion 308-213.

Xiao, D. K., Raiguel, S., Marcar, V., Koenderink, J., and Orban, G. A. (1995). Spatial heterogeneity of inhibitory surrounds in the middle temporal visual area. Proceedings of the National Academy of Sciences of the United States of America 92, 11303-11306.

Chapter 5

Direction specific spatial summation in motion sensitive area MST

János A. Perge, Kenneth H. Britten and Richard J. A. van Wezel

Abstract
Self-motion through a structured environment produces complex motion patterns on our retina, called optic flow. Visual processing of optic flow implies the existence of cortical mechanisms that sum local motion signals both over space and direction. We studied these summation mechanisms in medial superior temporal (MST) area of the macaque. This cortical area contains neurons with selectivity for optic flow components. We investigated whether summation depends on the relative difference in motion direction of two local motion inputs. We presented small, spatial Gabor functions moving simultaneously at nine different locations in the receptive field. At each Gabor location, we presented a pseudorandom sequence of brief motion impulses in any of four different directions independent from the other Gabor locations. This stimulus presentation allowed us to analyze a large number of Gabor combinations over both space and direction. We probed the mechanisms of summation by comparing the effect of Gabor pairs to the summed effect of their components. We found that summation is different if two local motion inputs are moving either to the same, orthogonal or opposite directions relative to each other. This direction dependent summation in MST indicates specific, context dependent selection of input signals. Such a mechanism could be the basis for increased specificity of MST neurons to complex motion patterns.

Introduction

The mammalian visual system is hierarchically organized into a succession of processing stages along the visual pathway. Receptive field size and complexity increase at higher processing stages. A comparison of middle temporal (MT) and medial superior temporal (MST) cortical areas is a clear example for this tendency. Neurons in MT respond selectively to the direction of local visual motion (Rodman and Albright, 1987). MT neurons supply afferents to area MST (Ungerleider and Desimone, 1986), which contains neurons responding selectively to optic flow components, such as expansion, contraction, clockwise or counterclockwise rotation (Sakata et al., 1985, 1986; Saito et al., 1986; Duffy and Wurtz, 1991a,b; Orban et al., 1992; Lagae et al., 1994; Orban et al., 1995; Geesaman and Andersen, 1996; Lappe et al., 1996; Heuer and Britten, 2004) and its linear combinations (Graziano et al., 1994). Because the receptive fields of MST neurons are substantially larger and more complex than that of their inputs (Lagae et al., 1994; Raiguell et al., 1997), MST neurons apparently integrate local motion signals from area MT neurons. However, it is not clear how exactly these complex receptive fields are build up from their simpler inputs.

One explanation for the selectivity of MST neurons for complex motion patterns is a template or mosaic model, in which local motion inputs in MT are lined up according to the preferred complex motion pattern of the MST cells (Tanaka et al., 1989; Duffy and Wurtz, 1991; Perrone and Stone, 1994; Lappe et al., 1996; Beintema and van den Berg, 1998; Royden, 2003;). These selected local motion inputs could be summed in a linear or a nonlinear fashion, depending only on the strength of the input signals, similar to what has been shown in area MT (Britten and Heuer, 1999; Heuer and Britten, 2002) and area MST (Recanzone et al., 1997). In contrast to these models, summation of local motion inputs could also depend on other properties such as the preferred direction of the local motion input signals. It is possible that summation is dependent on specific combinations of local motion signals that are characteristic to complex motion patterns. These interactions would increase the cell's selectivity for complex motion. These properties are suggested because it has been shown for instance that most MST neurons respond to complex motion patterns but not all to the separate local components of those patterns (Duffy and Wurtz, 1991). In this paper we will investigate whether besides linear summation and general non-linearities, interactions between different local motion directions occur in MST.

To test whether MST responses are summed in a direction specific manner we measured the summation properties of MST cells for multiple local stimuli moving in different directions. We presented stimuli moving

simultaneously in four different directions (left, right, up and down) at different locations within the receptive field. A large variety of possible pairs of local motion inputs was constructed this way. The simultaneous stimulation paradigm allowed us to examine the effect of a large number of stimulus combinations, which would be difficult if these combinations were presented individually. In this study, we examined if summation of stimulus pairs moving either in the same, orthogonal or opposite direction would be different from each other. The differences in summation that we report could be the basic mechanism that, besides linear summation, makes MST neurons even more selective for specific complex motion patterns.

Methods

Preparation

This study used three adult female rhesus macaques (*Macaca mulatta*). Before recording, each had been trained to fixate stationary targets in the presence of visual stimuli. Each was implanted with a scleral search coil (Judge et al., 1980) and equipped with a stainless steel head restraint post and recording cylinder located over the occipital cortex. A plastic grid secured inside this cylinder provided a coordinate system of guide tube support holes at 1 mm intervals (Crist et al., 1988). Animal procedures complied with the Institute for Laboratory Animal Research Guide for the Care and Use of Laboratory Animals and were approved by the University of California Davis Animal Care and Use Committee.

On recording days, guide tubes were inserted transdurally through these holes, and Parylene-insulated tungsten microelectrodes were inserted through the guide tubes. Initial mapping penetrations located the superior temporal sulcus (STS) and identified approximate boundaries of the motion-sensitive areas in its depths. MST was identified according to previously published methods (Celebrini and Newsome, 1994). To identify the STS, we used a combination of anatomical and physiological landmarks, including the depth from the brain surface, grey matter/white matter transitions, sulcus crossings and response properties. Within the STS, we located and mapped MT on the posterior bank, using its well-understood and consistent retinotopy and responses for physiological confirmation. MST was encountered after crossing the STS to its anterior bank and was identified by large receptive fields that often included the fovea or extended substantially into the ipsilateral hemifield. In addition, cells on the anterior bank often showed MST-like stimulus selectivities, preferring rapidly moving stimuli and complex optic flow stimuli. All recordings reported here came from penetrations in which the lumen of the STS were crossed and thus most likely from the dorsal subdivision of MST (MSTd). Histological verification

of recording sites has not yet been obtained, as all three monkeys are still being used in related experiments.

Once MST was localized, we would record and isolate activity using standard extracellular methods. Electrode signals were amplified and filtered, and single spikes were converted to digital pulses, whose time of arrival would be recorded with 1 msec resolution using the public domain software package REX (Hays et al., 1982). Search stimuli were chosen to match local multiunit preferences and could be moving bars, dot fields, or Gabor motion impulse stimuli. Once a cell was isolated, its receptive field location was crudely mapped using hand-held, moving bar stimuli, and quantitative testing commenced.

Stimuli.
All stimuli were presented on the face of a cathode ray terminal monitor, subtending 80° horizontally by 60° vertically (1280 x 1024 pixels), operating at a vertical refresh rate of 72 Hz and at a distance of 23 cm. Stimuli were generated by a Pentium personal computer running custom software hosting an ATI Technologies (Thornhill, Ontario, Canada) Mach 64 video card, running in 8 bit mode. Screen luminance was measured as a function of gray scale value using a Tektronix (Wilsonville, OR) photometer, fitted with a cubic polynomial; this was inverted to establish a linearized, gray scale lookup table. Average screen luminance was set to 30 cd/M^2, and maximum achievable contrast was effectively 100% (background luminance was 0.1 cd/M^2).

Stimuli for these experiments were similar to those described by Britten and Heuer (1999) and Heuer and Britten (2002). Stimuli were moving, two-dimensionally oriented "motion impulses," whose spatial luminance function was a Gabor function, or the product of a sine wave and a Gaussian function. These are members of the family that Watson refers to as "generalized Gabors" (Watson and Turano, 1995), which have the property that both the carrier (the sine wave) and the Gaussian contrast envelope are free to move. In our case, carrier and envelope moved together in one of four different directions. The motion directions were always horizontally left or right, or vertically up and down on the screen. The space–time luminance was described by the function:

$$L(x,y,t) = C(t) * \exp\left[-\frac{(x-\mu_x)^2}{\sigma_x^2}\right] * \exp\left[-\frac{(y-\mu_y)^2}{\sigma_y^2}\right] * \sin(\omega x) \quad (1)$$

where (μ_x, μ_y) are the instantaneous location of the center of the impulse, and (σ_x,σ_y) describe its dimensions. The constant ω establishes the spatial frequency of the carrier. The *x* coordinate of the center of the impulse moved linearly in time, and the spatial offset per frame was usually set to one-fourth of the cycle of the carrier. The contrast function *C*(*t*) was a trapezoid spanning seven frames (98 msec) as illustrated in Figure 1 of Britten (1999). The values for these parameters were 1.07 cycles/deg carrier spatial frequency, 18 Hz temporal frequency, σ_x= 0.56°, and σ_y= 1.12. We used these same stimulus settings for all recordings. The diameter of the Gabor functions was 1.5 deg.

Nine of these Gabor motion impulses were positioned along a grid as shown in Fig. 1. We used the same stimulus configuration and dimensions for all cells. The stimulus grid subtended an area of 12.5x12.5 deg, and was positioned on the most active part of the receptive field of the cell. The direction of each individual Gabor motion impulse was chosen randomly out of the four possible motion directions. All nine Gabor motion impulses were moving simultaneously during the trials.

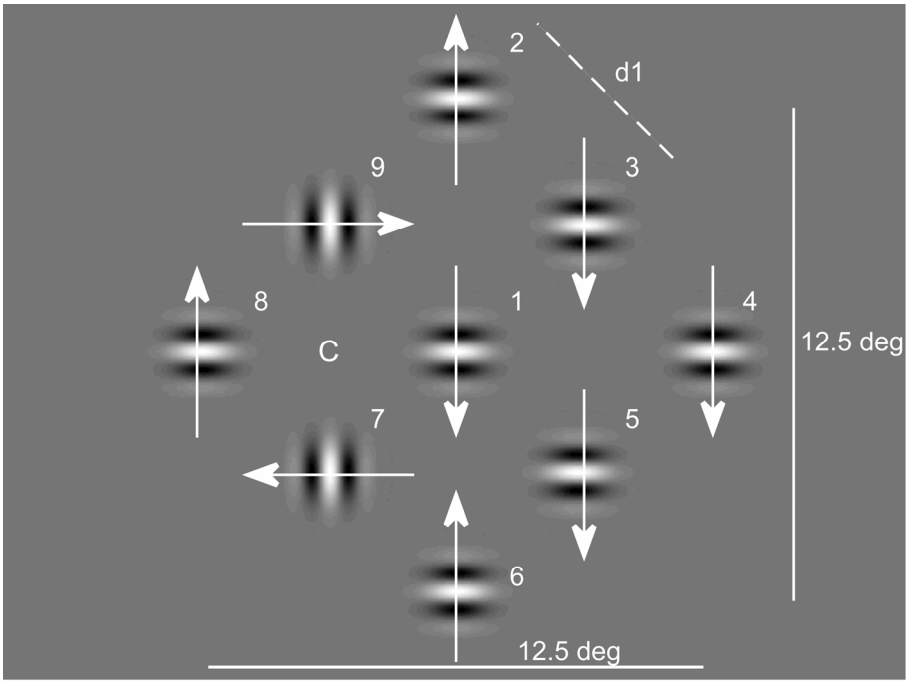

Fig. 1. Illustration of the stimulus field. Individual Gabor motion impulses (as described in the Methods Section) were presented at nine different locations simultaneously according to the configuration indicated in the figure. Each individual Gabor motion impulse could move in four different motion directions, either horizontally left or right or vertically up or down on the screen. The direction of motion for each Gabor motion impulse was chosen randomly and independently. The arrows show a possible combination of motion directions during one motion impulse as indicated by the arrows. The label d_1 indicates the closest distance between two Gabors (4.4 deg). Numbers indicate the reference number of the locations. Each motion impulse lasted 98 msec, which was followed by a 27 ms long blank period when only the gray background was presented. Motion impulses were presented 30 times during one trial, with each time a new randomly-chosen combination of motion directions.

Between each Gabor motion impulse two monitor frames were intervening, which results in a total Gabor motion impulse duration of 125 msec. Gabor motion impulse stimuli were presented sequentially. Single trials consisted of 30 Gabor motion impulse stimuli sequentially with a total duration of 3.8 seconds. The monkey was required to hold fixation during this trial duration and was rewarded for correctly maintaining fixation. There was no inter trial interval, and the monkey was trained to hold fixation over multiple trials. The final motion impulse in trials in which fixation was broken was discarded from subsequent analysis. The trials were run for as long as the cell could be held. In the dataset that we report here, each direction at each location was presented at least 492 times, and on average 2770 times.

Results

We recorded 57 MST neurons in three adult female macaques. The stimulus field consisted of nine Gabor motion impulses arranged along a grid as shown in Fig. 1. The motion directions of the Gabor impulses were randomly chosen and independent from each other. The directions were always either horizontally left or right, or vertically up or down. First, we will document the average response to a single Gabor motion impulse at one location and in one direction; then, we will turn to responses to Gabor pairs.

Response to single Gabor

Before we investigate how responses vary across the receptive field we need to establish an appropriate time window for measuring responses. We calculated the "grand average" PSTH for all cells and all stimulus presentations (Fig. 2). We averaged the responses of each cell for any stimuli and determined the maximal response in the average. We used this maximal response to normalize the cell's response to any stimulus. These normalized responses were then averaged over all cells to produce the histogram. As Fig. 2 shows, response onset starts ~60 ms after stimulus onset, reaches a peak at ~80 ms and decays until ~180 ms, when the response to the following stimulus starts. Notice that the lowest response (~0.62) is still high compared to the dynamic range of the responses (~0.62 - 0.8). This activity does not correspond to spontaneous activity, but is due to the average responses to all stimuli, temporal summation of subsequent stimuli and the different response latencies of individual neurons. Responses to the previous and following stimuli are based on a similar but not completely identical dataset, because the monkey breaks fixation. We chose a time window from 60 to 160 ms to analyze all of the neurons (as indicated in the figure by vertical lines). This way we avoid selecting individual windows for each neuron, which can be unreliable or subjective.

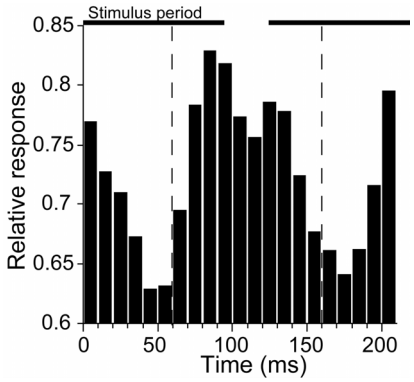

Fig. 2. The time course of responses for the total population. We averaged the responses of each cell for any stimuli and determined the maximal response in the average. We used this maximal response to normalize the cell's response to any stimulus. These normalized responses were than averaged over the whole population to produce the histogram. The vertical dashed lines indicate the boundaries of the temporal window used to calculate average response rates. The bold horizontal line indicates the stimulus period.

Next, we investigated the dependence of responses on location and direction for each cell separately. Figure 3 shows results for an example cell. It illustrates the average response after a specific stimulus occurrence at nine Gabor locations and for four different motion directions. This neuron showed higher activity when a motion direction to the left was presented at nearly all of the nine locations (bottom left panel). For this cell the middle location had the strongest direction selective response. Note that during the experiment, all nine locations were stimulated simultaneously with randomly chosen stimulus directions. Therefore, the calculated average response for each field is a result of the stimulus direction in the corresponding location plus the average response to the randomly-chosen stimulus directions at all other locations. Due to the simultaneous stimulation at multiple locations, these responses are not identical to firing rates evoked by individual Gabors presented alone at different locations. However, these results reveal the spatial dynamic range of the neuron, and its direction tuning at different spatial locations.

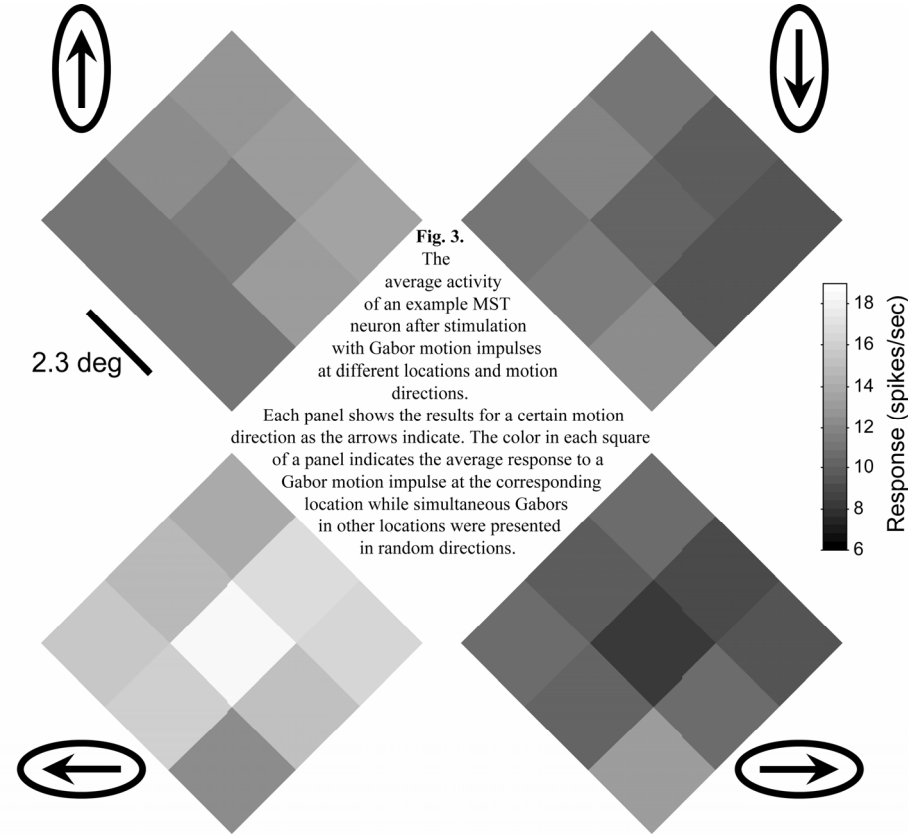

Fig. 3. The average activity of an example MST neuron after stimulation with Gabor motion impulses at different locations and motion directions. Each panel shows the results for a certain motion direction as the arrows indicate. The color in each square of a panel indicates the average response to a Gabor motion impulse at the corresponding location while simultaneous Gabors in other locations were presented in random directions.

It is important to note that the stimulus was not completely balanced, because directions were randomly chosen. The number of stimulus occurrences of one or another direction could be different at a certain location, due to chance variation. However, this unbalance was relatively small compared to the average number of stimulus presentations. To quantify this, we calculated the chance variation (CV) of the stimulus for each cell and stimulus location according to the form:

$$CV = \left(\frac{Count_{\max} - Count_{\min}}{Count_{mean}} \right) * 100 \quad (2)$$

where $Count_{max}$ and $Count_{min}$ indicate the number of presentations of the most often and the least often presented stimulus directions. $Count_{mean}$ indicates the average occurrence of Gabors in any direction. Thus CV expresses the difference between the smallest and largest stimulus occurrence as a percentage of the average stimulus occurrence in any direction. The average CV in the population was 4.3±2.4%, and the most extreme CV for a cell at one Gabor location was 15%.

Response to Gabor pairs

Based on the same data that was used to calculate responses to single Gabors we calculated responses to a combination of two Gabors. Similar to the response to a single Gabor, these average responses are the result of the response to the Gabor pair plus the average response of simultaneously-presented Gabors at other locations to random directions. Both Gabors in the pair could move to any of the four directions and could be presented at any of the nine Gabor locations, resulting in a total number of 1152 possible Gabor pairs. Note that the combination of a location with itself is not included in this subset.

Since Gabors were presented randomly, the number of repetitions for different combinations could be slightly different, and the actual number depended on the duration of the experiment. One specific Gabor pair was presented minimally 102 times and on average 757 times. Similarly to the single Gabor responses, we calculated CV for the Gabor pairs as well, to give an indication about how balanced the stimulus presentation was (equation 2). In this case, $Count_{max}$, $Count_{min}$ and $Count_{mean}$ refer to the occurrence of specific direction combinations rather than directions. The average CV for Gabor pairs was 15±5% and the most extreme CV was 39%. However, even in this case the least number of presentations for a Gabor pair was 185 times.

The main goal of these experiments was to compare responses to Gabor pairs with predicted responses based on the sum of the responses of the same Gabors presented individually. However, there are two reasons why this comparison is not identical to previous summation measurements when predictions to Gabor pairs were based on Gabors presented alone (Britten and Heuer, 1999). First, a substantial part of the response in our measurements is due to Gabors presented at other locations in random directions, resulting in a high baseline activity (see Fig. 2). Second, and more importantly, single responses and pair responses in our paradigm are not independent. Single responses are the result of one particular Gabor combined with all other Gabors, and thus all possible pairs are represented in the single response. Consequently, pair-responses are based on a subset of the single Gabor data.

General linear and nonlinear response summation properties of MT neurons, like a general static non-linearity (saturation) and those reported by Britten and Heuer (1999), re-scale our recorded single and pair responses equally. Therefore, our measurements will not reveal those general linear and nonlinear response properties. However, we are able to investigate nonlinear response summation properties by comparing predicted and measured pair-responses for specific Gabor combinations. As we will show, the relation between predicted and measured responses is different for specific subsets of Gabor combinations, dependent on the relative motion directions and position of the Gabor pairs. These differences indicate specific summation properties in MST that are highly nonlinear, since they depend on the relative directions and positions of the Gabor pairs.

We investigated the differences in response summation for Gabor pairs with same, orthogonal or opposite motion directions. First, we will only discuss the results for the most adjacent Gabor pairs, which were separated by a distance of 4.4 deg (d_1 in Fig. 1). Figure 1 shows examples of these adjacent Gabor pairs for same, orthogonal and opposite directions for locations 3-4, 6-7, and 5-6, respectively. For these most adjacent Gabor pairs, the motion directions are always 45 or 135 deg relative to the line that connects the two positions. The total number of these Gabor pairs in our stimulus is 192.

Figure 4 shows three cells, representative to the range of observations in our data set. In each panel we plotted the observed responses to simultaneous, adjacent Gabor pairs against the predicted response based on the sum of the component single responses. Since the average activity corresponding to the average response to any stimulus was the same for single Gabors and for Gabor pairs, it was necessary to subtract one average

activity from the prediction to bring it into a similar response range as the observed pair responses. The different direction combinations are indicated with different colors. After applying linear regression on the data of the three stimulus conditions separately, it is clear that different direction combinations have different slopes (Fig. 4A and B). In a purely linear system the slopes should be equal to one. The slope differences suggest that the response summation mechanism for different stimulus combinations is not the same.

The cell in Fig. 4C illustrates another characteristic, which we observed only in a small subset of the cells. The slopes for same, orthogonal and opposite direction combinations are very similar, but the linear regression lines are clearly shifted. This indicates that, for this neuron, the measured responses for same direction pairs are generally higher than predicted and for opposite direction pairs generally smaller. The data points are shifted not only for low or high, but in the total range of responses, indicating that the difference in summation mechanism for same and opposite direction is not related to the response level itself. This neuron was one of the clearest examples of this shift; most other neurons only showed slope differences.

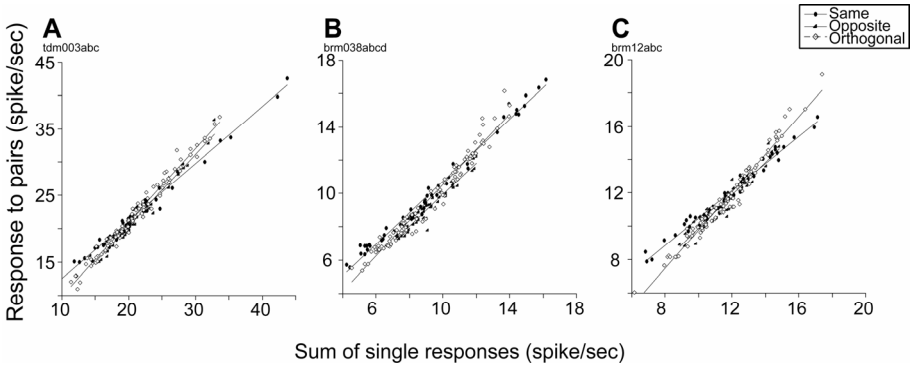

Fig. 4. Summation mechanisms are different for same, orthogonal or opposite direction combinations. Each symbol indicates the measured and predicted response for a pair of adjacent Gabors. Measured responses for Gabor pairs correspond to the average response to certain combinations of two Gabor motion impulses while other stimulus directions in other locations were randomly presented. Predicted responses correspond to the sum of the responses to individual Gabors. The large crosses indicate the average activity to all stimuli. A: Slope for orthogonal direction is the steepest, and same direction is the shallowest. B: Slopes for opposite and orthogonal directions are similar, while the slope for the same direction condition is shallower. C: Opposite directions show lower response than same directions.

To evaluate if two regression lines are significantly different from each other we compared the fit residuals of two linear regressions to the fit residuals of one regression on both groups of points. Evidently, fit residuals

of one linear regression will be larger than residuals for two regressions, because the number of parameters for one regression is less. We used an F-test to evaluate whether the worsening of the fit for one regression is significant, derived under the null hypothesis that the two groups of points are falling on the same line. We performed the test for the combination of any regression lines separately (same/orthogonal, same/opposite and opposite/orthogonal pairs). All of the three example cells in Fig. 4 showed a statistically significant difference between any of two regression lines (F-test, $p<0.05$). For 75% of the cells there was a significant difference between the regression lines of same and orthogonal pairs. For same/opposite and opposite/orthogonal comparison these values were smaller (56% and 38% respectively).

Figure 5 shows the slopes for the three different direction combinations for the whole population. This figure does not only show the slopes for different Gabor pairs, but also how these slopes are related to each other within a cell. The population as a whole shows steeper slopes, higher than 1 for orthogonal (1.07 ± 0.06) pairs and slopes, smaller than 1 for same direction pairs (0.90 ± 0.09). The slopes for opposite directions was on average 0.99 ± 0.11. Slopes for all three directional combinations were statistically significantly different from each other (ANOVA, $p<<0.01$). There was a negative correlation between slopes for same direction pairs and orthogonal direction pairs (Fig. 5A, $r =-0.62$, $p<0.01$) and a weaker, though statistically significant negative correlation between slopes for same/opposite and opposite/orthogonal direction pairs (Fig. 5B, $r =-0.39$ and -0.34 respectively, both p values < 0.05). Filled symbols indicate a statistically significant difference between the two regression lines (F-test, $p<0.05$), according to the statistical method described in the previous paragraph.

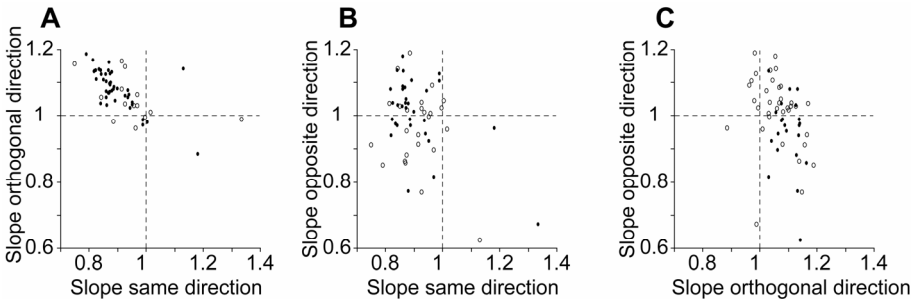

Fig. 5. The slopes of linear regression lines between predicted and measured responses of pairs of Gabors. Each symbol indicates one neuron. A: Slopes for same and opposite direction conditions are negatively correlated. ($r = -0.62$, $p<0.01$) B: Slopes of same and opposite direction conditions are weakly negatively correlated ($r = -0.39$, $p<0.05$). C: Slopes for orthogonal and opposite direction conditions are weakly negatively correlated ($r = -0.34$, $p<0.05$).

Effect of distance

All the preceding analysis was based on pairs of Gabor stimuli, which were the closest to each other. In the following, we investigate the spatial dependence of the spatial summation differences, by describing the slopes of linear fits for the three direction combinations as a function of stimulus distance. The procedure of this analysis was similar to that described above for the most adjacent Gabors. For each stimulus distance, responses to Gabor pairs were plotted against the sum of the component single responses. Linear fits were obtained for same, orthogonal and opposite directional combinations separately.

Figure 6 plots the average slopes of the linear fits for same, orthogonal and opposite Gabor pairs as a function of stimulus distance. The differences between slopes were significantly different for immediately-adjacent Gabor pairs, which we already described in the previous paragraph (ANOVA, $p<0.01$). The slopes were not significantly different for larger stimulus distances, although we still found a significant difference at the largest measured distance of 9.8 deg. Note that because of our stimulus configuration, a different distance also means a change in directions relative to the line that connects the two pairs. Furthermore, the envelope of the Gabor motion impulses was moving, which causes slight differences in distances for the different direction combinations. Therefore, it is not clear from our measurements whether or not the large difference between d_1 and the other distances is a result of the change in distance or in configuration.

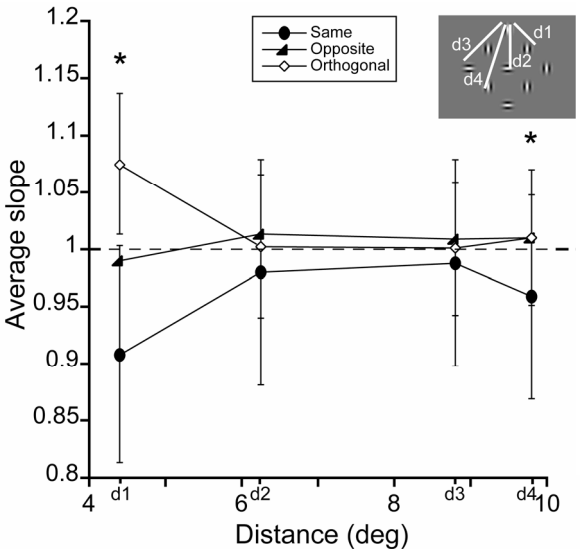

Fig. 6. The slopes of linear regression lines between predicted and measured responses of Gabor pairs as a function of distance. The distances are defined as the inset indicates. The distances for d_1 to d_4 in degrees are 4.4, 6.25, 8.83, and 9.8 deg respectively. The stars above d_1 and d_4 indicate significant differences between the three slopes (ANOVA, $p<0.01$).

Effect of time

We analyzed how the differences in summation mechanism for the three types of directional pairs evolve in time for the most adjacent pairs. We analyzed the slopes of same, opposite and orthogonal Gabor pairs during the time course of the responses. For this analysis, a 60 ms wide window was taken around a series of time points relative to stimulus onset. Figure 7 plots the average slopes as a function at corresponding time points. The average slope for same directions decreases from 1 to about 0.9 in about 100 msec and returns slowly back to 1. The average slopes for orthogonal directions have a similar time course but slopes get higher than 1 up to 1.07. The average slope for opposite directions changes in time. These results indicated different dynamic summation mechanisms for different relative directions.

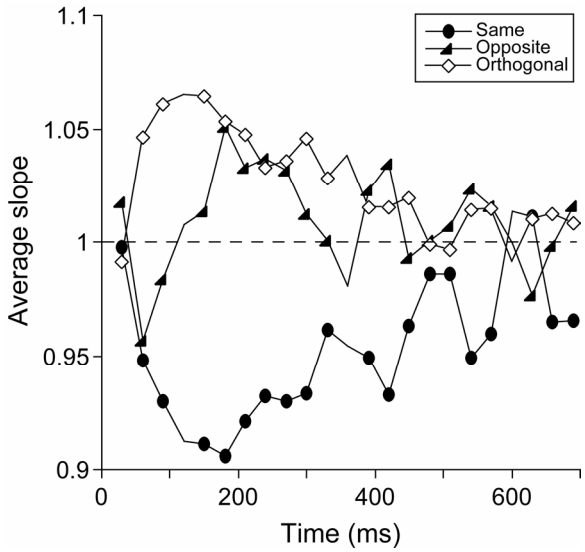

Fig. 7. The temporal development of the different summation properties for pairs of same, orthogonal and opposite direction combinations. The average slope was calculated from responses within a 60 ms wide window centered at different times during the response. Slopes were significantly different from each other at all delays except the first delay (ANOVA, $p<0.01$)

Relationship to tuning in spiral space

If our findings are related to the cell's sensitivity to complex motion patterns, we would expect that specific nonlinearities for directional combinations that we report here are correlated to the tuning of the cells in spiral space (Graziano et al., 1994; Heuer and Britten, 2004). Therefore, we calculated direction indices in spiral space for each neuron.

Since Gabors were presented simultaneously, specific complex motion patterns of four Gabor motion impulses occurred spontaneously. Four Gabor motion impulses can move expanding, contracting or in clockwise or counterclockwise rotation. Those specific combinations occured at least 27 times and on average 217 times at five different locations in the stimulus field. The motion vectors around letter "C" in Fig. 1 illustrate an example of such a complex pattern (clockwise rotation). We calculated the average response after the occurrence of four different complex motion patterns; clockwise rotation, counterclockwise rotation, expanding and contracting patterns. Data for the same complex pattern but at different locations were pooled together. It has been reported that spiral space tuning measured this way correlates strongly with spiral space measurements with four Gabor motion impulses presented alone (not imbedded in simultaneously presented 5 other Gabor motion impulses) or with moving random dots (van Wezel and Britten, 1997).

The Direction Index (DI) for the tuning in spiral space for each cell was calculated based on these four responses by using the method of Baker et al. (1981):

DI = 1 – (non-preferred direction in spiral space / preferred direction in spiral space) (4)

Since we found the largest differences between the regression lines of same and orthogonal direction pairs, we choose the test statistic of the F-test for same/orthogonal regression lines to compare it to the direction index (Fig. 8). Though there was a large variation both in the direction index and the F-value, we found a statistically significant correlation between the cell's sensitivity to specific Gabor combinations and complex motion patterns ($r = 0.39$, $p<0.01$). This indicates that the specific interactions that we describe could be the underlying mechanism for strong selectivity to complex motion in MST neurons.

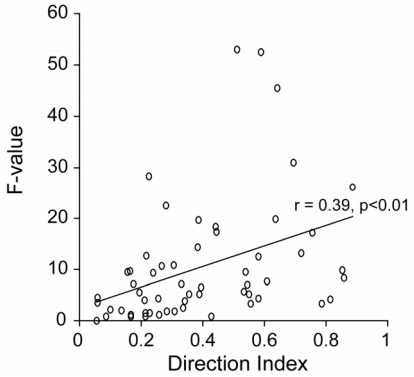

Fig. 8. Differences between same and opposite direction summation are positively correlated to the neuron's sensitivity to complex motion patterns. Each symbol indicates one neuron. The Direction Index corresponds to the cell's tuning in spiral space (see Formula 4. in the Results section). The F-value indicates the difference between same and orthogonal regression lines as indicated in Fig. 4. Larger F-values correspond to larger differences.

Discussion

We investigated spatial summation properties of different stimulus directions within MST receptive fields. Our method does not allow us to test general nonlinearities that operate similarly between a wide range of input signals. However, our analysis can capture specific interactions that might occur, for instance, between certain stimulus locations or by a specific timing of multiple signals. We measured the responses for pairs of Gabors moving in the same, orthogonal or opposite directions. We compared these responses to predicted ones based on the sum of responses to the individual motion directions. We found substantial and consistent differences between summation properties for the three direction combinations. In the following paragraphs we will discuss possible mechanisms causing these differences and their origins.

The slope differences for different Gabor pairs cannot be explained by firing rate dependent general nonlinearities, for instance a static nonlinearity (saturation) at the output of an MST neuron. Other models, such as scaled nonlinear summation models or normalization models (Britten and Heuer, 1999; Recanzone et al., 1997) also fail to describe our data. In area MT and MST, such models have proven to explain summation of two local motion inputs in the same direction, but it can never explain the different summation properties we find when the direction pairs are opposite or orthogonal. To explain our results, such a summation model should include summation properties that are dependent on the angular difference between the two local motion inputs.

Possible sources

Direction specific interactions could arise from local circuits in area MST, at the input of the MST neurons or originate from an earlier processing stage. The spatial extent of the interactions that we find is rather localized (Fig. 6). This indicates that the interactions occur either at the input of the MST cells or at an earlier processing stage with smaller receptive field sizes; at MT, for instance. A similar measurement in MT that targets the summation properties of different stimulus directions could reveal if our results are a specific feature of MST neurons or of direction specific interactions originating from earlier levels.

Slopes for opposite and orthogonal pairs are more similar to each other than are slopes for opposite and same pairs (Fig. 5). This excludes the possibility that the results are only due to orientation differences of the Gabors. When Gabor pairs are presented in the same or opposite directions, the orientations of the Gabors are the same. Therefore, if results were due to interactions between differently tuned cells located, for instance, in V1, we would expect that slopes for the same and opposite direction pairs are more similar than slopes for same and orthogonal pairs, which is not the case. If results were related to cross-orientation inhibition mechanisms (e.g. Blakemore and Tobin, 1972; Kapadia et al., 2000) between the Gabor motion impulses, we would expect that orthogonal Gabor combinations would show the shallower slopes, which it also not the case.

MT cells respond the most to their preferred direction, and in general, the responses are the lowest to the antipreferred direction, which is opposite to the preferred direction (Rodman and Albright, 1987). If our results were related to the tuning properties of MT neurons, we would expect larger differences between opposite and same direction pairs, and smaller differences between opposite and orthogonal pairs, which is exactly the opposite to our findings. The role of center-surround interactions in MT

(Xiao et al., 1995; Born, 2000) can be also excluded, because center-surround interaction is the strongest between opposite directions; therefore, we would expect the largest differences between slopes for the same and opposite direction pairs, and not between the same and orthogonal pairs. Both of these argue against the primary role of MT in the direction-specific interactions.

The most likely locus of direction-specific interactions is between MT and MST. Our results are in accordance with feedback models that assume dynamic feedback loops between MST and MT (Ambastha et al., 2004). In a feedback model, receptive fields are the representations of frequent or useful patterns in their input signals, learned by dynamic feedback loops. These mechanisms could result into the multiplicative and/or recruitement type of nonlinearities that we report, which increase the efficiency of MST neurons to detect complex stimuli. Furthermore, it could explain why certain stimulus combinations, which might be more informative about the complex motion pattern, are summed differently than others. These special mechanisms could be essential for MST to be able to play its important role in complex motion analysis tasks like structure from motion processing (Bradley et al., 1998; Sugihara et al., 2002) and heading detection from optic flow information (Britten and van Wezel, 1998, 2002).

Acknowledgements
We thank Bert van den Berg, Martin Lankheet, André Noest and Henk P. van Wijk for helpful discussions.

References

Ambastha, M., Logan, D., Ballard, D. H., and Duffy, C. J. (2004). Spatial summation data from cortical motion area MST is explained by feedback. Neuroscience 2004 poster.

Baker, J. F., Petersen, S. E., Newsome, W. T., and Allman, J. M. (1981). Visual response properties of neurons in four extrastriate visual areas of the owl monkey (Aotus trivirgatus). J Neurophysiol 45, 397-416.

Beintema, J. A., and van den Berg, A. V. (1998). Heading detection using motion templates and eye velocity gain fields. Vision Res 38, 2155-2179.

Blakemore, C., and Tobin, E. A. (1972). Lateral inhibition between orientation detectors in the cat's visual cortex. Exp Brain Res 15, 439-440.

Born, R. T. (2000). Center-surround interactions in the middle temporal visual area of the owl monkey. J Neurophysiol 84, 2658-2669.

Bradley, D. C., Chang, G. C., and Andersen, R. A. (1998). Encoding of three-dimensional structure-from-motion by primate area MT neurons. Nature 392, 714-717.

Britten, K. H., and Heuer, H. W. (1999). Spatial summation in the receptive fields of MT neurons. J Neurosci 19, 5074-5084.

Britten, K. H., and Van Wezel, R. J. (2002). Area MST and heading perception in macaque monkeys. Cereb Cortex 12, 692-701.

Celebrini, S., and Newsome, W. T. (1994). Microstimulation of extrastriate area MST influences perceptual judgements of motion direction. Invest Ophthal Vis Sci 35, 1828.

Crist, C. F., Yamasaki, D. S. G., Komatsu, H., and Wurtz, R. H. (1988). A grid system and a microsyringe for single cell recording. J Neurosci Meth 26, 117-122.

Duffy, C. J., and Wurtz, R. H. (1991). Sensitivity of MST neurons to optic flow stimuli. I. A continuum of response selectivity of large-field stimuli. J Neurophysiol 65, 1329-1345.

Duffy, C. J., and Wurtz, R. H. (1991). Sensitivity of MST neurons to optic flow stimuli. II. Mechanisms of response revealed by small-field stimuli. J Neurophysiol 65, 1346-1359.

Geesaman, B. J., and Andersen, R. A. (1996). The analysis of complex motion patterns by form/cue invariant MSTd neurons. J Neurosci 16, 4716-4732.

Graziano, M. S. A., Andersen, R. A., and Snowden, R. J. (1994). Tuning of MST neurons to spiral motions. J Neurosci 14, 54-67.

Hays, A. V., Richmond, B. J., and Optican, L. M. (1982). A UNIX-based multiple process system for real-time data acquisition and control. WESCON Conf Proc 2, 1-10.

Heuer, H. W., and Britten, K. H. (2002). Contrast dependence of response normalization in area MT of the rhesus macaque. J Neurophysiol 88, 3398-3408.

Heuer, H. W., and Britten, K. H. (2004). Optic flow signals in extrastriate area MST: comparison of perceptual and neuronal sensitivity. J Neurophysiol 91, 1314-1326.

Judge, S. J., Richmond, B. J., and Chu, F. C. (1980). Implantation of magnetic search coils for measurement of eye position: An improved method. Vision Res 20, 535-538.

Kapadia, M. K., Westheimer, G., and Gilbert, C. D. (2000). Spatial distribution of contextual interactions in primary visual cortex and in visual perception. J Neurophysiol 84, 2048-2062.

Lagae, L., Maes, H., Raiguel, S., Xiao, D. K., and Orban, G. A. (1994). Responses of macaque STS neurons to optic flow components: a comparison of MT and MST. J Neurophysiol 71, 1597-1626.

Lagae, L., Maes, H., Raiguel, S., Xiao, D. K., and Orban, G. A. (1994). Responses of macaque STS neurons to optic flow components: a comparison of MT and MST. J Neurophysiol 71, 1597-1626.

Lappe, M., Bremmer, F., Pekel, M., Thiele, A., and Hoffmann, K. P. (1996). Optic flow processing in monkey STS: a theoretical and experimental approach. J Neurosci 16, 6265-6285.

Orban, G. A., Lagae, L., Verri, A., Raiguel, S., Xiao, D., Maes, H., and Torre, V. (1992). First-order analysis of optical flow in monkey brain. PNAS 89, 2595-2599.

Perrone, J. A., and Stone, L. S. (1994). A model of self-motion estimation within primate extrastriate visual cortex. Vision Res 34, 2917-2938.

Raiguel, S., Van Hulle, M. M., Xiao, D. K., Marcar, V. L., Lagae, L., and Orban, G. A. (1997). Size and shape of receptive fields in the medial superior temporal area (MST) of the macaque. Neuroreport 8, 2803-2808.

Recanzone, G. H., Wurtz, R. H., and Schwarz, U. (1997). Responses of MT and MST neurons to one and two moving objects in the receptive field. J Neurophysiol 78, 2904-2915.

Rodman, H. R., and Albright, T. D. (1987). Coding of visual stimulus velocity in area MT of the macaque. Vision Res 27, 2035-2048.

Saito, H., Yukie, M., Tanaka, K., Hikosaka, K., Fukada, Y., and Iwai, E. (1986). Integration of direction signals of image motion in the superior temporal sulcus of the macaque monkey. J Neurosci 6, 145-157.

Sakata, H., Shibutani, H., Kawano, K., and Harrington, T. L. (1985). Neural mechanisms of space vision in the parietal association cortex of the monkey. Vision Res 25, 453-463.

Sakata, H., Shibutani, H., Ito, Y., and Tsurugai, K. (1986). Parietal cortical neurons responding to a rotary movement of visual stimulus in space. Exp Brain Res 61, 658-663.

Tanaka, K., Fukada, Y., and Saito, H. (1989). Underlying mechanisms of the response specificity of expansion/contraction and rotation cells in the dorsal part of the medial superior temporal area of the
Macaque monkey. J Neurophysiol 62, 642-656.

Ungerleider, L. G., and Desimone, R. (1986). Projections to the superior temporal sulcus from the central and peripheral field representations of V1 and V2. J Comp Neur 248, 147-163.

van Wezel, R. J. A., and Britten, K. H. (1997). Spatial interactions of translational motion impulses in area MST of the macaque monkey. Society for Neuroscience, 23, 15 (abstract).

Watson, A. B., and Turano, K. (1995). The optimal motion stimulus. Vision Research 35, 325-336.

Xiao, D. K., Raiguel, S., Marcar, V., Koenderink, J., and Orban, G. A. (1995). Spatial heterogeneity of inhibitory surrounds in the middle temporal visual area. Proceedings of the National Academy of Sciences of the United States of America 92, 11303-11306.

Summary and Conclusions

Cortical middle temporal (MT) and medial superior temporal (MST) areas play an important role in visual motion processing. We studied how neurons within these areas contribute to visual motion integration and segregation. Therefore, we investigated the response properties of the cells for multiple visual stimuli in space and time. We found evidence that MT and MST neurons integrate multiple motion signals in both space and time. The results present new insights on the mechanisms of motion integration and segregation.

First, we studied how direction selectivity of area MT cells changes in time. We found that in general the neurons respond the most actively when moving stimuli change direction from the antipreferred to the preferred direction. In addition, they are generally more responsive when sudden changes in motion directions occur, irrespective of the preferred direction of the cells. This indicates that the cells are sensitive to temporal motion contrast. This property might be behaviorally relevant for the detection of sudden changes in the visual environment.

We mapped direction selectivity of MT cells in space and in time in another set of experiments. These maps revealed center-surround receptive field organization in MT. Center-surround receptive fields make MT cells specifically sensitive to motion contrast in the spatial domain. This property might be perceptually relevant, for instance, in the segmentation of moving objects from their background. We found that the ability of MT cells to signal motion differences in space and time should be attributed to different mechanisms. Furthermore, we showed that the effect of antagonistic surround is slower than that of the center. The delayed surround might be the result of cortical computations related to the processing of motion segregation.

The neurophysiological results in MT inspired us to investigate the perceptual consequences of delayed antagonistic surrounds in human motion perception. Our assumption was that the activity of center-surround neurons is reflected in our percept of relative motion. However, we found no evidence for a relation between the observed neural characteristics and human motion perception.

Visual processing of optic flow implies the existence of cortical mechanisms that sum local motion signals both over space and direction. We investigated how spatial motion integration in area MST depends on the relative difference in motion direction of the local input signals. We found that summation is different if two local motion inputs are moving either to the same, orthogonal or opposite directions relative to each other. This

direction dependent summation in MST indicates specific, context dependent selection of input signals. Such a mechanism could be the basis for increased specificity of MST neurons to complex motion patterns.

The results of this thesis shed more light on the question how cortical neurons process visual motion and how they integrate or segregate multiple motion signals. This information is crucial for a better understanding on intriguing questions such as how visual information projected on the retina is transformed into visual perception and how this information is used by organisms to freely move around in a complex environment.

Nederlandse samenvatting

De medio-temporaalkwab (midden van de slaapkwab; MT) en de medio-superiore temporaalkwab (midden-boven van de slaapkwab; MST) zijn twee gebieden in de hersenschors die een belangrijke functie hebben bij de verwerking van visuele bewegingsinformatie. Wij hebben onderzocht welke rol zenuwcellen (= neuronen) in deze gebieden spelen bij de integratie en segregatie van visuele beweging. Hiervoor hebben we de respons van deze neuronen in de tijd gemeten terwijl we meerdere visuele stimuli tegelijkertijd aanboden. Uit de resultaten blijkt dat zenuwcellen in MT en MST meerdere bewegingssignalen zowel spatieel als temporeel integreren. Onze bevindingen geven een nieuw inzicht in de mechanismen van integratie en segregatie bij de verwerking van bewegingsinformatie door het visuele systeem.

Eerst hebben we bestudeerd hoe de richtingsgevoeligheid van MT neuronen verandert in de tijd. We hebben aangetoond dat neuronen het meest actief zijn wanneer een bewegende stimulus verandert van de niet-voorkeursrichting naar de voorkeursrichting van de onderzochte cel. Verder hebben we gevonden dat de neuronen een hogere activiteit vertonen wanneer de richting van beweging plotseling verandert, onafhankelijk van de voorkeursrichting van de cellen. Deze bevindingen laten zien dat deze cellen gevoelig zijn voor temporeel bewegingscontrast. Deze eigenschap kan gebruikt worden door de hersenen om plotselinge veranderingen in het visuele veld te detecteren.

In een ander experiment hebben we onderzocht hoe de bovenstaande eigenschap met betrekking tot de richtingsselectiviteit van MT zenuwcellen in de tijd zich spatieel (= ruimtelijk) gedraagt. Dit experiment brengt de centrum-omgeving structuur van de receptieve velden in kaart. Een centrum-omgeving structuur maakt MT cellen gevoelig voor bewegingscontrast in het spatiële domein. Deze eigenschap zou kunnen bijdragen tot het detecteren van een object ten op zichte van de achtergrond. We hebben gevonden dat de mechanismen voor de verwerking van spatiële en temporele bewegingscontrast verschillen. Daarnaast laten onze resultaten zien dat de latentie van het omgevende receptieve veld groter is dan die van het centrale receptieve veld. Deze vertraagde input naar de omgeving zou het resultaat kunnen zijn van signaalverwerking in de cortex die gerelateerd is aan segregatie van visuele beweging.

De hierboven beschreven neurofysiologische resultaten inspireerden ons om te onderzoeken hoe de gevonden eigenschappen van MT zenuwcellen het bewegingspercept bij mensen beïnvloeden. We hebben de hypothese getest dat de vertraagde input naar de omgeving een effect zou moeten hebben op het zien van relatieve beweging. Echter we hebben in onze experimenten geen relatie kunnen vinden tussen de eigenschappen van MT zenuwcellen en het bewegingspercept bij mensen.

De verwerking van de retinale beelden (= visuele informatie zoals die op het netvlies valt) die worden opgewekt door eigenbeweging (‘optic flow’) suggereert dat in de hersenschors lokale bewegingsinformatie zowel temporeel als spatieel wordt geïntegreerd. In een 4^{e} experiment hebben we onderzocht hoe de spatiële integratie van bewegingssignalen in het gebied MST afhangt van het verschil in bewegingsrichting van twee lokale bewegingsinputs. We hebben gevonden dat sommatie eigenschappen verschillen voor dezelfde, orthogonale en tegenovergestelde richtingen. Deze relatieve richtingsafhankelijke integratie in MST laat zien dat er een specifieke, context afhankelijke selectie van bewegingsinputs plaatsvindt. Een dergelijk mechanisme zou de basis kunnen zijn van de verhoogde gevoeligheid van MST zenuwcellen voor complexe bewegingspatronen.

De resultaten van dit proefschrift laten zien hoe zenuwcellen in de hersenschors visuele bewegingsinformatie verwerken en hoe ze meerdere inputs integreren en segregeren. Deze bevindingen zijn relevant voor een beter begrip van intrigerende vragen, zoals hoe de visuele informatie die op het netvlies wordt geprojecteerd getransformeerd wordt in een visueel bewegingspercept en hoe deze informatie door organismen wordt gebruikt om vrij rond te bewegen in een complexe omgeving.

Magyar összefoglaló

A medio-temporális (MT) és a medio-szuperio-temporális (MST) agyterületek fontos szerepet játszanak a vizuális mozgás feldolgozásában. Tanulmányoztuk ezen agyterületek idegsejteinek szerepét a vizuális mozgásfeldolgozásban. E célból mértük az idegsejtek aktivitását különbözõ térbeli és idõbeli vizuális ingerlés során. Munkánk által bizonyságot nyert, hogy az MT és MST idegsejtek összegzik a különbözõ eredetû mozgás-információt térben és idõben. Az eredmények új meglátásba helyezik a mozgásfeldolgozás mechanizmusait, a különbözõ mozgás-információk elkülönítésében és az összehangolásában.

Tanulmányoztuk, hogy az MT agyterület idegsejteinek mozgásirány-érzékenysége hogyan változik az idõben. Azt tapasztaltuk, hogy a vizuális mozgás által kiváltott sejtaktivitás akkor a legmagasabb, amikor a mozgó ingerlés irányt változtat az ellentétes, nem kedvezõ mozgásirányból a kedvezõ mozgásirányba. Továbbá, a sejtaktivitás általában magasabb, amikor a mozgás irányt változtat - függetlenül a kedvezõ mozgásiránytól. Ezek az eredmények arra utalnak, hogy a sejtek érzékenyek a mozgás idõbeli változására. Ez a tulajdonság fontos lehet a környezetben történõ hirtelen mozgásváltozások érzékelésében.

Egy másik kísérletsorozatban feltérképeztük az MT idegsejtek mozásirány-érzékenységét térben és idõben. Az így feltérképezett érzékenységi mezõk “központra” és “környékre” tagozódtak. A “központ-környék” érzékenységi mezõk létezése arra utal, hogy a tanulmányozott MT sejtek a térbeli mozgás-különbségekre is érzékenyek. Ez a tulajdonság szerepet játszhat például mozgó objektumok háttértõl való elkülönülésében. Úgy találtuk, hogy az MT sejtek térbeli mozgáskülönbség érzékenysége és idõbeli mozgásváltozás érzékenysége különbözõ folyamatok eredményének tulajdonítható. Arra is rámutattunk, hogy a “környék” ingerlésének hatása lassabb mint a “központ” hatása. A “környék” ingerlésére adott késleltetett reakció feltehetõen a mozgás-elkülönülés agykérgi feldolgozási folyamatainak eredménye.

Az itt közölt idegfiziológiai eredmények arra ösztönöztek bennünket, hogy a késleltetett “környék” következményeit vizsgáljuk az ember mozgás érzékelésében. Feltételezésünk szerint a “központ-környék” sejtek késleltetett aktivitása tükrözõdik az egyén relatív mozgásérzékelésében. Azonban semmilyen bizonyítékot nem találtunk arra, hogy az idegi jelenség valamilyen hatással lenne a mozgás érzékelésünkre.

A tény, hogy képesek vagyunk összetett vizuális mozgásmintázatok érzékelésére arra utal, hogy bizonyos agykérgi folyamatok összegzik a különbözõ eredetû mozgás-információt térben és idõben. Tanulmányoztuk, hogyan összegzõdik a térbeli mozgás-információ az MST agykéregben, és hogy ezt az összegzõdést hogyan befolyásolja az analizálandó helyi mozgáskomponensek iránya. Azt tapasztaltuk, hogy a mozgáskomponensek térbeli összegzõdése különbözik attól függõen, hogy a komponensek egymáshoz viszonyított mozgásiránya azonos, ellentétes vagy derékszögû. Ez az irány-függõ mozgásösszegzõdés az MST agyterületen arra utal, hogy meghatározott mozgáskomponensek speciális kombinációi kontextus-függõ módon összegzõdnek. Ez a mechanizmus lehet az alapja az MST sejtek összetett mozgásra mutatott speciális érzékenységének.

E munka eredményei új részletekkel gazdagítják tudásunkat arról, hogy az agykérgi idegsejtek hogyan elemzik a látótérben történõ mozgást és hogyan összegzik, vagy különböztetik meg a különbözõ eredetû mozgás-információt. Ezek az eredmények elengedhetetlenül fontosak annak megértéséhez, hogy a szemünk retinájára esõ vizuális információ hogyan alakul át mozgási érzékletté, továbbá, hogyan használjuk ezt az információt az összetett környezetben történõ mozgásunk során.

Credits

Over the past four years, I have been working in the nurturing atmosphere of the NEST (Neuro Ethology Station), surrounded by several elements of the Dutch countryside. I fully enjoyed my work there and the contact with my colleagues. The most important person who made this possible is my supervisor, Dr. Richard vanWezel. I am very grateful to him, for his mental support and supervision. His financial support also enabled me to travel to the United States several times, and made it possible to visit researchers working in the same scientific field, and to collect new and stimulating ideas.
I would also like to say thank to everybody, who positively contributed to this book, to my research, and to my mental/physical well-being in the Netherlands. Namely…

My family:
Mother, Pergéné Papp Veronika
Father, János Perge †
Sister, Perge Ildikó

Utrecht University:
Wim van de Grind
Albert van den Berg
Martin Lankheet
Mirjam van Hattum
Vajda Ildikó
Bart Borghuis
Roger Bours
André Noest
Jaap Beintema
Jeannette Lorteije
Jacob Duijnhouwer
Mieke Struik
Michiel Toolboom
Theo Stuivenberg
Erik Aarnoutse
Ervin Poljac
Hans Borgeld
Rob Peters
Frank Bretschneider
Jan Brascamp
Rob Loos
Rob vanWeerden
Gerard Stoker
Ed van der Veen
Tao Ran
Lonneke Eeuwes
My student, Remco Suer

Other relevant persons:
Gerencsér Andrea
Ruff János
Asli Mete
Fejes Szilvia
Peter Sterling
Jeanet van Zoelen
Marcel Smolenaars
Rinske Jellema
Chris Horn
Marije Beertema
Robert van Sluis
Sandra Souisa
Diet Borst
Ankie Delpeut
Antje Roedig
Bojan Babic
Jade Gundelach
Claudia Fila
Toldi József
Dunya Krause
Csajbók Éva
Hans de Cock
Janine Wichmann
Fiser József
Kürti Gréta
Martijn Agterberg
Német András
Huang Wei
Tóth Melinda
Henk P. van Wijk

The Church:
Bart Borghuis
Bas Dutilh
Sven vanEijl
Rikkert Hansler (who enlighted me about the use of rubber gloves in dishwashing)
Michael Drescher
Sander Borghuis
Harm-Wouter Snippe
Jacob Dutilh

Furthermore:
My dentist, Marcel Wes
Klimmuur Utrecht
Danscentrum Trianon
Albert Heijn (because there is always at least one pretty girl in A.H.)

Curriculum Vitae

Name: Perge, János Attila
Nationality: Hungarian
Date of birth: 17. December 1976,
Place of birth: Balassagyarmat, Hungary

2005 -	Post-doc at University of Pennsylvania, Philadelphia, USA in the group of Prof. Peter Sterling, working on retinal circuitry.
2005 March-April	Internship at Center for Neuroscience, Davis, California, USA, supervised by Prof. Kenneth H. Britten.
2000-2005	PhD study at the Dept. of Functional neurobiology, Utrecht University, The Netherlands, entitled: “Cortical mechanisms of visual motion integration”.
2000	Master of Science in Biology, University of Szeged, Hungary.
1999 Jun-July	TEMPUS scholarship on neural plasticity, Zentrum Anatomie Georg August Universitat, Götingen, Germany.
1998-2000	Worked as an undergraduate student at the Dept of Comparative Physiology, University of Szeged, Hungary, investigating the effect of peripheral nerve damage on the cortical inhibition level.
1997-1998	Worked as an undergraduate student at Bay Zoltán Applied Biotechnological Research Institute, on artificial symbiosisms in plant-bacterial cell cultures.
1995	Completed secondary school at Szent-Györgyi Albert Gimnázium, Balassagyarmat, Hungary.

List of publications

Perge, J. A., Borghuis, B. G., Bours, R. J., Lankheet, M. J., and van Wezel, R. J. (2005). Temporal dynamics of direction tuning in motion-sensitive macaque area MT. J Neurophysiol 93, 2104-2116.

Borghuis, B. G., Perge, J. A., Vajda, I., van Wezel, R. J., van de Grind, W. A., and Lankheet, M. J. (2003). The motion reverse correlation (MRC) method: a linear systems approach in the motion domain. J Neurosci Methods 123, 153-166.

Farkas T, Perge J, Kis Z, Wolff JR, Toldi J. (2000) Facial nerve injury-induced disinhibition in the primary motor cortices of both hemispheres. Eur J Neurosci. Jun;12(6):2190-4.

Toldi J, Farkas T, Perge J, Wolff JR. (1999)Facial nerve injury produces a latent somatosensory input through recruitment of the motor cortex in the rat. Neuroreport. Jul 13;10(10):2143-7.